

## Interactions with Arenes

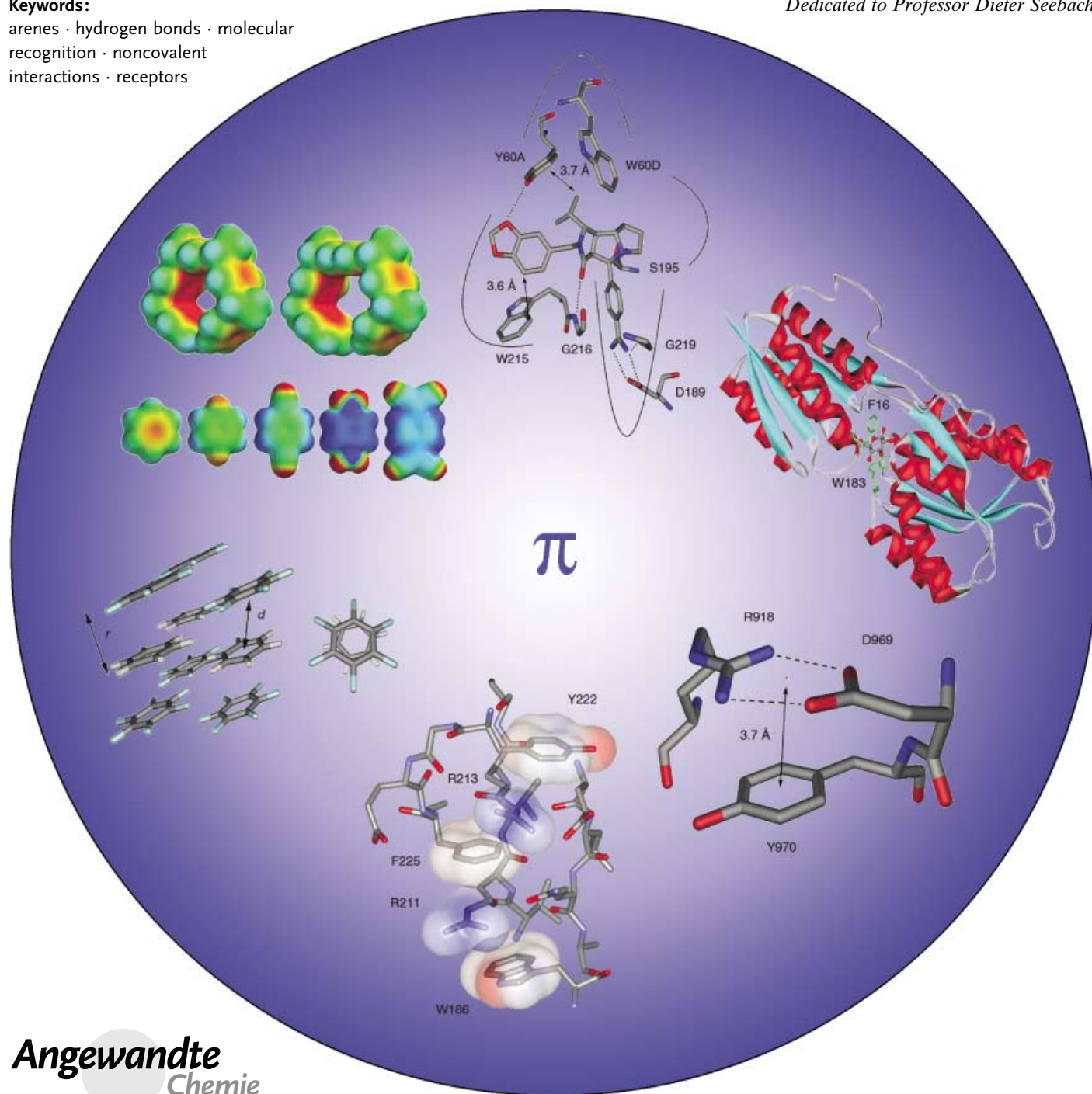
## Interactions with Aromatic Rings in Chemical and Biological Recognition

Emmanuel A. Meyer, Ronald K. Castellano,\* and François Diederich\*

## Keywords:

arenes · hydrogen bonds · molecular recognition · noncovalent interactions · receptors

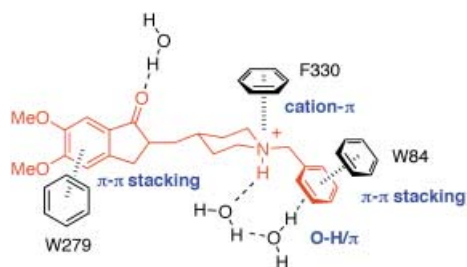
Dedicated to Professor Dieter Seebach



*Intermolecular interactions involving aromatic rings are key processes in both chemical and biological recognition. Their understanding is essential for rational drug design and lead optimization in medicinal chemistry. Different approaches—biological studies, molecular recognition studies with artificial receptors, crystallographic database mining, gas-phase studies, and theoretical calculations—are pursued to generate a profound understanding of the structural and energetic parameters of individual recognition modes involving aromatic rings. This review attempts to combine and summarize the knowledge gained from these investigations. The review focuses mainly on examples with biological relevance since one of its aims is to enhance the knowledge of molecular recognition forces that is essential for drug development.*

## 1. Introduction

Noncovalent interactions involving aromatic rings are pivotal to protein–ligand recognition and concomitantly to drug design. Indeed, the vast majority of X-ray crystal structures of protein complexes with small molecules reveals bonding interactions involving aromatic amino acid side chains of the receptor and/or aromatic and heteroaromatic rings of the ligand. The complex of the enzyme acetylcholinesterase (AChE) with the drug E2020 (Aricept), which was developed to treat symptoms of Alzheimer's disease, is one example of the diversity of these interactions (Figure 1).<sup>[1]</sup> The X-ray crystal structure analysis reveals  $\pi$ – $\pi$  stacking, O–H/ $\pi$ , and cation– $\pi$  interactions as major forces that stabilize the association. Accordingly, investigations aimed at an energetic quantification of individual interactions with aromatic rings in biological complexes are of paramount importance for improved drug design and lead optimization. Three main research approaches are pursued in order to reach this objective: 1) the biological recognition processes are analyzed in quantitative structure–activity relationships; 2) individual aromatic interactions are investigated in molecular recognition studies with designed synthetic receptors;<sup>[2]</sup> and increasingly 3) the magnitude of individual nonbonded interactions is addressed by high-level computational studies. This review attempts to present a unified picture of the understanding of the recognition of aromatic rings as it has



**Figure 1.** Binding mode of the anti-Alzheimer drug E2020 within the active site of acetylcholinesterase from *Torpedo californica* (PDB code: 1EVE).<sup>[1]</sup>

## From the Contents

1. Introduction	1211
2. Thermodynamics of Arene Complexation	1212
3. What Do We Learn from Crystals?	1216
4. Arene–Arene Interactions	1218
5. Hydrogen Bonding to Aromatic $\pi$ Systems	1225
6. Cation– $\pi$ Interactions	1227
7. Interactions between Aromatic and Perfluoroaromatic Compounds	1232
8. Sulfur–Arene Interactions	1235
9. Summary	1239

emerged from all three approaches. Given the enormity of the topic, this task can only be approached in an incomplete way, with a relatively small number of studies—preferentially those providing novel structural and thermodynamic insight—being addressed in detail. Nevertheless, this is a worthwhile, timely endeavor in light of the huge number of potential new therapeutic targets for drug design and development emerging from genomics and proteomics.<sup>[3]</sup>

The review begins with a discussion of the solvent dependency of the complexation of aromatic substrates in chemical and biological systems (Section 2). This topic has witnessed major extensions from the classical concepts of hydrophobically driven apolar complexation over the past 15 years. Section 3 highlights the crystal structures of small aromatic molecules and how analysis of their crystal-packing patterns provides a source of inspiration for the discovery of new intermolecular forces. For example, the crystal packing of a precursor to an inhibitor of thrombin,<sup>[4]</sup> a serine protease in the blood coagulation cascade targeted in the fight against thrombotic disorders, not only shows aromatic rings in classic

[\*] Prof. Dr. R. K. Castellano  
 Department of Chemistry  
 University of Florida  
 P.O. Box 117200  
 Gainesville, Florida 32611-7200 (USA)  
 Fax: (+1) 352-846-0296  
 E-mail: castellano@chem.ufl.edu  
 Prof. Dr. F. Diederich, Dipl.-Chem. E. A. Meyer  
 Laboratorium für Organische Chemie  
 Departement für Chemie und Angewandte Biowissenschaften  
 ETH-Hönggerberg, HCI, 8093 Zürich (Switzerland)  
 Fax: (+41) 1-632-1109  
 E-mail: diederich@org.chem.ethz.ch

edge-to-face (T-shaped) and parallel-displaced (stacking) arrangements, but also shows a notably short C(aromatic)–N(nitrile) distance (3.47 Å) that represents a type of weak H bond to the  $\pi$  system of the cyano group (Figure 2). Figure 3 shows the crystal structure of the complex of thrombin with a highly active inhibitor (inhibition constant  $K_i = 7$  nM), developed by structure-based de novo design.<sup>[5]</sup> The intermolecular contacts in this complex, such as the edge-to-face interaction in the distal D pocket, the C–H/ $\pi$  interactions in the proximal P pocket, and the contacts between the amidinium-substituted phenyl ring and the surrounding protein in the specificity pocket S1 are discussed in detail in Section 4.

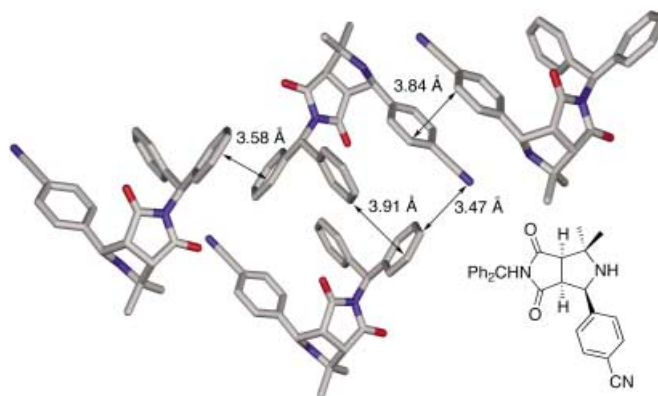
Since the seminal work of Burley and Petsko on aromatic–aromatic interactions in proteins,<sup>[6]</sup> database mining of the Cambridge Structural Database (CSD) and the Brookhaven Protein Data Bank (PDB) have increasingly been applied to identify and characterize weak intermolecular interactions in chemical and biological systems. H bonds to  $\pi$  systems provide examples for such weak bonding contacts and are discussed in Section 5. The importance of cation– $\pi$  interactions was first recognized by Ma and Dougherty, who reviewed this field comprehensively in 1997.<sup>[7]</sup> Section 6 will thus only survey the most recent investigations of this interaction in chemistry and biology. A beautiful example is the strong complexation of 7-methylated GTP (association constant  $K_a \approx 1.1 \times 10^8 \text{ M}^{-1}$ ,  $\Delta G^\circ = -11.0 \text{ kcal mol}^{-1}$ ) by a messenger RNA 5'-cap-binding protein, the eukaryotic translation initiation factor eIF4E. The cationic nucleobase in this complex is sandwiched at van der Waals distance (ca. 3.5 Å) between two Trp side chains (Figure 4).<sup>[8]</sup>

The last two sections address two emerging areas of research which have only been sparsely reviewed up to this point, namely fluoroaromatic interactions (Section 7) and those involving divalent sulfur (Section 8).

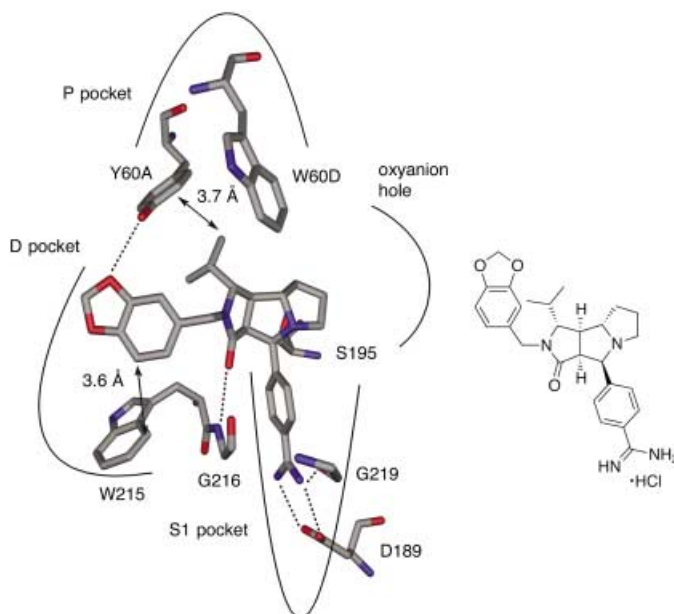
## 2. Thermodynamics of Arene Complexation

### 2.1. Complexation of Arenes with Chemical and Biological Receptors in Water

Inclusion complexation of aromatic solutes by cyclophanes in water has been intensively investigated over the past two decades, and these studies have been extensively



**Figure 2.** Edge-to-face and  $\pi$ -stacking interactions operative in the crystal packing of a precursor to an inhibitor of thrombin (CCDC-177644).<sup>[4]</sup> Color code: C: gray, N: blue, O: red, S: yellow, F: cyan. Unless noted otherwise, this color code is applied systematically in all subsequent figures.



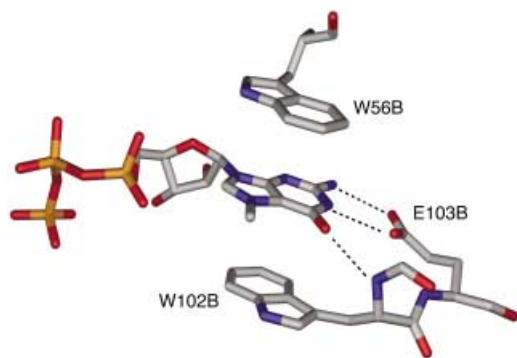
**Figure 3.** The active site in the X-ray crystal structure of the complex formed between thrombin and a designed inhibitor; edge-to-face and C–H/ $\pi$  contact distances are given; hydrogen bonds are represented as dashed lines.<sup>[5]</sup>



*François Diederich, born in 1952 in the Grand Duchy of Luxembourg, received his Ph.D. in 1979 from the University of Heidelberg. After postdoctoral studies at the University of California at Los Angeles (UCLA) from 1979–1981, he was a research associate at the Max-Planck-Institut für medizinische Forschung in Heidelberg. After his Habilitation in 1985, he joined the faculty of the Department of Chemistry and Biochemistry at UCLA where he became full professor in 1989. Since April 1992, he has been a professor of organic chemistry at ETH Zürich.*



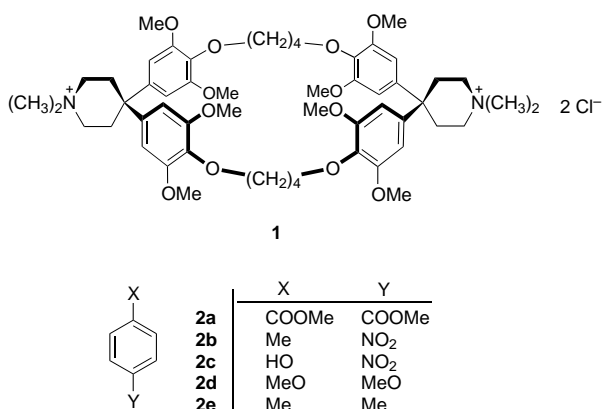
*Ronald K. Castellano was born in Toms River, New Jersey in 1973 and received his B.S. in chemistry from Gettysburg College in 1995. He received his Ph.D. in 2000 under the tutelage of Professor Julius Rebek, Jr., both at MIT and The Scripps Research Institute. His studies continued at the ETH Zürich as an NSF postdoctoral fellow with Prof. François Diederich. Since August 2002, he has been an Assistant Professor of Chemistry at the University of Florida.*



**Figure 4.** Partial view of the X-ray crystal structure (PDB code: 1L8B) of the messenger RNA 5'-cap-binding protein eIF4E bound to 7-methyl-GTP, which shows the sandwiching of the cationic nucleobase between the side chains of Trp102B and Trp56B.<sup>[8]</sup>

reviewed.<sup>[2d,9,10]</sup> Efficient apolar binding sites have not only been shaped by the covalent construction of large macrocycles with aromatic cavity walls, but also by metal-ion-mediated self-assembly.<sup>[11]</sup>

We conducted calorimetric studies with cyclophanes, such as **1**, to investigate the nature of the driving force for inclusion complexation of *para*-disubstituted benzene derivatives, such as **2a–e**, in water.<sup>[12–15]</sup> These cyclophanes form stable inclusion complexes in which the aromatic substrates undergo both aromatic  $\pi$ – $\pi$  stacking and edge-to-face interactions (see Section 4) with the cavity walls of the host.<sup>[16]</sup> We expected to



Emmanuel A. Meyer was born in 1975 in Zürich, Switzerland. From 1994 to 1999 he studied Chemistry at the ETH Zürich and Imperial College, London. He is currently a graduate student in the group of Prof. François Diederich, and his research is concerned with the design and synthesis of inhibitors for prokaryotic tRNA-guanine transglycosylase (TGT).

measure thermodynamic quantities characteristic for binding driven by the classical hydrophobic effect, namely, 1) a large favorable complexation entropy  $T\Delta S^\circ$ , 2) a small complexation enthalpy  $\Delta H^\circ$ , and 3) an increasingly favorable enthalpic term upon raising the temperature, as expressed by a large negative change in heat capacity  $\Delta C_p^\circ$ .<sup>[17,18]</sup> The classical hydrophobic effect had originally been defined to account for the thermodynamic characteristics measured for the transfer of small apolar solutes from the gas phase into water.<sup>[17,18]</sup>

We were at first rather surprised to obtain very different thermodynamic quantities, namely, a large enthalpic driving force for complexation, which was partially compensated by an unfavorable entropic term (Table 1). Only the measured negative changes in heat capacity were in agreement with our

**Table 1:** Thermodynamic parameters describing the complexation between cyclophane **1** and 1,4-disubstituted benzene guests in water and methanol.<sup>[a]</sup>

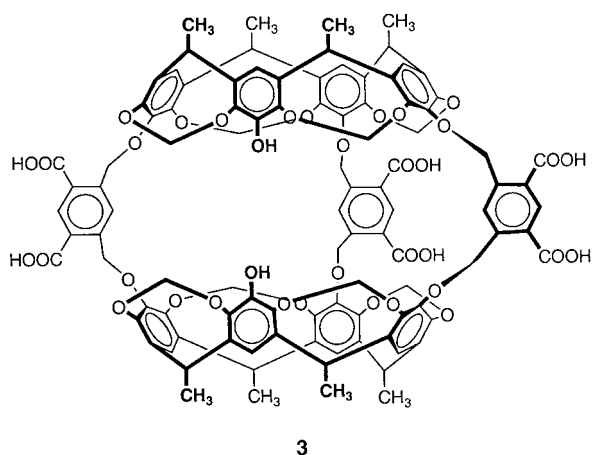
Guest	$\Delta G_{293K}^\circ$ [kcal mol <sup>-1</sup> ]	$\Delta H_{293K}^\circ$ [kcal mol <sup>-1</sup> ]	$\Delta C_p^\circ$ [cal mol <sup>-1</sup> K <sup>-1</sup> ]	$T\Delta S_{293K}^\circ$ [kcal mol <sup>-1</sup> ]
Complexes in water				
<b>2a</b>	–6.81	–11.8	–60	–5.0
<b>2b</b>	–6.01	–8.1	–50	–2.1
<b>2c</b>	–5.86	–10.5	–130	–4.6
<b>2d</b>	–5.38	–10.0	–20	–4.6
<b>2e</b>	–5.33	–7.2	–20	–1.9
Complex in methanol				
<b>2d</b>	–1.20	–3.7	–	–2.5

[a] The enthalpic terms have an uncertainty of  $\pm 0.2$  kcal mol<sup>-1</sup>; the binding free energies have an uncertainty of  $\pm 0.07$  kcal mol<sup>-1</sup> (in water) and  $\pm 0.17$  kcal mol<sup>-1</sup> (in methanol); for further details, see ref. [13].

initial expectations. On the other hand, negative changes in heat capacity had already been reported for cyclophane–arene inclusion complexation in organic solvents, such as methanol or chloroform, and therefore are not characteristic of complexation processes in water.<sup>[13,19]</sup> It, therefore, seemed unlikely that our inclusion complexation processes were promoted to a large extent by the classical hydrophobic effect.

Similar thermodynamic quantities—a large enthalpic driving force partially compensated by an unfavorable complexation entropy—have more recently been reported for the complexation of benzene derivatives and other substrates by the closed-shell hemicarcerand host **3** in an aqueous borate buffer at pH 9 (Table 2).<sup>[20,21]</sup> The complete and tight guest encapsulation by the spherical receptor results in the complexes being much more stable than those formed by the more open cyclophane **1**.

A literature search following our initial experimental work<sup>[15]</sup> readily showed that these complexation thermodynamics (that is,  $\Delta H^\circ \ll 0$ ;  $T\Delta S \ll 0$ ), which in the meantime had been named the “nonclassical hydrophobic effect” and which we also observed in the complexation of a steroid by a cyclophane receptor in water/methanol (1:1),<sup>[22]</sup> had been encountered in many arene binding studies with other synthetic and biological receptors. Thus, the inclusion com-



**Table 2:** Thermodynamic parameters describing the complexation between the spherical hemicarcerand host **3** and 1,4-disubstituted benzene guests in aqueous borate buffer (pH 9).<sup>[a]</sup>

Guest	$\Delta G_{293\text{K}}^{\circ}$ [kcal mol <sup>-1</sup> ]	$\Delta H_{293\text{K}}^{\circ}$ [kcal mol <sup>-1</sup> ]	$T\Delta S_{293\text{K}}^{\circ}$ [kcal mol <sup>-1</sup> ]
<b>2d</b>	-7.9	-10.9	-3.0
<b>2e</b>	-9.6	-12.3	-2.6

[a] Thermodynamic data for more complexation processes are reported in ref. [20].

plexation of benzene and naphthalene derivatives by natural and modified cyclodextrins is enthalpy driven, as demonstrated in a variety of calorimetric and other investigations.<sup>[23–27]</sup> The negative changes in the heat capacity recorded for these recognition processes are of similar magnitude to those reported in Table 1.<sup>[24,26]</sup> These and related thermodynamic data for cyclodextrin complexation have been compiled by Rekharsky and Inoue in a comprehensive review.<sup>[28]</sup>

Although calorimetric data on biological recognition processes remain disappointingly scarce,<sup>[29]</sup> the first examples reporting thermodynamic driving forces for apolar complexation different from those expected by the hydrophobic effect were reported as early as 1969 by Shiao and Sturtevant.<sup>[30]</sup> The authors measured the thermodynamic quantities for the complexation of small aromatic substrates in the arene binding pocket at the active site of the digestive serine protease  $\alpha$ -chymotrypsin by flow calorimetry. They determined that the complexation of indole ( $\Delta H^{\circ} = -15.2$  kcal mol<sup>-1</sup>), *N*-acetyl-D-tryptophan ( $\Delta H^{\circ} = -19.0$  kcal mol<sup>-1</sup>), and proflavin ( $\Delta H^{\circ} = -11.3$  kcal mol<sup>-1</sup>) at 298 K in aqueous buffer (pH 7.8) was strongly enthalpy driven. The authors noted that these data were not consistent with those expected for classical hydrophobic interactions. They rationalized their observations by invoking Coulombic enzyme–substrate interactions as well as large conformational changes of the enzyme upon complexation of the inhibitors—the nonclassical hydrophobic effect had yet to be recognized. A large variety of complexation processes between enzymes and aromatic substrates have subsequently been described that feature a strong enthalpic driving force at ambient temperature, with a compensating unfavorable entropic term and negative change in the heat capacity between 100 and 500 cal mol<sup>-1</sup> K<sup>-1</sup>.<sup>[31]</sup>

A favorable enthalpy and entropy of complexation have both been recorded for the complexation of aromatic substrates that also undergo ion pairing, which is well known to be entropically favored.<sup>[32]</sup> This is the case at ambient temperature for the complexation of *para*-substituted benzamidine substrates in the selectivity pocket of the serine protease trypsin (similar to thrombin, Figure 3) containing an Asp carboxylate group at its bottom.<sup>[33]</sup> Complexation at elevated temperatures is only enthalpy driven as a result of a large negative change in the heat capacity and a significant enthalpy–entropy compensation (see below).

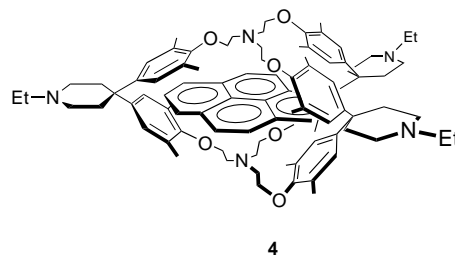
The examples of biological complexation processes featuring the thermodynamic characteristics of the nonclassical hydrophobic effect are not limited to enzyme–aromatic substrate binding, but also include: 1) DNA intercalation by arenes such as ethidium bromide,<sup>[34–36]</sup> 2) DNA association with intercalator/minor groove binders such as the antitumor drug daunomycin,<sup>[36]</sup> and 3) DNA minor groove intercalation of antitumor drugs such as netropsin and distamycin as well as hairpin polyamides.<sup>[37–39]</sup> An increasing number of studies also report enthalpic driving forces for protein–protein,<sup>[40,41]</sup> protein–DNA,<sup>[42]</sup> and protein–lipid interactions.<sup>[43]</sup> The stacking interaction between the antimalarial drug chloroquine and heme provides another example of enthalpy-driven association of aromatic rings in water.<sup>[44,45]</sup>

In view of this increasing amount of data, it is surprising that the nonclassical hydrophobic effect, with a strong enthalpic driving force for biological recognition, is almost entirely ignored in modern biochemistry textbooks. Instead, biological complexation processes are still mainly described as being driven by the classical hydrophobic effect.

It should be noted that many of the complexation studies cited in this section report strong enthalpy–entropy compensations upon variation of the host and/or guest: an increasingly favorable enthalpic driving force for complexation is compensated by an increasingly unfavorable entropic term.<sup>[26,35,38,41,42,44,46]</sup> The reader is referred to various theoretical models that have been proposed to explain the linear enthalpy–entropy compensation that is nearly universally observed in chemical and biological recognition processes.<sup>[47]</sup>

## 2.2. Solvent Dependency of the Inclusion Complexation of Aromatic Substrates

A very strong solvent dependence has been observed for the stability of pyrene complex **4**.<sup>[13,14,48]</sup> Upon changing from water, the most polar, to carbon disulfide, the least polar of the considered solvents, the complexation free enthalpy decreases from  $\Delta G^{\circ} = -9.4$  kcal mol<sup>-1</sup> to  $\Delta G^{\circ} =$



**Table 3:** Thermodynamic characteristics for the formation of complex **4** in solvents of differing polarity.<sup>[14]</sup>

Solvent	$\Delta G_{303K}^{\circ}$ [kcal mol <sup>-1</sup> ]	$\Delta H_{303K}^{\circ}$ [kcal mol <sup>-1</sup> ]	$T\Delta S_{303K}^{\circ}$ [kcal mol <sup>-1</sup> ]
water	-9.4	-	-
2,2,2-trifluoroethanol	-7.8	-20.0	-12.2
ethylene glycol	-7.3	-	-
methanol	-6.4	-12.0	-5.6
formamide	-6.2	-	-
ethanol	-6.1	-11.0	-4.9
<i>N</i> -methylacetamide	-5.8	-9.0	-3.2
<i>N</i> -methylformamide	-5.1	-5.6	-0.5
<i>N,N</i> -dimethylacetamide	-4.4	-2.0	+2.4
acetone	-4.3	-6.6	-2.3
dimethyl sulfoxide	-3.9	-6.4	-2.5
<i>N,N</i> -dimethylformamide	-2.9	-3.7	-0.8
dichloromethane	-2.9	-	-
tetrahydrofuran	-2.7	-3.0	-0.3
chloroform	-2.3	-3.1	-0.8
benzene	-1.5	-0.8	+0.7
carbon disulfide	-1.3	-	-

-1.3 kcal mol<sup>-1</sup> (303 K, Table 3). Thus, the apolar binding strength increases consistently from apolar to dipolar aprotic solvents, to protic solvents, and to water. Since complex **4** has nearly the same geometry in all solvents, the measured modulation of association strength is mostly solvent-controlled.<sup>[49]</sup>

A strong linear free-energy relationship was found to exist between the free enthalpy of formation of complex **4** and the solvent polarity parameter  $E_T(30)$ <sup>[50]</sup> of the various solvents investigated, including water.<sup>[48]</sup> Thus, the apolar complexation-promoting characteristics of water can be correlated with such characteristics of other solvents (as expressed by  $E_T(30)$ ) and are predictable solely on the basis of physical constants and properties. Linear free-energy relationships with  $E_T(30)$  or related empirical solvent parameters have also been useful in describing the solvent dependencies of other host-guest complexation processes,<sup>[12,48,51]</sup> conformational reorganizations,<sup>[52]</sup> and chemical transformations.<sup>[53]</sup>

A calorimetric study (Table 3) revealed that the formation of complex **4** is enthalpy driven in all solvents.<sup>[13,14]</sup> The complexation in alcohols are the most exothermic and, in general, the enthalpic driving force decreases from polar protic solvents, to dipolar aprotic solvents, and to apolar solvents. Correspondingly, the complexation entropy becomes increasingly less favorable as the exothermicity increases, which results in a strong enthalpy-entropy compensation. This calorimetric investigation, which revealed the thermodynamic signatures for arene complexation in solvents of all polarities, provided substantial support for our explanation of the nonclassical hydrophobic effect.

### 2.3. The Nonclassical Hydrophobic Effect

We identified favorable changes in solvent cohesive interactions and a gain in dispersion interactions as the main components of the enthalpic driving force for apolar

complexation in aqueous solution, that is, the nonclassical hydrophobic effect.<sup>[12-15]</sup> Thus, the stability of complex **4** (Table 3) is highest and the complexation enthalpy the most favorable in solvents characterized by high cohesive interactions and low molecular polarizability.

Solvents with high cohesive interactions prefer to interact with bulk solvent molecules rather than to solvate the complementary apolar surfaces of host and guest molecules. We proposed that “water molecules around apolar surfaces participate in fewer strong hydrogen bonds than bulk solvent molecules”.<sup>[54]</sup> Therefore, enthalpy is gained upon release of surface-solvating molecules to the bulk during the complexation step. Water has the highest cohesive interactions and, therefore, the enthalpic driving force in this solvent is particularly favorable. Saenger, in his seminal review on cyclodextrin complexation in 1980, already stated correctly that water molecules solvating the cavities of the receptors are higher in energy than water molecules in the bulk solvent.<sup>[55]</sup>

A similar explanation for the role of internal solvent-cohesive interactions in promoting apolar binding processes in water had already been proposed by Sinanoglu as early as in 1968.<sup>[56]</sup> As a result of the strong cohesive forces in water, energy is required to create a cavity in the bulk liquid to accommodate an apolar guest molecule. Such cavities are also created when water molecules enter the binding site of the free host for solvation. Other authors have also pointed to the unfavorable energetics for cavitation in pure solvent.<sup>[18,57]</sup> Free-enthalpy calculations on the pyrene complex **4** in water and chloroform indeed provided impressive support for the major role of internal solvent-cohesive interactions.<sup>[49]</sup> This computational study revealed that the key process which determines the difference in binding in the two solvents ( $\Delta\Delta G^{\circ} = 7.1$  kcal mol<sup>-1</sup>; Table 3) is the elimination of pyrene molecules from the solvent and not directly the cyclophane-pyrene interactions, which are of similar magnitude in both solvents. From the calculated difference in the free enthalpy of complexation between water and chloroform ( $\Delta\Delta G = 10.2$  kcal mol<sup>-1</sup>), 8.6 kcal mol<sup>-1</sup>, that is, about 84 %, is caused by the differences in the free enthalpy of solvation of the pyrene molecule in the two solvents!

Recent computational studies provide further evidence for the importance of the proposed large contribution of solvent-cohesive interactions to enthalpy-controlled apolar binding processes. Rossky and co-workers<sup>[58]</sup> carried out simulations of the hydration structure of the aromatic binding pocket at the active site of the digestive serine protease  $\alpha$ -chymotrypsin. They found that the highly constrained concave geometry of the pocket prevents the formation of a hydrogen-bonding network between the solvating molecules. Correspondingly, solvent displacement by the incoming substrate is associated with a large enthalpic driving force.

Southall and Dill<sup>[59]</sup> observed in Monte Carlo simulations a large dependence of the hydration efficiency on the shape and curvature of the solute. Small solutes, for which the classical hydrophobic effect was derived, undergo an ordered “iceberg”-like solvation (characterized by  $\Delta S \ll 0$ ) to avoid breaking H bonds. In contrast, the geometry of larger non-polar solutes, in particular planar ones such as arenes, force

first-shell water molecules to break their H bonds ( $\Delta H^{\circ} \gg 0$ ). This study also analyzes in greater detail the origin of the negative changes in heat capacity accompanying apolar binding processes in water. Similar conclusions with respect to topography-dependent H-bonding sacrifices upon the hydration of apolar surfaces have also been drawn by other authors.<sup>[60]</sup>

A second major contribution to the favorable enthalpic driving force in water results from the substitution of less favorable dispersion interactions between water molecules and the complementary surfaces of the host and guest molecules by more favorable dispersion interactions between the hydrocarbon surfaces in the complex.<sup>[12–15, 48, 61]</sup> The attractive  $B$  term in the Lennard–Jones potential [Eq. (1);  $U$ : potential energy] that describes the London dispersion interactions is directly proportional to the polarizability  $\alpha$  [ $\text{\AA}^3$ ] of the interacting atoms and groups [Slater–Kirkwood equation (2);  $\alpha$ : polarizability,  $e$ : charge on an electron,  $m$ : mass of an electron,  $\hbar$ : Dirac's constant,  $N$ : effective number of electrons in the outer shell].<sup>[62]</sup>

$$U = \frac{A}{r^{12}} - \frac{B}{r^6} \quad (1)$$

$$B = \frac{3/2 e (\hbar/m^{1/2}) \alpha_i \alpha_j}{(\alpha_i/N_i)^{1/2} + (\alpha_j/N_j)^{1/2}} \quad (2)$$

At constant distances between interacting atoms, attractive dispersion interactions increase with increasing atom polarizability. The constituents of water (O:  $\alpha = 0.84 \text{ \AA}^3$ ; HO:  $\alpha = 1.20 \text{ \AA}^3$ ) have much lower polarizabilities than hydrocarbon groups (CH<sub>2</sub>:  $\alpha = 1.77 \text{ \AA}^3$ ; CH<sub>3</sub>:  $\alpha = 2.17 \text{ \AA}^3$ ; aromatic CH:  $\alpha = 2.07 \text{ \AA}^3$ ).<sup>[62]</sup> Therefore, the dispersion forces between water molecules and a hydrocarbon surface are weaker than those between two hydrocarbon surfaces. Thus, upon apolar complexation, less favorable water–solute contacts are replaced by more favorable contacts between the surfaces of the binding partners. The importance of molecular polarizability for apolar binding in water has also been recognized in other investigations.<sup>[26, 27, 63]</sup>

The tightness of the fit between the associating molecules affects the thermodynamic characteristics of host–guest binding.<sup>[24, 25, 27, 64, 65]</sup> Efting and co-workers showed in calorimetric studies that tight inclusion of apolar aromatic and aliphatic guests in the smaller cavity of  $\alpha$ -cyclodextrin at 298 K is characterized by a much larger enthalpic driving force than the inclusion of the same guest in the wider cavity of  $\beta$ -cyclodextrin.<sup>[24, 25, 64]</sup> In some cases involving aliphatic guests, changing from the smaller to the larger binding site was associated with a change from an enthalpy- to an entropy-driven process. The strongly distance-dependent (ca.  $1/r^6$ ) attractive van der Waals interactions between the host and guest in a tight complex<sup>[66]</sup> are much more effective than in a loose complex, whereas translational and rotational degrees of freedom of the interacting partners become substantially reduced. A loose association, on the other hand, is predominantly driven by the desolvation entropy.

In view of the lack of calorimetric data for apolar complexation processes of biological and chemical systems

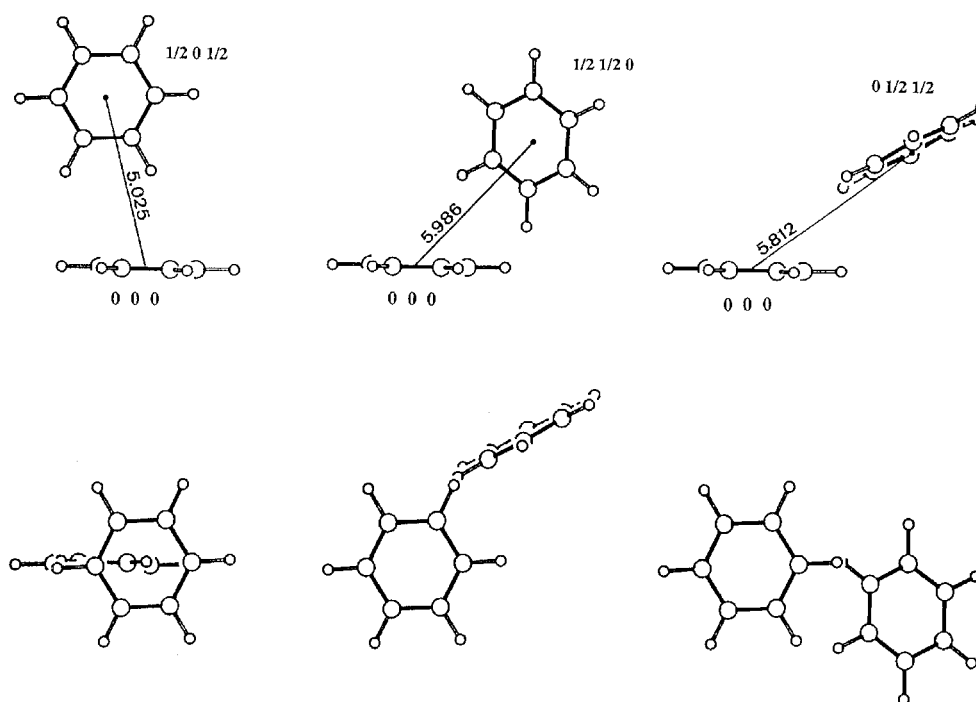
in water, we suggested around 1990<sup>[10, 12–15]</sup> that characterizing apolar binding processes in water as hydrophobically driven should not imply a predominant enthalpic or entropic driving force. However, it is also becoming increasingly clear that tight complexation in deep apolar pockets of biological and synthetic receptors is mostly enthalpy driven, that is, obeys the nonclassical hydrophobic effect.

### 3. What Do We Learn from Crystals?

A crystal is an ordered supramolecular system, and according to Dunitz “a supermolecule par excellence”.<sup>[67]</sup> X-ray crystallography provides accurate information on the structures of molecular complexes and the nature of the nonbonded interactions between the binding partners in the solid state. This technique has become a central one in molecular recognition studies.

Rational drug design, as a biological extension of the supramolecular sciences, is increasingly dependent on available protein crystal structures taken from the Protein Data Bank (PDB) or in-house databases.<sup>[68]</sup> In addition, new programs, such as Isostar,<sup>[69a]</sup> SuperStar,<sup>[69b]</sup> and the impressive Relibase,<sup>[69c]</sup> permit the systematic investigation of protein–protein or protein–ligand interactions. The use of the Cambridge Structural Database (CSD) is also important for the life sciences.<sup>[70]</sup> Both sets of databases are growing at an exponential rate,<sup>[71]</sup> and have been vaults for finding information on chemical interactions: they have been the basis for extensive investigations of classical H bonds in the past,<sup>[72, 73]</sup> and more recently have been used to explore weaker H bonds, such as C–H $\cdots$ O, C–H $\cdots$ N, and C–H $\cdots$ Cl.<sup>[74]</sup> Directionality, energetics, distance relative to van der Waals radii, and bond length are useful criteria for classifying H bonds. In this context, the C–H/ $\pi$  interaction between aromatic rings has been defined as an H bond (see Section 5). Moreover, although of controversial importance, the C–H $\cdots$ O hydrogen bond remains a prominent example because of its wide occurrence in crystal structures and its postulated structural role in biology.<sup>[75]</sup> We shall conclude these introductory remarks with the statement that “atoms have to go somewhere”, a perhaps discouraging view of a crystallization process, but one that reminds us of the maximization of dispersive and minimization of repulsive interactions in crystals—“real” and measurable structure-determining processes—that need to be considered when describing weak intermolecular forces.<sup>[76]</sup>

Parallels can be drawn between molecular recognition events that occur within model systems in the liquid phase and those that define the supramolecular nature of a molecular network in the solid state. The crystal structure of benzene laid the structural basis for recognizing attractive interactions between aromatic rings (Section 4).<sup>[77]</sup> Benzene crystallizes in the space group  $Pbca$ , with four molecules in the unit cell, and each molecule being surrounded by twelve neighbors. Three types of next-neighbor interactions are observed (Figure 5): The most favorable interaction is the edge-to-face arrangement with a distance of  $5.025 \text{ \AA}$  between the ring centers. However, as pointed out by Williams and Xiao,<sup>[78]</sup> none of the



**Figure 5.** Two orthogonal views (upper and lower rows) of the basic next-neighbor motifs in crystalline benzene (*Pbca*). Left: most favorable edge-to-face orientation with a center-to-center distance of 5.025 Å; rings located at (0,0,0) and  $(\frac{1}{2}, 0, \frac{1}{2})$  in the unit cell. Middle: dimer with perpendicular arrangement but a larger offset (5.986 Å, rings at (0,0,0) and  $(\frac{1}{2}, \frac{1}{2}, 0)$ ). Right: pairing with inclined ring moieties (5.812 Å, rings at (0,0,0) and  $(0, \frac{1}{2}, \frac{1}{2})$ ); Reprinted with permission from The Royal Society (London).<sup>[80]</sup>

pairs in the benzene crystal corresponds to the lowest energy arrangements observed in the gas-phase dimer. This discrepancy arises from the presence of *several* nearest neighbor molecules in the vicinity of an individual benzene molecule and of long-range intermolecular interactions in the solid state. Modifications to the benzene lattice structure have been realized experimentally by using different pressures, with many of the attempts being made with the aim of predicting the resulting crystal structure.<sup>[79]</sup> The search for polymorphic structures facilitates a deeper understanding of the thermodynamics of crystallization and comparisons with predicted models. The smaller polycyclic aromatic hydrocarbons (PAHs), such as naphthalene or pyrene, prefer T-shaped interaction geometries, similar to benzene. The larger aromatic molecules (such as coronene, kekulene, or hexabenzocoronene) show offset  $\pi$ - $\pi$  stacking, since for these molecules there is a substantial gain in dispersion interactions that results from the contact of such large polarizable surfaces. In each of these crystals, however, there also exist edge-to-face interactions between molecules of neighboring stacks in the so-called “herringbone pattern”.

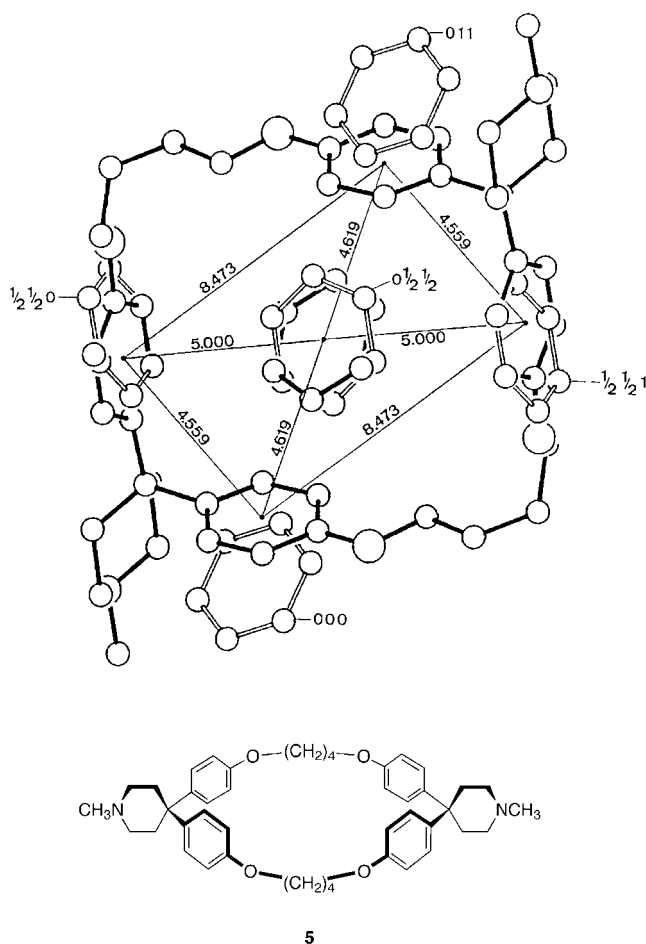
The crystal structure of benzene, in a least-squares superimposition, was matched geometrically with the structure of an inclusion complex of cyclophane **5** with benzene (Figure 6).<sup>[80]</sup> This study revealed that the interactions of the benzene rings in the host with the included benzene ring are similar to those seen between nearest neighbors in crystalline benzene. Klebe and Diederich concluded that the self-recognition of molecules in the solid state provides a guide for the design of hosts that are specific receptors for the molecule in question. This analysis has been useful for

modeling a pseudoreceptor during drug design.<sup>[81]</sup> The analysis of the benzene crystal has been extended to other systems displaying similar packing modes, such as the self-assembling cyclic peptide nanocylinders of Bong and Ghadiri.<sup>[82]</sup>

The Holy Grail of crystallography remains the prediction of crystal structures from molecular structures.<sup>[83]</sup> The last workshop held on this subject produced only a few correct predictions, which emphasizes how limited our knowledge is in this area.<sup>[84]</sup> The problem of crystal-structure prediction has been recognized as more complex than originally thought, but steady progress has been made. By considering molecular size, shape, stoichiometry, and topology; Desiraju and Gavazzotti were able to assign a set of 32 PAHs into four different crystal packings.<sup>[85]</sup> Correlations between molecular size, packing energy, and other crystal properties made it possible to predict physical properties, such as sublimation enthalpy and density of unknown aromatic hydrocarbons.<sup>[76]</sup>

Crystal engineering has enabled connections between molecular and supramolecular structure to be established on the basis of intermolecular interactions.<sup>[86]</sup> In this context, supramolecular synthons have been defined as structural units within supermolecules that can be formed and/or assembled by known or conceivable synthetic operations involving intermolecular interactions. The aryl-aryl synthons, for example, are based on edge-to-face and stacking arrangements of two aromatic rings. An example of an application of the latter lies in the topochemical solid-state synthesis of 3,4-diphenyl-substituted cyclobutane-1,2-dicarboxylic acids using the attractive interactions between aromatic donor and acceptor moieties.<sup>[87]</sup>





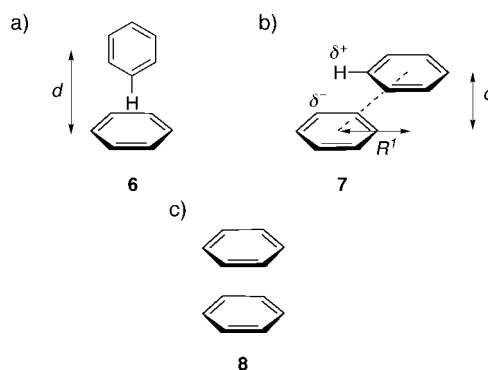
**Figure 6.** Superimposition of a subset from the packing of crystalline benzene (empty bonds, classified by their centering in the crystal packing) with the molecular structure of the benzene-5 complex in the crystal (solid bond). Mutual center-to-center distances between the aromatic rings in the cyclophane complex are given.<sup>[80]</sup>

## 4. Arene–Arene Interactions

### 4.1. Biological Relevance

Arene–arene interactions play an essential role in the structure of biological macromolecules such as DNA and proteins, as well as in their interaction with small molecules.<sup>[88]</sup> However, their weak and poorly directional character hindered for some time the development of a general, structural, and energetic model for their description.<sup>[89]</sup>

Interactions between aromatic amino acid side chains are abundant in proteins, as shown by the pioneering work of Burley and Petsko.<sup>[6, 90]</sup> They demonstrated in a study involving 34 proteins that on average 60% of aromatic side chains (Phe, Trp, Tyr) are involved in  $\pi$ – $\pi$  interactions, where the predominant arrangement was found to be the T-shaped edge-to-face structure **6** (Figure 7). McGaughey, et al. extended the analysis to a larger sample of proteins and suggested that the parallel-displaced geometry **7** was a preferred orientation.<sup>[91]</sup> Remarkably, none of these studies described the face-to-face geometry **8**.



**Figure 7.** Proposed lowest energy structures of the benzene dimer.  $d$ : distance between planes,  $R^1$ : lateral offset.

Several other statistical analyses of PDB structures have elucidated the preferential arrangement of specific aromatic amino acid pairs in proteins or  $\alpha$ -helices.<sup>[92, 93]</sup> When these results are combined with computational work, the general view is a competition between stacked and T-shaped complexes; however, an uneven distribution can be seen depending on the aromatic amino acid pair analyzed, the distance of the two aromatic rings, their location in the protein (in the core or on the surface), and whether clustering of the aromatic amino acids is involved.<sup>[94]</sup>

Although  $\pi$ – $\pi$  interactions are accepted as weak, they have been recognized to play an important role in the folding<sup>[93]</sup> and the thermal stability of proteins.<sup>[95]</sup> Other biological contributions are noteworthy. The recent literature provides several illustrative examples: Edge-to-face interactions are implicated in the decrease of the  $pK_a$  value of Tyr9, which is located in the vicinity of Phe10 in the active site of glutathione *S*-transferase A1-1. This enzyme catalyzes the conjugation of glutathione to electrophilic substrates (drugs, toxins, endogenous compounds).<sup>[96]</sup> Stacking interactions play an essential role in mRNA-cap recognition by proteins (in combination with cation– $\pi$  interactions, see Figure 4 and Section 6),<sup>[97]</sup> in the arrangement of porphyrin units in water or inside proteins,<sup>[98]</sup> in the binding of carotenoids in a light-harvesting complex,<sup>[99]</sup> and have been suggested to govern the self-assembly of amyloid fibrils.<sup>[100]</sup> Introduction of aromatic side chains in a hairpin motif of a *de novo* designed  $\beta$  sheet produces an enthalpy-driven interaction between  $\beta$  strands.<sup>[101]</sup> The self-association of a 12-residue  $\beta$  hairpin through aromatic side chains was investigated, and the Phe–Phe pair that are found in an edge-to-face geometry gave an increment in the interaction free enthalpy of  $-0.55 \text{ kcal mol}^{-1}$ .<sup>[102]</sup> This value is similar in magnitude to that found by double mutant cycles in the cold-shock protein CspA (Phe  $\rightarrow$  Leu),<sup>[103]</sup> but lower than what has been previously observed in barnase by Fersht and co-workers (Tyr  $\rightarrow$  Ala,  $-1.3 \text{ kcal mol}^{-1}$ ).<sup>[104]</sup> Moreover, the Phe–Phe interaction can stabilize monomeric  $\alpha$  helices by up to  $\Delta G = -0.8 \text{ kcal mol}^{-1}$ , as determined recently by circular dichroism studies.<sup>[105]</sup>

#### 4.2. Geometrical and Energetic Aspects

The benzene dimer has often been chosen as a model system for the investigation of  $\pi$ - $\pi$  interactions. The earliest gas-phase studies began with the work of the Klemperer research group who deduced, by using molecular beam spectroscopy, there was an edge-to-face arrangement between neighboring molecules.<sup>[106]</sup> This T-shaped arrangement has been confirmed in a large number of experimental studies. Although the observed intermolecular arrangements have been shown to be often dependent upon the experimental technique used,<sup>[107]</sup> the T-shaped motif also appears as the preferred one for both liquid benzene (as revealed by <sup>1</sup>H NMR investigations)<sup>[108]</sup> and, as seen in Section 3, for benzene in the crystal.

Molecular mechanics, ab initio, and density functional calculations at several levels of theory have been employed to describe and predict the structure of the benzene dimer.<sup>[109]</sup> Different minima have been proposed, where the interaction energy is often dependent on the method used.<sup>[110]</sup> Very recent calculations gave two nearly isoenergetic minima for the edge-to-face and parallel-displaced arrangements with values for the CCSD(T) (coupled cluster calculation with single and double substitutions with noniterative triple excitations) interaction energy of  $D_e = -2.48$  and  $-2.46$  kcal mol<sup>-1</sup>, respectively.<sup>[111]</sup> This low calculated difference in binding energy is in good qualitative agreement with the observation that no strong preference for either arrangement has been found for Phe, Tyr, and Trp side chains in proteins. Experimental measurements in the gas phase have shown the stabilization enthalpy of the benzene dimer to range from  $D_0 = -1.6 \pm 0.2$  kcal<sup>[112]</sup> to  $-2.4 \pm 0.4$  kcal.<sup>[113]</sup> Finally, the sandwich structure **8** (Figure 7) is more unfavorable ( $D_e = -1.48$  kcal mol<sup>-1</sup>) than the other two, even though it is an energy minimum and still attractive in nature. The energy barriers for interconversion of the three most stable minima geometries are very low, and hence they are in dynamic equilibrium.<sup>[114]</sup> We should mention the geometric values that describe the most stable arrangements **6** and **7**. Structure **6** has an experimentally determined ring-center separation of 4.96 Å, with the partially positively charged H atom pointing perpendicular into the partially negatively charged center of the second ring (Figure 7). The parallel-displaced stacking dimer **7** has an interplanar distance  $d$  of 3.4–3.6 Å with a displacement  $R^1 = 1.6$ –1.8 Å. The application of ab initio techniques to even larger polycyclic aromatic hydrocarbon dimers has upheld the arrangement seen in the corresponding crystal structures (Section 3).<sup>[115]</sup>

It is nowadays recognized that London dispersion interactions are the major source of stabilization energy between two aromatic molecules; however, the electrostatic component associated with the large quadrupole moment<sup>[116]</sup> of benzene ( $-28.3 \times 10^{-40}$  C m<sup>2</sup>)<sup>[117]</sup> is an influential factor in determining the geometry of the interaction. For example, the parallel-displaced arrangement is a compromise between optimal surface overlap that maximizes the dispersive attraction (distance dependency  $r^{-6}$ ) and quadrupole moment positioning ( $r^{-5}$ ). Short-range repulsive interactions (Pauli-exchange/repulsion forces) also influence the interplanar

distance.<sup>[118]</sup> Assessment of these binding interactions in aqueous solution is complicated by additional hydrophobic effects; these of course lead to apolar complexation or to intramolecular hydrophobic collapse (Section 2).<sup>[119]</sup> A deeper view of the solvent-dependency of the interaction energy in the benzene dimer is available from computational studies. The calculated Gibbs free energy minimum ( $\Delta G$ ) for the benzene dimer in liquid benzene, chloroform, and water is  $-0.4$ ,  $-1.0$ , and  $-1.5$  kcal mol<sup>-1</sup>, respectively.<sup>[120]</sup> Thus, there appears to be a solvophobic enhancement of the binding on progression to more polar solvents. The more favorable gas-phase interaction is considerably dampened by solvent competition and entropic effects.<sup>[120]</sup> Finally, it is interesting to note that the T-shaped structure has been confirmed through computational investigations to be an energetic minimum in aqueous solutions.<sup>[121,122]</sup>

The parallel-stacked arrangement **8** that would permit a HOMO–LUMO charge-transfer interaction is estimated to be 0.7–1.5 kcal mol<sup>-1</sup> (gas phase or aqueous solution) less stable than the T form.<sup>[122]</sup> This geometry is unfavorable because of repulsive interactions between the negatively charged electron clouds or quadrupole moments of equal sign.

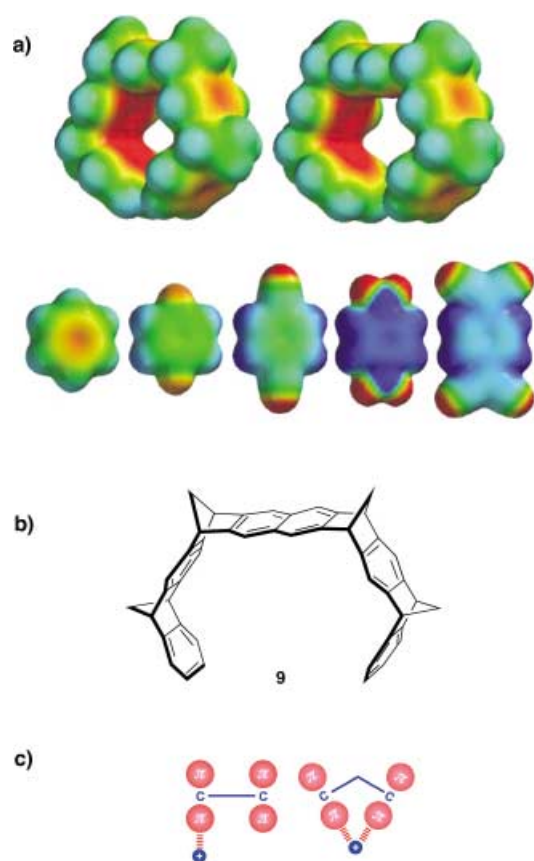
The benzene dimer is not necessarily a good model for the  $\pi$ - $\pi$  interaction since polarization or enlargement of the  $\pi$  system changes the preferred intermolecular arrangement dramatically. To this end, the toluene dimer has been shown to have stacked arrangements as global minima as a result of a small dipole originating from the methyl group. Toluene has, therefore, been proposed as an improved model for phenylalanine for the study of  $\pi$ - $\pi$  interactions in proteins.<sup>[122,123]</sup>

#### 4.3. Experimental Study of $\pi$ - $\pi$ Interactions

##### 4.3.1. Background Information

We have shown that one of our cyclophane receptors (similar to **1** (Section 2) but with the eight MeO groups exchanged for Me groups) is able to complex 2,6-disubstituted naphthalene derivatives in CD<sub>3</sub>OD, with the cavity-bound guests undergoing both edge-to-face and  $\pi$ -stacking interactions with the receptor.<sup>[124]</sup> Complementarity between the electron-rich host and electron-poor guests led to particularly stable association (for example,  $K_a = 280$  M<sup>-1</sup>,  $-\Delta G = 3.4$  kcal mol<sup>-1</sup> for the complex of 2,7-dicyanonaphthalene as compared to  $K_a = 50$  M<sup>-1</sup>,  $-\Delta G = 2.3$  kcal mol<sup>-1</sup> for the complex of 2,7-dimethoxynaphthalene;  $T = 303$  K), which stresses the importance of polar contributions in  $\pi$ - $\pi$  interactions.<sup>[125]</sup>

Klärner and co-workers have shown that the convex-concave topology of aromatic surfaces influences the binding properties of tweezer-shaped receptors.<sup>[126a]</sup> Computational methods at different levels of theory have been used to generate electrostatic potential surfaces for both the convex and concave faces (Figure 8). The results are striking: the concave surface features convergent  $\pi$ -electron systems (Figure 8c) that lead to a considerably larger negative potential within the tweezer's interior than at the exterior. This observation explains the experimentally observed high preference of receptor **9** (Figure 8b) for complexing electron-



**Figure 8.** a) Electrostatic potential surfaces of molecular tweezers with benzene (left) and naphthalene (right) spacers developed by Klärner and co-workers (top) and aromatic guests (bottom, from left to right: benzene, *p*-difluorobenzene, *p*-dicyanobenzene, *p*-dinitrobenzene, and 7,7,8,8-tetracyanoquinodimethane) calculated by semiempirical methods. The color code spans from  $-25$  (red) to  $+25$  kcal mol<sup>-1</sup> (blue). b) Receptor **9** for which the electrostatic potential surface is shown in (a). c) Schematic representation of the interaction of a positive test charge with nonconjugated “idealized” sp<sup>2</sup> C atoms with linear (left) and concave geometry (right).<sup>[126a]</sup>

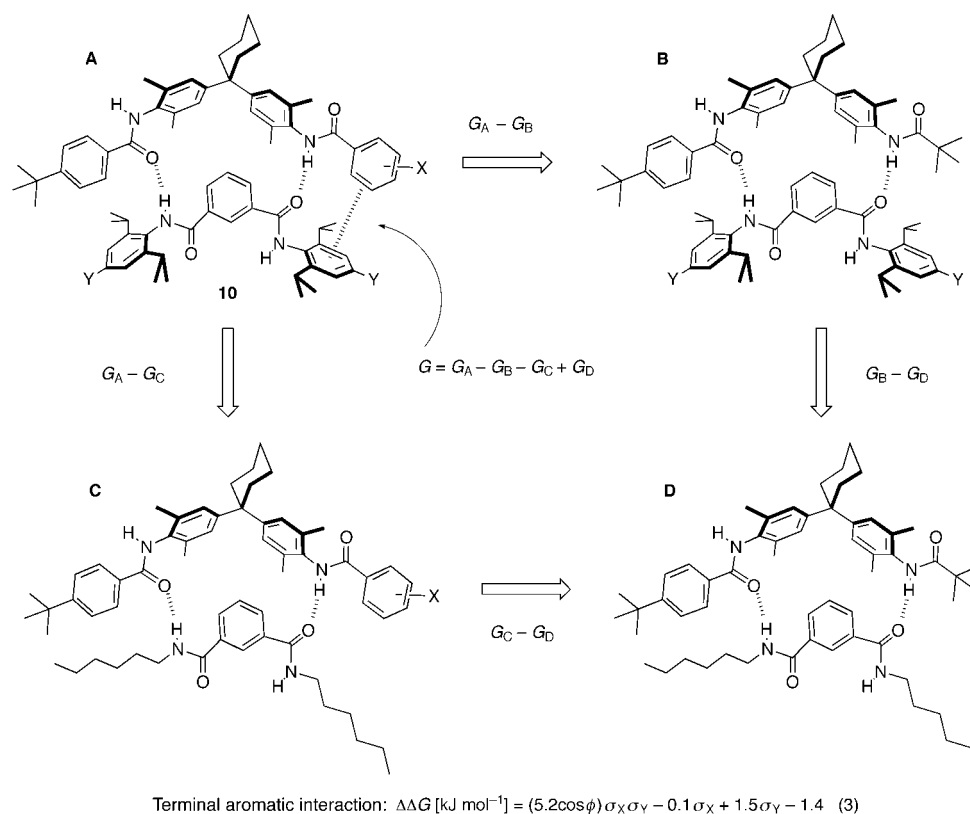
deficient guests in its interior in a position parallel to the central naphthalene spacer.<sup>[126b]</sup> This result demonstrates the importance of molecular receptor topology: evaluation of host–guest complexation processes needs to take into account the complementarity of both the shape and molecular electrostatic potential (MEP). This principle has been employed to rationalize the complexation behavior of various curved aromatic hosts and even cyclic peptides.<sup>[127,128]</sup>

In 1990 Hunter and Sanders developed a simple electrostatic model where a set of point charges is used to represent the electrostatic charge distribution in a  $\pi$  system. Useful general rules have been derived from this work for a qualitative understanding of  $\pi$ – $\pi$  interactions.<sup>[129]</sup> The key feature of the model is that it considers  $\pi$  electrons and the  $\sigma$ -bonding system separately, and reveals  $\pi$ – $\pi$  repulsions and  $\pi$ – $\sigma$  attractions to be the governing factors in the interaction between two aromatic molecules. This model has been challenged recently by ab initio studies, which contend it should be sufficient to recognize solely the role of molecular quadrupoles when describing aromatic interactions.<sup>[130]</sup>

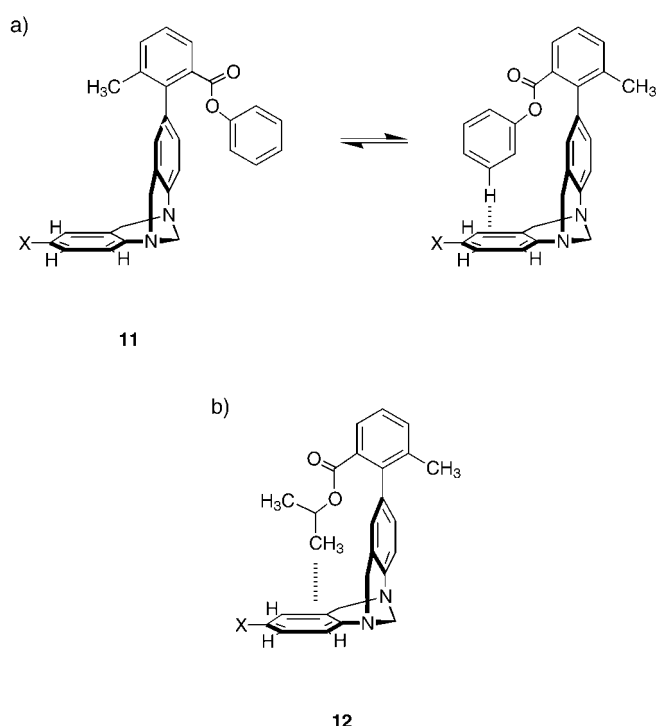
#### 4.3.2. Edge-to-Face Interactions

Many chemical model systems have been designed to investigate both edge-to-face and  $\pi$ -stacking geometries of interacting aromatic rings, and a plethora of receptors, in particular cyclophanes, have demonstrated these arrangements during complexation.<sup>[2,9–16,126,131]</sup> The intermolecular edge-to-face aromatic interactions have been analyzed by Hunter and co-workers using chemical double-mutant cycles.<sup>[132]</sup> This elegant method allows individual assignment of the contribution from T-shaped interactions between differently substituted terminal phenyl rings in the host (substituent X) and guest (substituent Y) to the overall binding free enthalpy in the molecular zipper complexes **10** (Figure 9). The obtained increment in free enthalpy for the edge-to-face interaction,  $\Delta\Delta G$ , is on average  $-0.3$  kcal mol<sup>-1</sup> (for X=Y=H) and is sensitive to the nature of the substituents on the aromatic rings, and varies from unfavorable ( $\Delta\Delta G = +0.29$  kcal mol<sup>-1</sup> when X=NO<sub>2</sub> and Y=NO<sub>2</sub>) to favorable ( $-1.1$  kcal mol<sup>-1</sup> when X=NO<sub>2</sub> and Y=NMe<sub>2</sub>).<sup>[133]</sup> Thus, the highest edge-to-face attraction is found when an electron-attracting substituent renders the interacting H atom more acidic (higher positive partial charge) and an electron-donating substituent increases the basicity ( $\pi$ -electron density) of the interacting  $\pi$  system. Equation (3) in Figure 9 gives the relationship between the Hammett substituent constants  $\sigma$  and the observed interaction energies for this system: In addition to the attraction between the partially positively charged edge H atoms (of the host) with the terminal aromatic ring (of the guest), the crucial influence of the global dipoles can be seen (cross-term  $5.2 \cos(\phi)\sigma_X\sigma_Y$ ). However, the incremental free enthalpy values  $\Delta\Delta G$  are not likely to be universal values for edge-to-face interactions between aromatic rings as a result of the lack of rigidity in the zipper complex, as pointed out by Martínez et al.<sup>[134]</sup>

Wilcox and co-workers developed the molecular torsion balance **11** based on rotational isomerism (Figure 10) to quantify edge-to-face interactions.<sup>[135]</sup> The following findings were made in this study that was recently reviewed:<sup>[136]</sup> 1) The folded conformation in a series of phenyl esters (X in **11**: Me) is preferred by  $-\Delta G^\circ = 0.4$  to  $0.65$  kcal mol<sup>-1</sup> (298 K), with the variation depending on the nature of substitution on the phenyl ring ( $0.24$  kcal mol<sup>-1</sup> for the *p*-methoxyphenyl ester, and  $0.65$  kcal mol<sup>-1</sup> for the *p*-nitrophenyl ester). 2) The folded conformation of the corresponding cyclohexyl ester was also stabilized to a similar extent ( $0.37$  kcal mol<sup>-1</sup>). 3) Variation of the substituent X in **11** from donor (NH<sub>2</sub>) to acceptor (CN) did not affect the magnitude of the energetic preference for the folded conformation ( $\Delta G = -0.18$  to  $-0.30$  kcal mol<sup>-1</sup>). 4) The folding of isopropyl ester **12** (Figure 10b) was more exergonic ( $\Delta G = -0.34$  to  $-0.64$  kcal mol<sup>-1</sup>, depending on substituent X) than the folding of the phenyl ester. These results support the notion that dispersion, and not electrostatic forces, are largely responsible for the attractive edge-to-face interaction. However, computational investigations suggested that the preference for the folded state arising from the aromatic interactions could have been underestimated.<sup>[137a,b]</sup> The calculations showed that differences in the solvent-accessible surfaces of the two conformations in **11** may push



**Figure 9.** Chemical double-mutant cycle by Hunter and co-workers for probing the magnitude ( $\Delta\Delta G$ ) of the edge-to-face aromatic interaction between the terminal phenyl rings of molecular zipper **10** and isophthalic acid diamide guests.<sup>[132,133]</sup>

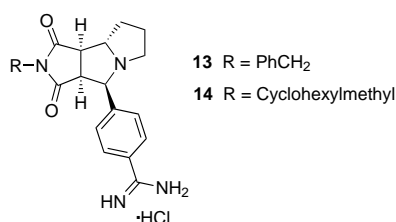


**Figure 10.** a) Molecular torsional balance **11** described by Wilcox and co-workers to quantify aromatic edge-to-face interactions. T-shaped aromatic interactions are effective only in the folded conformation.<sup>[135]</sup> b) Preferred folded state of isopropyl ester **12**. X = NO<sub>2</sub>, CN, I, Br, Me, OH, NH<sub>2</sub>.

the equilibrium toward the unfolded state; thus, a more favorable free enthalpy of interaction might be expected when solvent effects are fully considered.<sup>[137c]</sup>

Clearly, solvent effects greatly increase the challenge—not only in computational work but also in studies of elegantly designed supramolecular model systems—to quantify a single individual intermolecular bonding interaction, such as an edge-to-face aromatic contact. Over the past few years we have recognized this challenge with model systems, and have complemented our molecular-recognition studies on synthetic receptors with the analysis of intermolecular interactions in structurally well-defined enzyme–inhibitor complexes. In this approach, we introduce defined mutations in substrates that form complexes of similar geometry with the biological receptor (which we prove by X-ray crystallography) and evaluate the differences in binding free enthalpy, thereby obtaining valuable information on the magnitude of individual intermolecular interactions.

We found for a series of inhibitors of thrombin (such as the one shown in Figure 3, Section 1) that measured changes in binding free enthalpy can be directly correlated with the bonding contributions of individual substituents of the inhibitors.<sup>[5]</sup> Thus, similar binding affinities were obtained for the benzyl- and cyclohexylmethyl-substituted inhibitors **13** (inhibition constant  $K_i = 220$  nM) and **14** ( $K_i = 350$  nM) that adopt an edge-to-face geometry with respect to Trp215 in the D pocket of the enzyme active site (Figure 3).<sup>[138]</sup> This result suggests, in agreement with the studies of Wilcox and co-workers, that specific electrostatic C–H/ $\pi$  interactions need



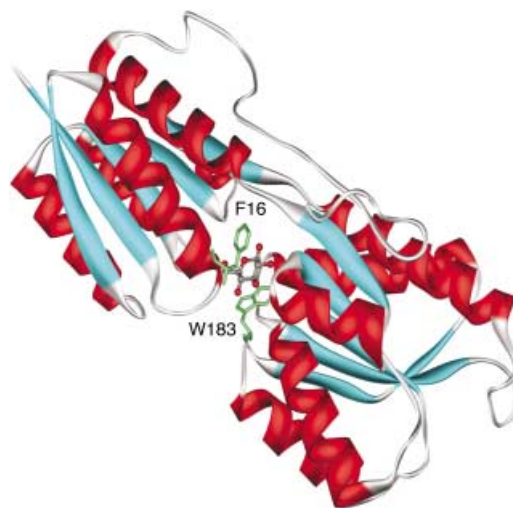
not be invoked. Model investigations by Turk and Smithrud also came to the conclusion that aliphatic–aromatic and aromatic–aromatic edge-to-face contacts provide similar energetic stabilization.<sup>[139]</sup>

Clearly, there remains some controversy with respect to the directional, electrostatic component of the edge-to-face interactions, which have been identified in a variety of X-ray crystal structures of other protein–inhibitor complexes.<sup>[140]</sup> We presume that a substantial electrostatic component of the interaction, in addition to the dominating dispersion term, only exists if the partial positive charge on the interacting edge H atoms is substantially enhanced by strong electron-withdrawing *ortho*- and/or *para* substituents, which the aromatic amino acid side chains are lacking.

#### 4.3.3. The C–H/ $\pi$ Interaction

Although the attraction between arenes, alkenes, or alkynes with hydrocarbons (the C–H/ $\pi$  interaction) is not an interaction between aromatic rings, it should be briefly discussed here, in view of its similarity to the edge-to-face aromatic interaction. The C–H/ $\pi$  interaction, while considerably weaker than classical H bonding, also plays notable structure-determining and structure-stabilizing roles throughout chemistry and biology.<sup>[141,142]</sup> High-level ab initio calculations of benzene–hydrocarbon complexes give interaction energies ( $D_c$ ) of  $-1.82$ ,  $-2.06$ , and  $-2.83$  kcal mol<sup>-1</sup> for the ethane, ethylene, and acetylene complexes, respectively, with benzene.<sup>[143]</sup> An increase in the electrostatic contribution upon changing from ethane ( $-0.17$  kcal mol<sup>-1</sup>) to acetylene ( $-2.01$  kcal mol<sup>-1</sup>) clearly reflects the differences in the hybridization state and the acidity of the C–H residue participating in the binding.<sup>[143]</sup> Even for alkanes, the orientation of the C–H bond toward the ring center is controlled to some extent by the relatively weak, but directional electrostatic interaction; however, the dispersion term provides the major source of attraction in all the complexes.

We limit our discussion of C–H/ $\pi$  interactions to a few examples since the field is comprehensively and continuously overviewed by Nishio et al., who published a pertinent monograph on the subject and provide a constantly updated reference list on the internet.<sup>[144,145]</sup> The C–H residues of sugars have been shown in many X-ray crystal structures of protein complexes to undergo interactions with aromatic amino acid side chains. A beautiful example of C–H/ $\pi$  interactions in biology is provided by the complex of the D-galactose/D-glucose binding protein with  $\beta$ -D-glucose, in which the aromatic side chains of Trp 183 (on the  $\beta$  face) and Phe 16 (on the  $\alpha$  face) sandwich the hexose ring at van der Waals distance (Figure 11).<sup>[146]</sup> The sugar C–H residues have a



**Figure 11.** Complexation of  $\beta$ -D-glucose by the D-galactose/D-glucose binding protein (PDB code: 2GBP).<sup>[146]</sup>

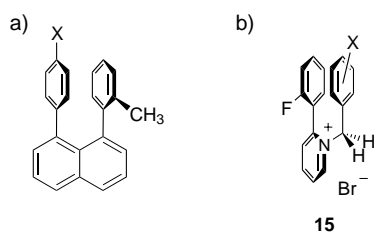
significant partial positive charge on their H atoms as a consequence of an inductive effect provided by the neighboring O and OH groups which should enhance their interactions with the aromatic rings.

As a second example for the ubiquitous C–H/ $\pi$  interactions, we refer to the close contacts ( $3.3$ – $4.1$  Å) established by the isopropyl group of our thrombin inhibitor with the aromatic rings of Tyr 60A and Trp 60D in the narrow P pocket of the enzyme (Figure 3).<sup>[5]</sup>

#### 4.3.4. Stacking Interactions

The other important arrangement of aromatic rings, besides the edge-to-face contact, is the parallel alignment. It is well known that two aromatic partners, one bearing strong electron-donor and the other strong electron-acceptor groups, form parallel stacking complexes in solution and often in the solid state, with the geometry largely determined by molecular orbital interactions (charge-transfer complexes). On the other hand, few chemical model systems have been designed to evaluate the optimum orientation, the role of substitution, and the underlying forces in the attraction of aromatic rings which do not differ greatly in their ionization potential (and electron affinity).

The forced face-to-face arrangement in 1,8-diarylnaphthalenes has offered the possibility to investigate the stacking interactions of substituted aromatic rings (Figure 12a). <sup>1</sup>H NMR measurements by Cozzi and Siegel of the barrier to rotation about the aryl–naphthyl bond in (CD<sub>3</sub>)<sub>2</sub>SO demonstrated there was a linear relationship between the barrier of rotation  $\Delta G^\ddagger$  and the Hammett parameter  $\sigma_{para}$ .<sup>[147]</sup> The barrier to rotation depends on the strength of the parallel-stacked interaction in the ground state, which is much larger when the substituent X is electron withdrawing ( $X = \text{NO}_2$ :  $\Delta G^\ddagger = 17.3$  kcal mol<sup>-1</sup>) than if X is electron donating ( $X = \text{MeO}$ :  $\Delta G^\ddagger = 13.9$  kcal mol<sup>-1</sup>). This finding that electron-deficient rings prefer stacking interactions over electron-rich ones is in agreement with the electrostatic model by



**Figure 12.** Dynamic  $^1\text{H}$  NMR investigations of 1,8-diarylnaphthalenes (a)<sup>[147]</sup> and pyridinium bromide **15** (b)<sup>[149]</sup> have provided evidence for polar effects in aromatic stacking interactions.

Hunter and Sanders.<sup>[129]</sup> The term “polar/ $\pi$ ” interaction was introduced to emphasize the importance of the electrostatic term in  $\pi$  stacking and the fact that the aromatic ring with the substituent X possesses a distinctly polar character. This support for the relevance of polar, electrostatic effects in  $\pi$ - $\pi$  stacking is in good agreement with the semiempirical AM1 study of the conformational equilibria performed on *cis*-1,3-diphenylcyclohexanes.<sup>[148]</sup>

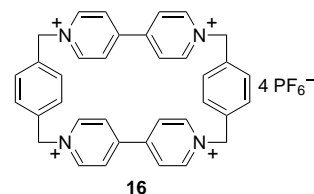
$^1\text{H}$  NMR spectroscopic measurements in water were carried out by Rashkin and Waters to determine the barriers to rotation about the biaryl bond in pyridinium bromides **15** (Figure 12 b) which, according to ab initio geometry optimization studies, features an offset stacking arrangement between the fluorinated phenyl and the benzyl ring.<sup>[149]</sup> In agreement with the results obtained by Siegel and co-workers, they found a rise in the barrier of rotation when the *para* substituent X in the benzyl ring was changed from electron donating (Me) to electron accepting ( $\text{NO}_2$ ). This effect was even more pronounced when the nitro group was in the *meta* position; the authors explained this effect by interannular electrostatic attraction between the nitro group and H atoms of the fluorinated phenyl ring.

It is often possible to rationalize stacking interactions by considering the quadrupole moments of the aromatic partners, or alternatively through visualization of the molecular electrostatic potentials (MEPs). Examples are anthracene-dinitrobenzene conjugates with flexible spacers (which prefer to adopt U-shaped conformations),<sup>[150]</sup> stacks formed by fluoroaromatic compounds (Section 7), and multichromophoric oligomers which fold into a pleated structure in water as a result of interactions between alternating electron-rich (1,5-dialkoxynaphthalene) and electron-poor (1,4,5,8-naphthalenetetracarboxylic diimide) moieties.<sup>[151]</sup> Although the latter system exhibits a strong charge-transfer band, the driving forces for formation of such “charge-transfer complexes” are mainly dispersion and dipolar interactions as well as—in water—hydrophobic effects. Charge transfer contributes very little to ground-state stabilization, but is very effective in the excited state.

#### 4.3.5. Aromatic Interactions Involving Heteroaromatic Compounds

The tetracationic cyclophane **16** is one of the most versatile hosts known for the inclusion complexation of electron-rich aromatic rings (such as dialkoxy-substituted

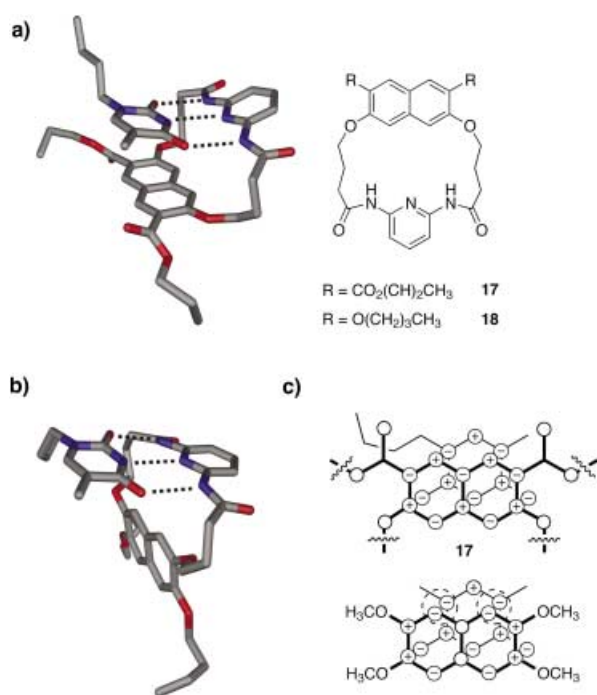
benzene and naphthalene derivatives or tetrathiafulvalene (TTF))<sup>[152]</sup> and has been used by Stoddart and co-workers as a fundamental component in the construction of a large diversity of catenanes and rotaxanes. This work has already been comprehensively reviewed.<sup>[153]</sup> The encapsulated  $\pi$  donors undergo both  $\pi$ - $\pi$  stacking with the two sandwiching bipyridinium rings in **16**—which includes a cation- $\pi$  interaction component (Section 6)—as well as edge-to-face interactions with the *p*-xylylene bridges.<sup>[154]</sup>



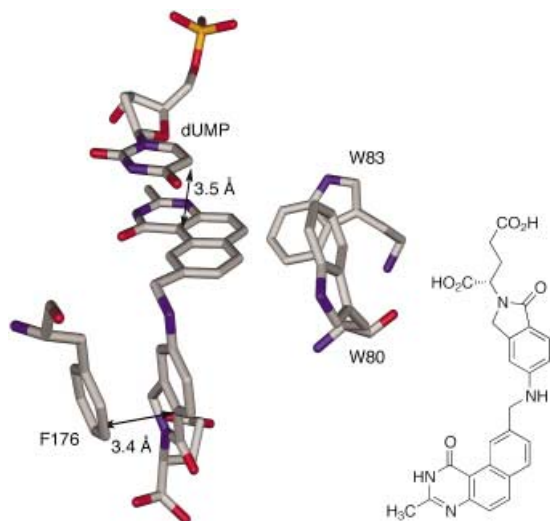
The introduction of heteroatoms into aromatic rings has a significant influence on the  $\pi$ - $\pi$  interaction. Electrostatic attraction between atoms with positive or negative partial charges<sup>[155]</sup> and the alignment of molecular dipoles become important in determining how two or more heterocyclic  $\pi$  systems interact. This has been nicely illustrated in molecular-recognition studies with the 1-butylthymine receptors **17** and **18** by Hamilton and co-workers.<sup>[156]</sup> Whereas **17** forms a solid-state complex in which thymine undergoes  $\pi$  stacking with the naphthalene ring of the host, an edge-to-face orientation is found in the complex of **18**, with the naphthalene ring adopting an orthogonal orientation with respect to the host-guest H-bonding array (Figure 13). The geometrical preferences are best explained by considering the distribution of the electronic charge on the atoms of the thymine guest and the naphthalene moiety of the host. In the stacking geometry seen with **17**, atom centers of opposite partial charges face each other, which provides a favorable electrostatic stabilization of the complex. On the other hand, a stacking complex of **18** would place centers of the same (+ or -) charge opposite each other, which would destabilize the association. The edge-to-face geometry is, therefore, adopted in the complex to avoid this electrostatic repulsion.

Since attractive electrostatic interactions between atoms of opposite partial charges often overcome the repulsion between closed-shell  $\pi$  clouds,  $\pi$ - $\pi$ -stacking interactions are abundant between heterocyclic  $\pi$  systems. In addition, the orientations of the molecular dipoles between the interacting chromophores may play a prominent role in determining the orientation of stacking heterocycles, as shown by Rotello and co-workers for flavin-substrate recognition in chemical model systems.<sup>[157]</sup> A nice example of heterocyclic  $\pi$  stacking is provided by the ternary complex of the anticancer drug 1843U89 and dUMP formed at the active site of thymidylate synthase (Figure 14).<sup>[158]</sup>

Many other receptors have been designed for complexation by  $\pi$ - $\pi$  stacking of nucleobases and related heteroaromatic systems.<sup>[159]</sup> Moreover, supramolecular architectures, such as helices, have been constructed through stacking interactions; the reader is referred to the pertinent literature references.<sup>[160]</sup>



**Figure 13.** X-ray crystal structures of the complexes formed by receptors **17** (CSD code: VABVID; a) and **18** (CSD code: VABVO); b) with 1-butylthymine.<sup>[156]</sup> c) Consideration of atomic partial charge interactions in the complexes explains the preference for the face-to-face orientation in the complex of **17** as well as why **18** (2,3,6,7-tetramethoxynaphthalene as model for **18** interacting with 1-butylthymine)<sup>[156c]</sup> avoids the stacking geometry.



**Figure 14.** Heterocyclic  $\pi$  stacking between dUMP and the anticancer drug 1843U89 bound at the active site of thymidylate synthase (PDB code: 1TSD).<sup>[158]</sup>

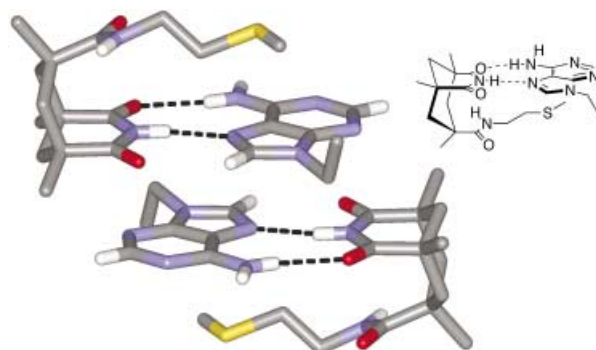
The geometries of DNA duplexes are largely determined by H-bonded nucleobase pairing,<sup>[161a]</sup> offset base stacking at a vertical base distance of 3.4 Å, the conformation of the sugar backbone,<sup>[161b]</sup> the base sequence, the hydrophobic effect, and presumably specific solvation patterns in the minor and major

grooves.<sup>[161c]</sup> The geometries of DNA duplexes have increasingly been subjected to high-level theoretical calculations, and the results have been summarized in a recent review.<sup>[162]</sup> According to these studies, the stacking of nucleic acids in the gas phase is dominated by dispersion forces. A terminal (dangling) base has been reported to contribute up to 1 kcalmol<sup>-1</sup> in stacking energy to the total stability of the DNA duplex in water.<sup>[163]</sup> The main driving force for base stacking in water, be it the hydrophobic effect, polar and dipolar interactions, or dispersion forces, remains a matter of some debate.<sup>[164]</sup>

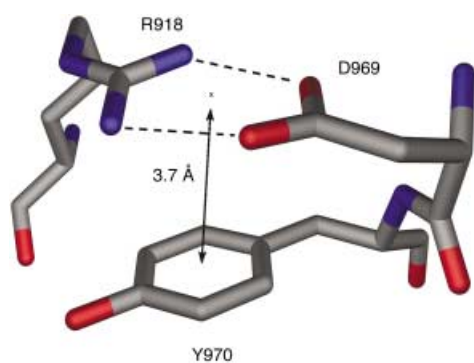
Natural bases in the DNA duplex can be substituted by apolar artificial ones (nucleobase isosteres) that do not undergo Watson–Crick H bonding but fit geometrically and electronically into the stacking base-pair array.<sup>[165]</sup> Furthermore, stacking is the dominant feature of DNA-intercalating agents, such as nogalamycin, 9-aminoacridine, and ethidium bromide.<sup>[166]</sup>

As was already shown in Figure 13 for the complex of 1-butylthymine with the artificial receptor **18**,  $\pi$ - $\pi$  stacking and edge-to-face interactions may also occur between H-bonding arrays and aromatic or heteroaromatic rings.<sup>[156,167,168]</sup> H-bonding arrays such as those between the guanidinium residue of Arg and the carboxylate of Glu or Asp are planar and only require additional solvation within the plane. Perpendicular to this plane they are rather apolar, and their highly polarizable bonds enables them to undergo efficient interactions with aromatic rings. To this end, Castellano et al. provided X-ray structural evidence for  $\pi$  stacking (3.4 Å) between a 9-ethyladenine molecule and the Hoogsteen H-bonding array formed from an imide-type receptor designed by Rebek and co-workers and a second adenine molecule (Figure 15).<sup>[167]</sup>

However, attractive examples can also be found in the crystal structures of proteins. Thus, Figure 16 shows the stacking of Tyr970A parallel to the hydrogen-bonding network formed between the side chains of Arg918A and Asp969A in the furoloyl esterase module of xylanase 10B.<sup>[169]</sup> Related to this topic is the flanking of aromatic rings by carboxylate groups, a positioning that can dramatically influence their pK<sub>a</sub> values,<sup>[170]</sup> facilitate desolvation, and promote the formation of salt bridges (see Section 6).<sup>[171]</sup>



**Figure 15.**  $\pi$  Stacking over a H-bonding network in the solid-state structure of the complex formed by H bonding between a Rebek imide-type receptor and 9-ethyladenine (CCDC-167543).<sup>[167]</sup>



**Figure 16.** Parallel-stacking interaction between Tyr 970A and the H-bonding network between the side chains of Arg 918A and Asp 969A in the feruloyl esterase module of xylanase 10B (PDB code: 1GKK).<sup>[169]</sup>

The implications of  $\pi$ - $\pi$  interactions in chemistry and biology are broad, and we conclude this section by listing a few additional examples. Aromatic-aromatic interactions can play a key role in synthesis (for example, in asymmetric induction),<sup>[172]</sup> in separation science (for example, in chiral chromatography),<sup>[173]</sup> and transition-metal complexation.<sup>[174]</sup>  $\pi$ - $\pi$  Stacking has also recently been shown to be influential in stereoselective epoxidations with *m*-chloroperbenzoic acid;<sup>[175]</sup> in this study, polar/ $\pi$  effects similar to those reported by Siegel and co-workers were observed.

## 5. Hydrogen Bonding to Aromatic $\pi$ Systems

### 5.1. Introductory Remarks

Traditionally, hydrogen bonds have been defined as A-H $\cdots$ B, wherein both the donor A and acceptor B are electronegative atoms, such as N, O, or F. Since there is no strictly defined cut-off for an atom's ability to participate in hydrogen bonding, this concept has been extended to weaker donor atoms such as carbon (in all three hybridization states) or unusual acceptors such as  $\pi$  systems.<sup>[74,176]</sup> Commonly encountered hydrogen-bond energies calculated for gas-phase complexes  $-0.5$ – $1.5$  kcal mol<sup>-1</sup> for neutral C-H/ $\pi$  interactions to greater than  $-10$  kcal mol<sup>-1</sup> for the strongest ionic H bonds such as O-H $\cdots$ O<sup>-</sup> ( $-23$  kcal mol<sup>-1</sup>) or F-H $\cdots$ F<sup>-</sup> ( $-39$  kcal mol<sup>-1</sup>).<sup>[74]</sup> As a comparison, the widely occurring N-H $\cdots$ O (for example, in proteins) and O-H $\cdots$ O hydrogen bonds (for example, in the water dimer) are considered to be of intermediate strength, that is, about  $-5$ – $7$  kcal mol<sup>-1</sup>.<sup>[177,178]</sup> The contribution of a hydrogen bond can be reduced dramatically in solution or the solid state because of entropic effects, solvation, or dielectric conditions imposed by the environment.<sup>[179]</sup>

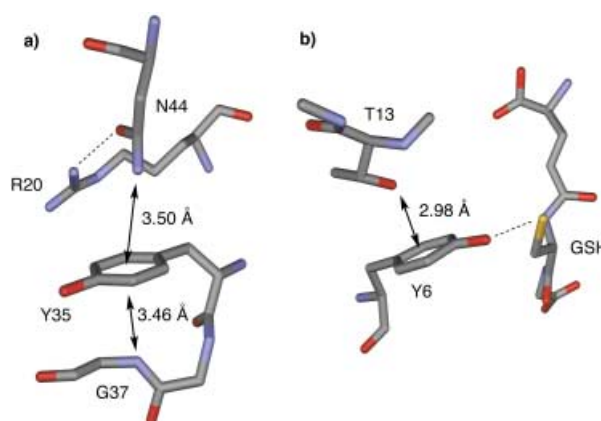
The energetically attractive contacts involving hydrogen-bond donors and aromatic rings are called  $\pi$ -hydrogen bonds; they are several kcal mol<sup>-1</sup> weaker than classical H bonds. The often observed contraction of the A-H bond in these arrangements is opposite to what is observed for classical H bonds, where the H-bond strength is proportional to the elongation of the A-H bond. This contraction leads to a shift

of the A-H stretch to higher frequency in the IR spectrum, and the bonds displaying this feature have been described as anti-hydrogen bonds, and more recently, blue-shifting hydrogen bonds.<sup>[180]</sup>

### 5.2. Biological Aspects

Each amino acid has a potential N-H hydrogen-bond donor in its backbone, and several possess additional donor centers in their side chains (for example, Lys, Arg, Asn, Gln, His), thus making N-H/ $\pi$  contacts statistically probable. One of the earliest examples of an N-H/ $\pi$  interaction was seen by Perutz et al. in the X-ray crystallographic study of the interaction of hemoglobin with the drug bezafibrate. In this association an asparagine side chain N-H residue points into the center of the *p*-chlorobenzamide ring of the drug.<sup>[181]</sup> Many other examples of X-H/ $\pi$  contacts (X=N, O, S) occurring at a mean distance of X to centroid of the aromatic ring of 3.2–3.8 Å can be found in proteins.<sup>[182]</sup> Peptides have also been used as model systems to investigate the effect of N-H/ $\pi$  interactions on the secondary structure of proteins.<sup>[183]</sup> In this context, the crystal structure of bovine pancreatic trypsin inhibitor (BPTI) has been solved and shown to display a backbone N-H/ $\pi$  interaction between Gly37 and Tyr35 with an N $\cdots$ ring centroid distance of 3.5 Å. The other face of the tyrosine ring interacts with the side chain NH<sub>2</sub> group of Asn44 at a distance of 3.5 Å (Figure 17 a).<sup>[184]</sup>

A rare example of O-H/ $\pi$  hydrogen bonding in proteins is provided by the complex of the enzyme glutathione transferase with glutathione (GSH), in which the side chain of Thr13 is arranged face-on to the aromatic face of Tyr6 (Figure 17b).<sup>[185]</sup> This interaction decreases the p*K*<sub>a</sub> value of the Tyr HO group and strengthens its hydrogen-bonding capacity to the HS group of GSH, thereby influencing the reactivity of the latter.<sup>[186]</sup> The occurrence of O-H/ $\pi$  and N-H/ $\pi$  interactions in proteins has been investigated in detail through several PDB searches.<sup>[187–191]</sup> Mitchell et al. showed that there is a preference for sp<sup>2</sup>-hybridized nitrogen atoms to be located above aromatic rings.<sup>[188]</sup> In this case, parallel



**Figure 17.** a) N-H/ $\pi$  interaction in the bovine pancreatic trypsin inhibitor (PDB code: 4PTI)<sup>[184]</sup> and b) O-H/ $\pi$  interaction in the complex of glutathione transferase with glutathione (GSH; PDB code: 6GST).<sup>[185]</sup>



stacking of N–H bonds is favored relative to the T-shaped arrangement. Recently, Steiner and Koellner performed a comprehensive structural analysis of X–H/ $\pi$  hydrogen bonding in a set of 592 high-resolution protein crystal structures.<sup>[182]</sup> They found that about 1 out of 11 aromatic amino acids acts as a  $\pi$  acceptor for H bonding with O–H, N–H, and S–H donors, with the best aromatic acceptor being Trp. This relatively high frequency, although small compared to classical hydrogen bonds, supports the postulated role that these contacts play in stabilizing the secondary structures of proteins.<sup>[192]</sup>

O–H/ $\pi$  contacts are observed in protein–water interactions and, if attractive, they contribute to the hydration energy.<sup>[193]</sup> Furthermore, water molecules interacting with the aromatic rings of Phe, Trp, and Tyr inside hydrophobic cavities may make significant contributions to stabilizing the local protein structure.<sup>[194]</sup> In this context, water molecules have been shown to fill and be conducted through carbon nanotubes (CNTs).<sup>[195]</sup> On the other hand, statistical analyses of protein structures show that water molecules are generally found at the edges of aromatic rings when a C–H $\cdots$ O interaction with the  $\delta^+$  polarized hydrogen atoms occurs.<sup>[196]</sup> This arrangement is also preferentially found for all types of oxygen atoms in amino acids.<sup>[189]</sup>

### 5.3. Physical and Theoretical Aspects

Complexes between benzene and H-bonding partners have been the subject of numerous theoretical and experimental investigations.<sup>[178]</sup> In particular, the solvation of benzene has attracted considerable attention.<sup>[197]</sup> We refer here to recent ab initio studies from Tsuzuki et al.,<sup>[198]</sup> although we are well aware that other notable contributions have been published on this subject. The stabilization enthalpy for monodentate H bonding of water to the  $\pi$  system of benzene (Figure 18a) has been calculated by high-level CCSD(T) calculations to give  $D_0 = -2.0$  kcal mol<sup>-1</sup> (O $\cdots$ centroid distance = 3.4 Å),<sup>[198]</sup> which agrees nicely with the experimental value ( $D_0 = -2.44 \pm 0.09$  kcal mol<sup>-1</sup>).<sup>[199]</sup>

The calculated potential well is extremely flat over the aromatic surface, which makes benzene an excellent target as a hydrogen-bond acceptor.<sup>[200]</sup> The attractive character of the water–benzene interaction could explain the higher solubility of aromatic hydrocarbons in water relative to alkanes,<sup>[201]</sup> as

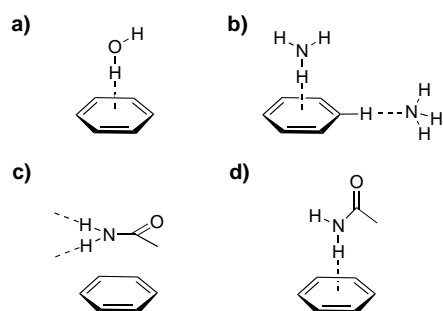
reflected by the  $\lg(P_{ow})$  values (the partition coefficients  $P$  between octanol and water) for benzene and cyclohexane (2.13 and 3.44, respectively).<sup>[202]</sup>

Another model system of H bonding to aromatic rings in proteins is the complex formed between benzene and ammonia.<sup>[203]</sup> This H-bond donor interacts more weakly with aromatic rings, a fact rationalized by the lower electronegativity of nitrogen relative to oxygen.<sup>[203]</sup> The stabilization enthalpy for H bonding to the  $\pi$  system of benzene (Figure 18b) was determined experimentally in the gas phase to be  $D_0 = -1.84 \pm 0.12$  kcal mol<sup>-1</sup>,<sup>[204]</sup> which is similar to the value derived from CCSD(T) calculations ( $D_0 = -1.61$  kcal mol<sup>-1</sup>,  $d(\text{N}\cdots\text{centroid}) = 3.6$  Å).<sup>[198,205]</sup> Only slightly lower  $D_0$  values, however, were calculated for the edge binding through a C–H $\cdots$ N contact (Figure 18b). Of course, ammonia is only a limited model for the side chain of Lys, which under physiological conditions is mostly protonated and, therefore, participates more frequently in cation– $\pi$  interactions (Section 6). Hydrogen bonding between the  $\pi$  systems of aromatic compounds and thiols has been very recently probed by ab initio calculations and protein database analyses (interactions between divalent sulfur and aromatic rings are described in Section 8).<sup>[206]</sup> High-level ab initio calculations have shown this contact can achieve a stabilization enthalpy of  $-2.6$  kcal mol<sup>-1</sup>, and is thus stronger than the corresponding hydrogen bonds formed by amino or hydroxy groups. It should be noted, however, that out of 609 studied X-ray crystal structures of proteins, only 4 Cys residues (among the 2542 Cys residues, 1860 form disulfide bonds) were found in hydrogen-bonding arrangements with Phe.

H bonds are composed of electrostatic (ES), dispersive, charge-transfer, exchange-repulsion (EX), and polarization terms. The ES and EX terms account for more than 80% of the interaction energy in classical, moderate H bonds.<sup>[72]</sup> Separation of the binding energies into individual terms for the X–H/ $\pi$  contacts gives insight into the observed differences in interaction when X is varied. Thus, there is an increase in the electrostatic term from X = C, to N, and to O, as expected from atom electronegativity, while the dispersive and repulsive terms remain essentially constant across the series.<sup>[198]</sup>

Searches for X–H/ $\pi$ (phenyl) contacts in the CSD have revealed that the optimum T-shaped geometry, where the H atom points into the centroid of the aromatic ring, is rarely adopted and that the preferred geometry instead involves direct interaction of the X–H group with the carbon atoms of the ring.<sup>[207]</sup> In general, X–H/ $\pi$  hydrogen bonds are rather uncommon in biology, although they have been recognized for many years.<sup>[208]</sup>

MP2 calculations of the benzene–formamide complex have been performed to better model the aromatic–amide–(backbone) interaction found in proteins. They revealed a significant stabilization energy ( $-4.0$  kcal mol<sup>-1</sup>),<sup>[209]</sup> with two energetically similar conformations of the complex—the parallel stacking (Figure 18c) and the perpendicular, T-shaped geometry with the N–H/ $\pi$  contact (Figure 18d).<sup>[210]</sup> The pyrrole dimer displays, similar to its benzene counterpart, a T-shaped structure wherein the N–H bond is directed into the  $\pi$  system of a neighboring ring.<sup>[211]</sup>

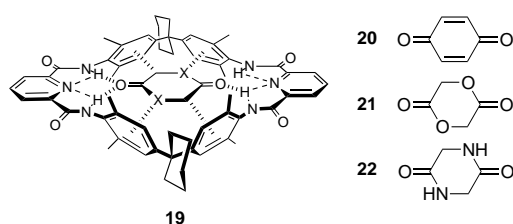


**Figure 18.** a) Preferred interactions of benzene with water (a), ammonia (b), and amides (c, d).

The origin of the chaotropic effect of the urea and guanidinium ions has been studied by Monte Carlo simulations in water and in the gas phase by Jorgensen and co-workers. Their results indicate that the interaction of these species with aromatic rings, which may involve both  $\pi$  stacking and T-shaped geometries, likely promotes protein denaturation.<sup>[212]</sup>

#### 5.4. Studies with Synthetic Receptors

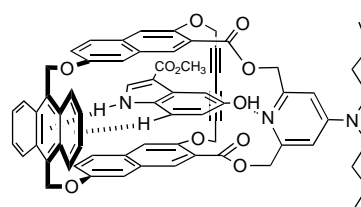
In contrast to aromatic  $\pi$ - $\pi$  interactions, hydrogen bonding to  $\pi$  systems has not been extensively investigated in supramolecular chemistry. Hunter and co-workers investigated the inclusion complexation of six-membered ring dicarbonyl compounds by cyclophane **19** (Figure 19).<sup>[213]</sup> <sup>1</sup>H NMR titrations in CDCl<sub>3</sub> provided the association con-



**Figure 19.** Inclusion complexation of cyclic 1,4-dicarbonyls by the macrocyclic tetramide receptor **19**. The complex formed by diamide **22** is additionally stabilized by N–H/ $\pi$  interactions.<sup>[213, 214]</sup>

stants  $K_a$  for the 1:1 complexes of **19** with **20** ( $2.3 \pm 0.4 \times 10^2 \text{ M}^{-1}$ ), **21** ( $3.4 \pm 0.6 \times 10^2 \text{ M}^{-1}$ ), and **22** ( $1.0 \pm 0.5 \times 10^6 \text{ M}^{-1}$ ). While all three complexes are stabilized by H bonding between the two C=O groups of the guests to the four amide N–H residues of the host, the complex of diamide **22** finds extra stabilization through favorable N–H/ $\pi$  contacts (Figure 19). Indeed, the X-ray crystal structure of the **19**–**22** complex was later determined and showed clearly that the amide N–H groups of **22** are pointing directly into aromatic rings of the receptor.<sup>[214]</sup> The complexation of **22** was sufficiently strong that it was even observed in water ( $70 \text{ M}^{-1}$ ). From chemical double mutant cycles, Hunter and co-workers estimated the Gibbs free energy contribution of individual N–H/ $\pi$  interactions as  $\Delta\Delta G = -1.1 \pm 0.1 \text{ kcal mol}^{-1}$ ,<sup>[215]</sup> a higher value than deduced for C–H/ $\pi$  interactions ( $0.35 \text{ kcal} \pm 0.2 \text{ mol}^{-1}$ ) in similar experiments (see Section 4.3.2). This result reflects the higher acidity of the N–H donor (pyrrole in this case) relative to C–H.

Another example for N–H/ $\pi$  interactions in a supramolecular complex has been provided by Cloninger and Whitlock<sup>[216]</sup> who prepared the complex of a serotonin mimic (methyl 5-hydroxy-3-indolecarboxylate) with a macrobicyclic cyclophane receptor ( $K_a = 4840 \pm 1280 \text{ M}^{-1}$ , CDCl<sub>3</sub>, 298 K; Figure 20). The very large complexation-induced downfield shift of the NH proton of the guest ( $\Delta\delta = 5.46 \text{ ppm}$ ) observed in the <sup>1</sup>H NMR spectrum strongly supports the proposed T-shaped N–H/ $\pi$  interaction geometry.



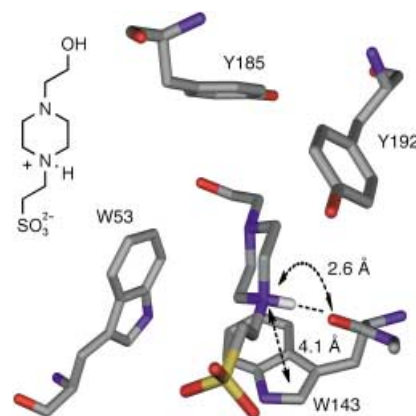
**Figure 20.** N–H/ $\pi$  interaction in the complex formed between a macrobicyclic cyclophane receptor with a serotonin mimic.<sup>[216]</sup>

## 6. Cation– $\pi$ Interactions

### 6.1. Introductory Remarks

The cation– $\pi$  interaction between a protonated HEPES buffer molecule (*N*-2-hydroxyethylpiperazine-*N'*-2-ethanesulfonic acid) and Trp in the acetylcholine (ACh) binding site of an ACh binding protein (Figure 21)<sup>[217]</sup> more than suggests these contacts to be important contributors to the structure and function of biomolecules.<sup>[7, 218, 219]</sup> This study represents a perceptible advance from the earliest structural studies that elucidated the “amino–arene” interaction between positively polarized N–H groups and aromatic amino acid side chains in proteins.<sup>[181, 190, 220]</sup> The protonated tertiary ammonium center is snugly located in a “box” of four aromatic residues where it comes into contact with Trp143 (4.1 Å) and makes cation– $\pi$  interactions, as shown for a variety of nicotinic ACh receptor agonists.<sup>[221–223]</sup>

While these and other discoveries in structural biology<sup>[218, 224]</sup> continue to inspire research on the cation– $\pi$  interactions, early solution studies with chemical systems in the Dougherty research group were responsible for defining its energetic features and establishing the interaction as a general one among the well-known noncovalent forces.<sup>[7]</sup> The use of elaborate mass-spectrometric techniques, computational protocols, and the possibility to routinely manipulate biological systems has enabled our ability to dissect this and other weak, noncovalent binding forces to burgeon in the past few years.



**Figure 21.** Cation/ $\pi$  interactions between a HEPES molecule and Trp143 in the ACh binding site of an ACh-binding protein.<sup>[217]</sup> Most H atoms have been omitted for clarity (PDB code: 119B).


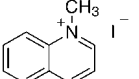
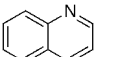
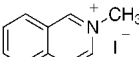
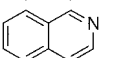
The key review of Ma and Dougherty<sup>[7]</sup> outlines the essential features of the cation- $\pi$  interactions (namely, its structure and energetics, applications, and biological implications). Subsequent accounts have since appeared which focus on its consequences in structural biology,<sup>[218]</sup> contribution to ligand structure and catalysis,<sup>[224]</sup> theoretical investigations,<sup>[178]</sup> and applications in host-guest chemistry.<sup>[225-230]</sup> We have chosen to limit our discussion to recent contributions that describe the energetic features of the cation- $\pi$  interaction; emphasis will be placed on experimental studies using synthetic receptors and biological macromolecules, although essential contributions of gas-phase, solid-state, and theoretical investigations will also be highlighted.

## 6.2. Cation- $\pi$ Interactions with Ammonium and Iminium Ions

### 6.2.1. Energetic Aspects of Host-Guest Chemistry

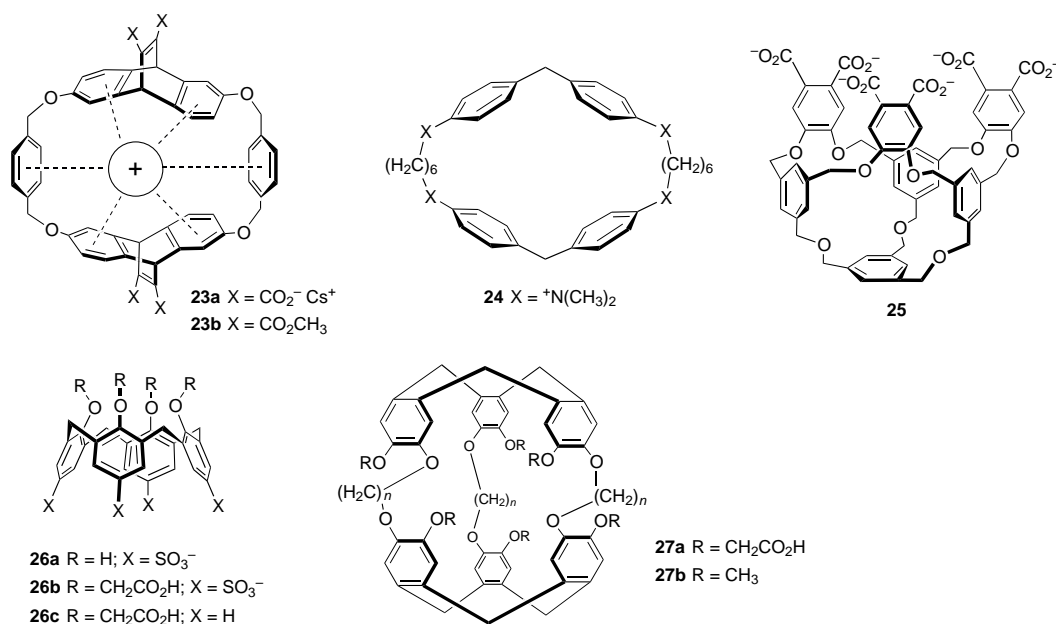
Dougherty and co-workers found that the anionic cyclophane **23a** (Figure 22) is a better receptor for quaternary ammonium and iminium ions in aqueous borate buffer (pD 9) than for the corresponding neutral molecules.<sup>[7,231]</sup> Thus, the complex of **23a** with methylquinolinium is 2.2 kcal mol<sup>-1</sup> more stable than with neutral quinoline (Table 4), even though the cationic guest is better solvated than its neutral counterpart by 46.5 kcal mol<sup>-1</sup>.<sup>[7,232]</sup> Host **23a** also complexes the neurotransmitter ACh with  $K_a = 20000 \text{ M}^{-1}$  ( $\Delta G = -5.8 \text{ kcal mol}^{-1}$ ). This result prompted the researchers to postulate a similar motif—an aromatic binding site instead of an environment rich in anionic carboxylate or phosphate groups—for the binding of ACh by acetylcholine esterase. The X-ray crystal structure of the enzyme from the Pacific electric ray, *Torpedo Californica*, indeed revealed an onium binding site. The modeling of ACh complexation with this site suggested that its quaternary ammonium ion does not interact

**Table 4:** Free enthalpy of complexation  $\Delta G^\circ$  for the 1:1 complexes of **23a** in aqueous deuterated borate buffer (pD = 9) and **23b** in  $\text{CDCl}_3$  ( $T = 295 \text{ K}$ ).<sup>[231]</sup>

Guest	<b>23a</b> $-\Delta G^\circ$ [kcal mol <sup>-1</sup> ]	<b>23b</b> $-\Delta G^\circ$ [kcal mol <sup>-1</sup> ]
	6.7	2.1
	7.6	3.5
	5.4	0.0
	7.2	2.5
	6.3	0.2

with a negatively charged “anionic site” but rather with some of the 14 aromatic residues that line the active site.<sup>[233]</sup>

The earliest investigations by Ma and Dougherty established the currently accepted “electrostatic model” of the cation/ $\pi$  interaction, namely, the electrostatic attraction between a cation and the permanent quadrupole moment associated with the  $\pi$  system.<sup>[7]</sup> Replacement of the two *p*-phenylene linkers of **23a** with cyclohexane-1,4-diyl groups indeed reduces its binding to quaternary ammonium guests. However, the contributions of the positively polarized C-H bonds of the onium ion that interact with the negatively polarized  $\pi$  systems should not be ignored (Section 5);<sup>[234]</sup> in effect, solvation of the positively charged onium ion by the aromatic rings of the host in terms of C-H/ $\pi$  interactions.



**Figure 22.** Various hosts employed in the study of cation- $\pi$  interactions.

Binding studies with tetrazoniacyclophane **24** in water by Schneider et al.<sup>[235,236]</sup> (Figure 22) as well as with other model systems<sup>[237–239]</sup> reinforced these observations. Linear free energy relationships showed that the binding free enthalpy is proportional to the number of aromatic rings surrounding a cationic center and that the gain in free energy can be as high as 0.5 kcal mol<sup>-1</sup> per ring. Additional early studies with host–guest systems in aqueous solution, including the cyclophane receptors **25–27**,<sup>[240–245]</sup> have produced the most efficient receptors for onium ions to date. Moreover, these studies demonstrated that multiple cation– $\pi$  interactions, particularly those involving hosts with electron-rich concave aromatic binding surfaces<sup>[126,246]</sup> (see Section 4.3.1), are capable of overcoming the desolvation penalty associated with binding various cations or ion pairs (see below) in aqueous media.<sup>[247]</sup> These investigations have been extensively reviewed.<sup>[7,225,226]</sup>

While studies of many receptor systems have since been extended to the gas phase<sup>[248]</sup> and the solid state,<sup>[249]</sup> the bulk of our knowledge concerning the energetics of cation– $\pi$  interactions continues to come from solution-phase investigations. Recent calorimetric studies show the binding of quaternary ammonium ions by calixarene hosts to be enthalpy driven ( $\Delta H^\circ < 0$ ) and entropy opposed ( $\Delta S^\circ < 0$ ).<sup>[250,251]</sup> The data reported for hosts **26b** and **26c** (Table 5)

**Table 5:** Thermodynamic parameters describing the complexation of tetramethylammonium (TMA) and *N,N,N*-trimethylanilinium (TMAN) ions (as their chloride salts) by calixarenes **26b** and **26c** in water (pH 7,  $T = 298$  K).<sup>[a]</sup>

Host	Guest	$\log K_a$	$\Delta C_{298K}^\circ$ [kcal mol <sup>-1</sup> ]	$\Delta H_{293K}^\circ$ [kcal mol <sup>-1</sup> ]	$T\Delta S_{293K}^\circ$ [kcal mol <sup>-1</sup> ]
<b>26b</b>	TMA	3.5(1)	-4.8(1)	-5.8(3)	-0.9(3)
<b>26c</b>	TMA	2.1(1)	-2.1(1)	-5.2(3)	-2.4(3)
<b>26c</b>	TMAN	2.2	-3.0	-4.9	-1.9

[a] Standard deviation  $\sigma$  in parentheses; for further details, see ref. [251].

binding tetramethylammonium (TMA) and *N,N,N*-trimethylanilinium (TMAN) ions reveal that the entropies of complexation ( $T\Delta S^\circ$ ) are slightly less unfavorable than for complexation processes involving neutral guest molecules in water (see Section 2, Table 1). This result can be rationalized by a more favorable desolvation entropy for ammonium guests relative to their neutral counterparts (that is,  $(\text{CH}_3)_4\text{N}^+$  versus  $(\text{CH}_3)_4\text{C}$ ).<sup>[252]</sup> Additionally, several binding studies have shown that the sulfonate substituents present on host **26b** serve to further desolvate the cationic guest relative to neutral host **26c** ( $\Delta(T\Delta S^\circ) = -1.5$  kcal mol<sup>-1</sup>, Table 5).<sup>[253,254]</sup>

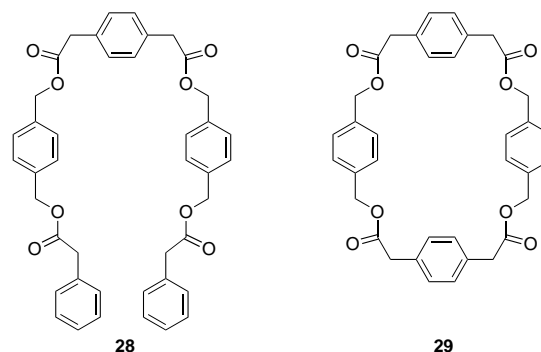
Recent investigations have employed cation– $\pi$  interactions in the recognition of a plethora of biologically important cations in aqueous solution. Phosphonate-based amino acid receptors of Schrader and co-workers combine ion-pairing interactions with cation– $\pi$  contacts to efficiently bind amino acids (for example, Lys, His, and Arg),<sup>[255]</sup> adrenaline,<sup>[256]</sup> and small peptides (for example, the RGD sequence).<sup>[257]</sup> Likewise, the molecular clips of Klärner, Schrader, and co-workers are efficient binders of *N*-alkylpyridinium salts ( $-\Delta G = 4.9$ – $5.5$  kcal mol<sup>-1</sup>), including the sizeable  $\text{NAD}^+$  ion, in aqueous solution.<sup>[258,259]</sup> These hydrophobic binding events are driven

by cation– $\pi$  interactions and not formation of a salt bridge, which lends further support to the importance of such contacts for the stabilization of protein structures and substrate recognition in biology.

While water is often considered the most “biorelevant” medium for investigating cation– $\pi$  interactions, measurement of the intrinsic binding affinity between a cation and a  $\pi$  surface is problematic in aqueous solution where competing effects are of some concern.<sup>[253]</sup> These include significantly different solvation properties of the host and guest, the hydrophobic effect, and may include electrostatic interactions between the cation and a negatively charged host (although this has generally been ruled out through control experiments). Dougherty and co-workers were the first to demonstrate that although the driving forces for apolar complexation (dispersion and desolvation) are too weak in organic solvents such as  $\text{CDCl}_3$  to ensure binding of neutral guests, cation– $\pi$  interactions can, and do, induce inclusion complexation of onium ions ( $-\Delta G^\circ = 2$ – $3$  kcal mol<sup>-1</sup>, Table 4). Other work with cryptophanes demonstrated the unprecedented complexation of TMA by **27b** (Figure 22) in  $(\text{CDCl}_2)_2$  with a  $K_a = 225,000 \text{ M}^{-1}$  ( $\Delta G^\circ = -7.4$  kcal mol<sup>-1</sup>),<sup>[244]</sup> a value significantly exceeding the gas-phase  $\Delta G^\circ$  value of  $-3.5$  kcal mol<sup>-1</sup> that describes the interaction of TMA with a single benzene ring.<sup>[260]</sup> The TMA cation clearly prefers solvation by the aromatic rings of host **27b** to the chloroalkane solvent.

Host–guest complexation in organic solutions based on cation– $\pi$  interactions continues to be an active research area, where cyclophanes,<sup>[261–263]</sup> cyclic peptides,<sup>[128,254,264,265]</sup> and molecular clefts<sup>[266]</sup> have been among the most versatile receptor scaffolds employed. Remarkable recent

examples are the acyclic, “open-phane” receptors by Roelens and Torriti, such as **28** (Figure 23) that are capable of binding the picrate salts of TMA and ACh in  $\text{CDCl}_3$  without the facilitation of preorganization.<sup>[253]</sup> The open-chained **28** and cyclic receptor **29** display similar binding free enthalpies for



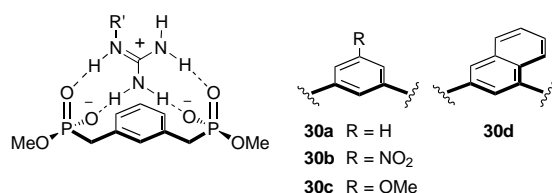
**Figure 23.** The “open” (**28**) and “closed” (**29**) cyclophane receptors of Roelens and Torriti bind quaternary ammonium species equally well in  $\text{CDCl}_3$ .<sup>[253]</sup>

tetramethylammonium picrate ( $\Delta G^\circ = -7.0 \text{ kcal mol}^{-1}$  and  $-7.3 \text{ kcal mol}^{-1}$ , respectively). The results reiterate that loose association is acceptable, if not required, for strong binding of quaternary ammonium species by aromatic hosts (that is, wherein the contact of the cation with the  $\pi$  surface is maximized).<sup>[232]</sup> In other words, the solvation requirements of the onium ion determine the conformation of the host in the complex. Free enthalpy increments for the interaction of TMA and ACh with individual aromatic rings were calculated as  $\Delta\Delta G = -0.46 \text{ kcal mol}^{-1}$  and  $-0.45 \text{ kcal mol}^{-1}$ , respectively, from the additivity principles based on linear free energy relationships.<sup>[238]</sup> These results are in excellent agreement with earlier ones determined by Schneider et al.<sup>[237,238]</sup>

### 6.2.2. Substituent Effects and Electrostatics

Although the electrostatic component does not represent the total binding energy in the cation– $\pi$  interaction (ca. 60% for many arenes<sup>[267,268]</sup>), Dougherty and co-workers have shown that molecular electrostatic potential (MEP) maps of aromatic rings are useful for rationalizing cation– $\pi$  binding trends.<sup>[7,268–270]</sup> Electrostatics and cation-induced polarization taken together can nearly quantitatively rationalize the variance in binding energy in alkali-metal– $\pi$  interactions.<sup>[271,272]</sup> Additionally, while caution is warranted when employing these analyses for ammonium ions, where contributions from dispersive interactions are intensified relative to the “harder” alkali-metal cations,<sup>[178,212,234,267,273–275]</sup> recent solution-phase studies has reinforced the MEP trend. Modulation of the electrostatic potential (ESP) of the central benzene ring in the receptors **30a–c** (Figure 24) from **30a** ( $R = \text{H}$ ) to **30b** ( $R = \text{NO}_2$ ), for example, results in a decrease in binding of guanidinium derivatives in  $\text{Me}_2\text{SO}$  by 0.2–0.3  $\text{kcal mol}^{-1}$ .<sup>[276]</sup> Likewise, the complexation free enthalpy  $-\Delta G$  increases by 0.5–0.6  $\text{kcal mol}^{-1}$  upon changing from **30b** ( $R = \text{NO}_2$ ) to **30c** ( $R = \text{OMe}$ ). Similar substituent trends have been reported in the complexation of ammonium salts by cyclic peptide receptors.<sup>[128]</sup> Incorporation of the naphthalene spacer into **30d** results in a cation affinity equivalent to that exhibited by **30c** (namely, 0.2–0.4  $\text{kcal mol}^{-1}$  greater than the one of **30a**), thus demonstrating the effect of aromatic size (that is, polarizability) on binding. This result is in qualitative agreement with recent *ab initio*<sup>[268]</sup> and DFT<sup>[277]</sup> calculations of  $\text{Na}^+$ /benzene and  $\text{Na}^+$ /naphthalene complexes.

Hunter et al. have employed their chemical double-mutant cycles (see Section 4) for the investigation of cation– $\pi$  interactions between pyridinium cations and substituted phenyl rings in chloroform.<sup>[278]</sup> Again, a clear dependence of



**Figure 24.** Substituent effects and the size of the aromatic platform modulate the cation-binding ability of synthetic guanidinium receptors.<sup>[276]</sup>

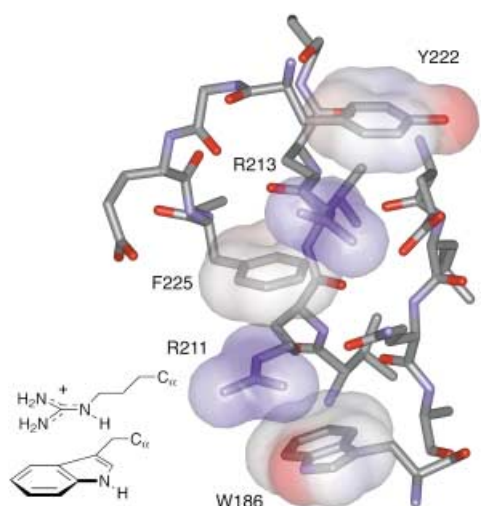
the interaction strength is found related to the electrostatics of the individual components; the calculated increment in free enthalpy for the cation– $\pi$  interaction  $-\Delta\Delta G$  decreases by 2.5  $\text{kcal mol}^{-1}$  upon changing from electron-rich ( $-\text{NMe}_2$ ) to electron-poor ( $-\text{NO}_2$ ) phenyl rings. This trend was illustrated through a Hammett plot which showed a steep positive slope. It is worth noting that the role of the anion has not been directly addressed in these systems, although the cation is presumably binding as its ion pair.

### 6.2.3. Counterion Dependence and Salt Bridges

Tight ion pairs exist<sup>[279]</sup> in polar, aprotic media which makes the electrostatic contribution of the anion to cation binding particularly important. While several studies have reported counterion-dependent cation– $\pi$  binding,<sup>[262,280,281]</sup> generally in the context of ditopic receptors,<sup>[282]</sup> it was not until recently that this phenomenon was systematically explored.<sup>[253,263,283–285]</sup> The stability of aromatic host–cation (TMA, ACh, and *N*-methylpyridinium (NMP)) complexes in  $\text{CDCl}_3$  and  $(\text{CDCl}_2)_2$  has been shown in numerous studies to decrease in the following anion sequence: picrate > trifluoroacetate >  $\text{I}^-$  >  $\text{Br}^-$  >  $\text{Cl}^-$  > tosylate  $\approx$  acetate.<sup>[263,265,281,284,286]</sup>

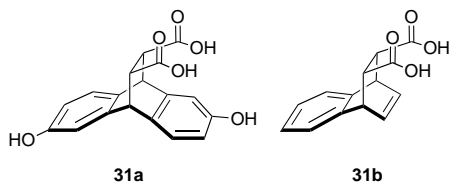
Although this sequence can be seemingly straightforwardly rationalized on the basis of the ion size (for the spherical halides) or ion-pair dissociation energy, Bartoli and Roelens have shown in a detailed study of their cyclophane systems, such as **29** ( $\text{CDCl}_3$ ), that there is a linear correlation between the binding free enthalpy ( $-\Delta G^\circ$ ) and solubility of the ammonium salt ( $\text{lg } S$ ).<sup>[285]</sup> The cations of ion pairs, wherein the cation and anion are not strongly interacting (that is, for large charge-diffused cations, such as TMA and ACh, and highly charge dispersed anions), are bound more strongly. These salts (ion pairs) also feature the lowest solubility. Additionally, a definitive linear correlation was found between the calculated electrostatic potential of the ion pair and the experimental binding free enthalpy ( $-\Delta G^\circ$ ). Extrapolation of the  $-\Delta G^\circ$  value to that denoting binding of the TMA cation to the aromatic host in the absence of its counterion reveals that more than 80% of the binding energy is lost as a result of the presence of the anion.<sup>[287]</sup>

The notion of the charge density of the counterion affecting the polarization of the cation charge has been implicated for some time in protein studies; the earliest crystallographic analyses of proteins often revealed aromatic amino acid side chains involving Lys and Arg in the proximity of salt bridges.<sup>[188,191,222,288,289]</sup> A variety of computational studies have considered ammonium–benzene (see above) and ammonium–carboxylate interactions separately, and have evaluated their intrinsic energies and solvation dependencies.<sup>[290]</sup> *Ab initio* calculations have shown that a cation– $\pi$  interaction in water should be more stabilizing than an analogous salt bridge ( $-\Delta\Delta G_{\text{bind}} \approx 2.6 \text{ kcal mol}^{-1}$ ),<sup>[289]</sup> while systematic database analysis has revealed the tendency for Lys and Arg to interact with aromatic amino acid side chains.<sup>[218,274]</sup> An example lies in the preference of Arg to interact with Trp in a facial manner,<sup>[218]</sup> as shown in the X-ray structure of the human growth hormone receptor (hGHR, Figure 25).<sup>[291,292]</sup>



**Figure 25.** Alternating cationic (Arg, Lys) and aromatic (Tyr, Phe, Trp) amino acid residues shown by X-ray crystallography (2.8 Å) within the human growth hormone receptor (hGHR) extracellular domain (PDB code: 3HHR).<sup>[291]</sup> The van der Waals and electrostatic potential surfaces (blue: positive, red: negative of the side chains) are shown as generated in WebLabViewer (ViewerPro V. 5.0, Accelrys, San Diego, CA). Hydrogen atoms have been omitted for clarity.

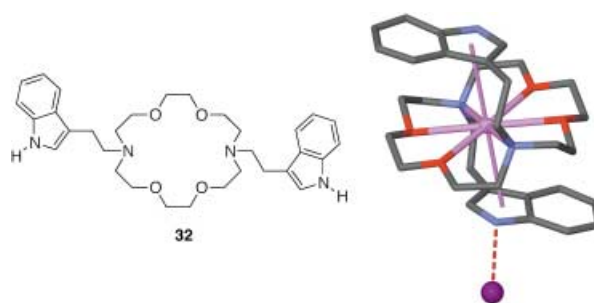
However, the analysis of ternary complexes involving salt bridges and aromatic compounds has only recently been investigated by computational analysis<sup>[289,293]</sup> and synthetic studies.<sup>[171,294]</sup> Dvornikovs and Smithrud, for example, have recently shown for their receptors (Figure 26) that Arg and Lys derivatives, while bound in water (pH 7.5, sodium phosphate buffer) by the carboxylates of **31a** ( $-\Delta G^\circ = 1.2$ – $1.5$  kcal mol<sup>-1</sup>), are not bound when the aromatic surface is absent, as in **31b**.<sup>[171][295]</sup>



**Figure 26.** The role of aromatic groups in stabilizing the formation of a salt bridge: Receptor **31a** binds Arg and Lys derivatives in aqueous phosphate buffer whereas **31b** does not.<sup>[171]</sup>

### 6.3. Alkali-Metal-Ion- $\pi$ Interactions

It is well-established that alkali-metal ions,<sup>[296–298]</sup> and although not specifically treated here, transition-metal ions,<sup>[298,299]</sup> form complexes with benzene and other aromatic molecules in the gas phase. The interaction energy is generally high (18.3 kcal mol<sup>-1</sup> for K<sup>+</sup>-benzene<sup>[297]</sup>) and the ion-molecule binding energy follows the expected electrostatic trend (namely, K<sup>+</sup> < Na<sup>+</sup> < Li<sup>+</sup>).<sup>[300]</sup> In aqueous solution, however, an aromatic ring cannot effectively compete with water for solvation of the alkali-metal cation.<sup>[301]</sup> Alkali-metal-cation-



**Figure 27.** Alkali-metal- $\pi$  interactions in the solid state. Di(indolyl) crown ether receptor **32** binds potassium (iodide) in a “sandwich” complex, with a K<sup>+</sup>...arene distance of 3.45 Å.<sup>[303]</sup> The iodide counterion is shown as the purple sphere.

$\pi$  interactions have been extensively reviewed by Gokel and co-workers,<sup>[228–230,302]</sup> who used crown ether derived receptors to study these contacts in solution and the solid state. Figure 27 shows the X-ray crystal structure of di(indolyl) receptor **32** with K<sup>+</sup> that reveals the sandwich complexation motif unique to these structures.<sup>[303]</sup> The K<sup>+</sup>...arene distance in the complex is 3.45 Å. These studies have subsequently provided the chemical basis for understanding interactions between alkali metals and aromatic amino acid side chains in a variety of media.<sup>[227,230,304]</sup> The interest in these interactions has also been extended to the gas phase<sup>[305,306]</sup> through advances in mass-spectrometric techniques and computational protocols.<sup>[305,307,308]</sup>

Many of the fundamental energetic features of the cation- $\pi$  interaction are applicable to both onium and alkali-metal cations. Extensive theoretical investigations on relatively simple C<sub>6</sub>H<sub>6</sub>...M<sup>+</sup> complexes are currently providing valuable information on these contacts.<sup>[309–312]</sup> It is clear that these efforts pave the way for more complete models describing the cation- $\pi$  interaction in chemistry and biology.

### 6.4. Energetics from Biological Systems

Experiments designed to quantify cation- $\pi$  interactions in biological systems, although sparse, have convincingly demonstrated the stabilizing role that such contacts can make within proteins and at their surface.<sup>[218,313–320]</sup> The most recent studies are summarized in Table 6. On average, the reported interaction energies for positively charged amino acid residues (namely, Lys, His, Arg) and aromatic side chains (Phe, Trp, Tyr) in water lie between  $-0.4$  and  $-2.4$  kcal mol<sup>-1</sup>. Although these values are somewhat lower than those predicted theoretically ( $-3.2$  to  $-3.6$  kcal mol<sup>-1</sup>),<sup>[274,289]</sup> they are surprisingly consistent given the many different systems employed. Known variables include differing intrinsic solvation energies for each amino acid<sup>[321]</sup> and solvent exposure of the interacting groups (that is, on the surface or buried), as well as indeterminate conformational changes that occur upon substitutions (or protonations) that can markedly affect the entropic and/or enthalpic components of  $\Delta G^\circ$ . The use of non-natural amino acids to investigate cation- $\pi$  interactions has been one way to sidestep these uncertainties, as recently

**Table 6:** Strength of cation– $\pi$  interactions involving amino acids in water based on biological model systems.

A <sup>+</sup> -Ar <sup>[a]</sup>	– $\Delta G^\circ$ [kcal mol <sup>-1</sup> ] <sup>[b]</sup>	Experimental technique	Biological system	Ref.
His-Trp	ca. 0.9	double-mutant cycles and pH dependence	$\alpha$ -helix (barnase)	[313]
His-Trp (C→N) <sup>[c]</sup>	0.8 ± 0.1	mutagenesis, AGADIR <sup>[d]</sup> analysis	<i>i,i</i> +4 residues in Ala-based $\alpha$ -helices	[314b]
His-Phe	0.5	double-mutant cycles and pH dependence	apoflavodoxin	[316]
Arg-Trp (C→N) <sup>[c]</sup>	0.4	mutagenesis	<i>i,i</i> +4 residues in Ala-based $\alpha$ -helices	[317, 320]
S-MeMet-Ar <sup>[e]</sup>	≤ 2.6 <sup>[f]</sup>	non-natural amino acids, mutagenesis	staphylococcal nuclease	[315]
serotonin-Trp	ca. 4	non-natural amino acids, fluorination plots	serotonin 5-HT <sub>3A</sub> receptor	[270]
ACh-Trp	ca. 2	non-natural amino acids, fluorination plots	nicotinic acetylcholine receptor	[270]

[a] A<sup>+</sup> = positively charged component, Ar = aromatic component. [b] Generally reported as  $\Delta\Delta G^\circ$  between folded proteins/peptides. [c] The directionality (positioning of the residues with respect to the helix termini) appears to be important in these systems. See ref. [320] wherein no interaction was observed in the N→C direction. [d] AGADIR is a computer program described in ref. [314a]. [e] S-MeMet = (S)-methylmethionine. [f] The exact quantity is unknown as the value reported may represent multiple (1, 2, or 3) interactions; see ref. [315].

shown by the research groups of Schultz<sup>[315]</sup> and Dougherty<sup>[221, 270]</sup> (Table 6, rows 5–7).

The contribution of the cation– $\pi$  interaction in proteins can be significant in mixed organic/aqueous solvents, although this has yet to be fully explored. The work of Kostic and co-workers<sup>[318]</sup> with associating protected single amino acids has shown that Lys–Phe and Lys–Tyr interactions, which are worth (from <sup>1</sup>H NMR titration) –2.4 and –2.1 kcal mol<sup>-1</sup> in water, are magnified to –3.4 and –2.9 kcal mol<sup>-1</sup> in chloroform/methanol/water mixtures. Likewise, Hamilton and co-workers<sup>[322]</sup> have recently designed guanidinium receptors for  $\alpha$ -helical peptides and postulated that there are significant cation– $\pi$  interactions between the charged centers of the receptor and a tryptophan residue in the binding site.

### 6.5. Outlook

Studies of the cation– $\pi$  interaction, while broad, have reached considerable consensus in describing the basic energetics of the simplest systems. This is a prerequisite, with the aid of advanced computational protocols, superior mass-spectrometric tools, and design creativity, for the continued exploration of these interactions in more complex systems. Particularly exciting are approaches that employ cation– $\pi$  interactions in the active sites of enzymes for de novo drug design,<sup>[8, 270]</sup> catalysis in both synthetic<sup>[323]</sup> and biological systems,<sup>[324]</sup> and organic synthesis (for example, stereocontrol in organic reactions<sup>[325]</sup>). Cation– $\pi$  interactions are increasingly observed at protein–DNA interfaces.<sup>[326]</sup> Although not specifically addressed here, recent reports of anion–arene interactions suggest that these may also be promising contacts for future study.<sup>[327, 328]</sup>

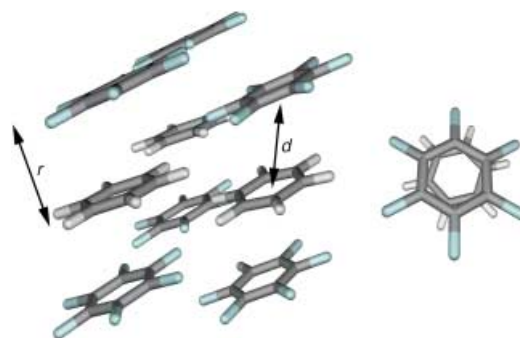
## 7. Interactions between Aromatic and Perfluoroaromatic Compounds

### 7.1. Benzene–Hexafluorobenzene

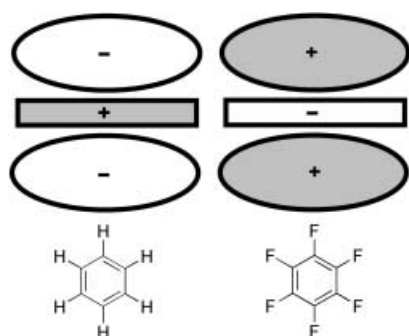
Hints of the unusual properties of perfluoroaromatic compounds came four decades ago from formation of a crystal from an equimolar mixture of hexafluorobenzene and benzene: A solid was formed with a melting point of 23.7 °C,

approximately 19 °C higher than either of the two components.<sup>[329]</sup> Unlike the crystal-packing patterns of benzene and hexafluorobenzene, which feature herringbone arrangements arising from T-shaped interactions (see Section 3), the C<sub>6</sub>H<sub>6</sub>–C<sub>6</sub>F<sub>6</sub> cocrystal shows nearly parallel molecules stacked alternately in infinite columns (Figure 28) with an interplanar distance (*r*) of about 3.4 Å and an intercentroid distance (*d*) of 3.7 Å.<sup>[330, 331]</sup> Weak C<sub>aryl</sub>–H...F contacts help to stabilize neighboring columns (see above). Early calorimetric and NMR studies demonstrated thermodynamic phase transitions for the equimolar mixture at 199 K (most ordered), 247.5, and 272 K (least ordered);<sup>[332]</sup> the lowest temperature structure (measurement at 30 K) is shown in Figure 28.<sup>[331]</sup> This general crystal-packing morphology has been reproduced with many complexes of aromatic–perfluoroaromatic compounds,<sup>[116, 333–335]</sup> and has led to the conclusion that the stacking interaction is a general one.<sup>[334]</sup>

Most, but perhaps not all, of the structural features of the hexafluorobenzene–benzene cocrystal can be rationalized on the basis of the quadrupole moments of the two components<sup>[334, 336, 337]</sup>—the values are equal in magnitude but opposite in sign (C<sub>6</sub>H<sub>6</sub>: –29.0 × 10<sup>-40</sup> Cm<sup>-2</sup>; C<sub>6</sub>F<sub>6</sub>: +31.7 × 10<sup>-40</sup> Cm<sup>-2</sup>),<sup>[338]</sup> as shown schematically in Figure 29.<sup>[337, 339]</sup> Spectroscopic studies have shown that the complexes do not have charge-transfer ( $\pi$ – $\pi^*$ ) properties, as demonstrated by the absence of characteristic bands in the UV spectra,<sup>[340]</sup> and there are only small shifts in the internal vibrational



**Figure 28.** The structure of the lowest temperature phase of the benzene–hexafluorobenzene cocrystal at 30 K.<sup>[331]</sup> Views along the approximate *b* axis (left) and *c* axis (right) are shown. *r* = interplanar distance (ca. 3.4 Å); *d* = intercentroid distance (ca. 3.7 Å); atom coloring: white, H; aqua, F; CSD code: BICVUE01.

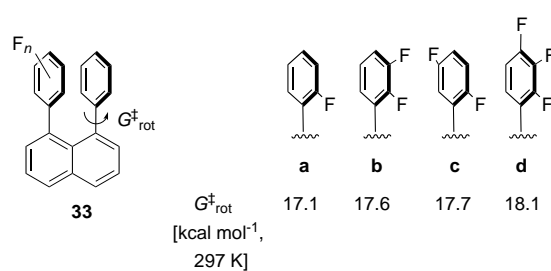


**Figure 29.** Schematic representations of the quadrupole moments of benzene (left) and hexafluorobenzene (right).

frequencies relative to the pure components;<sup>[331,341]</sup> this is not the case for complexes of  $C_6F_6$  with aromatic amines<sup>[342]</sup> or metal complexes.<sup>[343]</sup> The crystal-packing motif indeed reflects the maximizing of favorable quadrupole–quadrupole interactions (distance dependency:  $r^{-5}$ ) and the minimizing of unfavorable electrostatic repulsions (for example, edge-to-face arrangements).

Estimations of the interaction energy describing the  $C_6H_6$ : $C_6F_6$  dimer have come from both computational and experimental studies. Ab initio calculations have determined a stabilization energy of  $-3.7$  kcal mol $^{-1}$  ( $r = 3.6$  Å; CP-corrected MP2/6-31G\*\*<sup>[344]</sup>) and  $-4.3$  kcal mol $^{-1}$  ( $r = 3.7$  Å; SCF-MP2)<sup>[345]</sup> for the hexafluorobenzene–benzene dimer in the face-to-face eclipsed arrangement. More recent semi-empirical calculations<sup>[148]</sup> that include extended electron distribution (XED)<sup>[343]</sup> give a somewhat higher value of  $-5.6$  kcal mol $^{-1}$  ( $r = 3.6$  Å).<sup>[346]</sup> Finally, a value of  $-4.7$  kcal mol $^{-1}$ <sup>[347]</sup> has been reported from DFT calculations that consider the eclipsed, offset geometry. In all cases the values for the heterodimer are 1.5–3 times higher than the corresponding interaction energies for the two homodimers. Additionally, and perhaps most importantly, the calculations and crystal-structure analysis<sup>[337]</sup> have revealed dispersion interactions to be at the very least as large in magnitude (but generally larger, 70–85 %<sup>[346,347]</sup>) as the electrostatic component in these complexes.<sup>[67]</sup>

While many solution-based experiments have observed the consequences of the formation of the  $C_6H_6$ : $C_6F_6$  dimer,<sup>[108,348–351]</sup> we concern ourselves here with strategies used to quantify interactions between aromatic and perfluoroaromatic compounds. The 1,8-diarylnaphthalenes **33a–d** prepared by Siegel and co-workers have been employed to correlate fluorine substitution with barriers to rotation about aryl–naphthalene bonds (Figure 30; see also Figure 12).<sup>[147,352]</sup> Each additional fluorine atom in the series **33a** to **33d** increases the  $\Delta G_{rot}^\ddagger$  term by 0.5 kcal mol $^{-1}$ , which indicates there is a decrease in the repulsion in the stacked ground state upon removal of electron density from the ring. The results are consistent with the so-defined “polar/ $\pi$ ” interactions that feature significant electrostatic contributions to  $\pi$ – $\pi$  stacking (see Section 4.3.4). Experimental<sup>[221,270,353,354]</sup> and theoretical<sup>[221,268,355]</sup> investigations of cation– $\pi$  complexes (see Section 6) with *perfluorinated* aromatic compounds similarly demonstrate electrostatic-dominated interactions. In accor-



**Figure 30.** Progressive fluorine substitution results in an increase in the barrier to rotation of the phenyl–naphthalene bond in 1,8-diarylnaphthalenes.<sup>[147,352]</sup>

dance with this model, the interaction energy decreases strongly in all cases upon incremental substitution of fluorine atoms.<sup>[356]</sup>

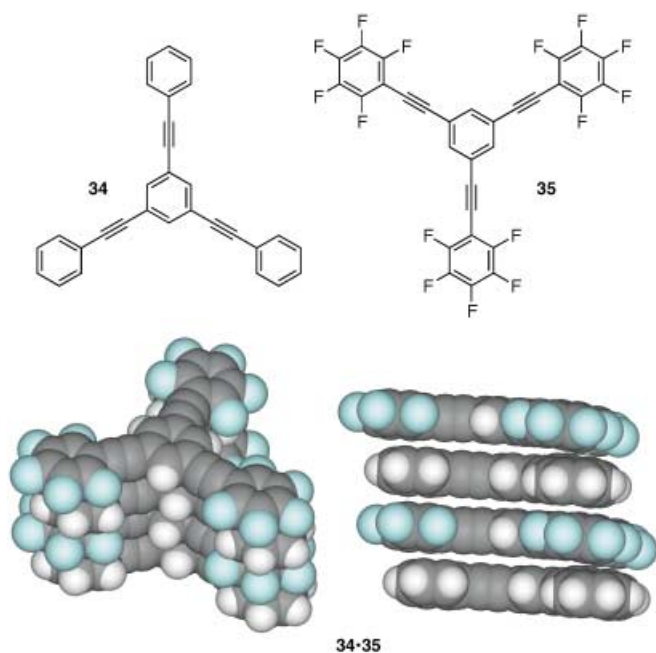
The chemical double-mutant cycles of Hunter and co-workers (Sections 4 and 6) have been employed to investigate interactions between aromatic and perfluoroaromatic compounds.<sup>[357]</sup> The experiments show a stabilizing interaction between a face-to-face-oriented dimethylamino-substituted aromatic compound and a pentafluorophenyl ring of 0.4 kcal mol $^{-1}$ . Coincidentally, this value is similar to the enthalpy of formation calculated for the solid hexafluorobenzene–benzene complex from differential scanning calorimetry (DSC) measurements (0.24 kcal mol $^{-1}$ ).<sup>[358]</sup> Further experiments by Hunter and co-workers revealed the edge-to-face arrangements between the two aromatic rings to be destabilizing, as expected for positively polarized aryl C–H protons directed toward the electron-poor  $\pi$  face of the pentafluorophenyl group. In summary, experimental investigations have nicely demonstrated the important electrostatic contribution to phenyl–perfluorobenzene interactions,<sup>[359,360]</sup> while theoretical studies have probed the role of dispersion forces in these contacts.

## 7.2. Stacking Interactions and Molecular Organization

The interaction between phenyl and perfluorophenyl groups fulfills the prerequisites of structural predictability for consideration as a supramolecular synthon.<sup>[86]</sup> To this end, the interaction has been used elegantly in crystal-engineering studies and the design of novel supramolecular architectures in much the same way as hydrogen-bonding donors and acceptors have been employed for these tasks.<sup>[361]</sup> A representative example is provided in the stacking of 1,3,5-tris(phenylethynyl)benzene (**34**) and 1,3,5-tris(perfluorophenylethynyl)benzene (**35**) in the solid state (Figure 31).<sup>[362]</sup> While **34** and **35** form slipped stacks with their terminal aryl rings twisted with respect to the plane of the central ring (namely, a twisted rotor conformation is formed, not shown) when crystallized separately, the 1:1 heterocomplex is essentially planar with markedly less slippage. These results provide excellent evidence for the structural control attainable when using the phenyl–perfluorophenyl synthon.

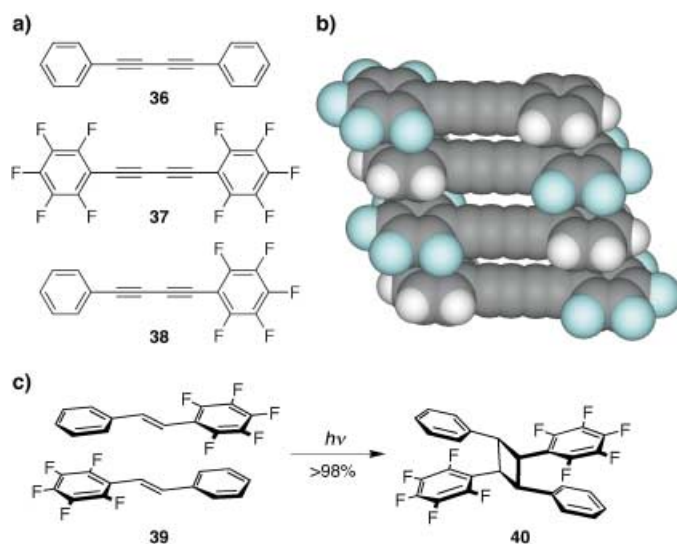
Dougherty, Grubbs, and co-workers were the first to use the phenyl–pentafluorophenyl motif to exert topological and





**Figure 31.** Well-defined solid-state organization that results from the phenyl–perfluorophenyl synthon. Cocrystallization of **34** and **35** gives nearly perfectly aligned alternating layers of the two components.<sup>[362]</sup> CSD code: WEVYIF.

stereochemical control over the photopolymerization reactions of 1,3-diynes in the condensed phase (Figure 32a).<sup>[363]</sup> Cocrystallization of **36** with **37** gives a solid (**36-37**) that melts at 152 °C, which is considerably higher than either of the two homodimers (87 °C for **36-36**, 114 °C for **37-37**). Similar to the cocrystal formed from benzene and hexafluorobenzene, the diynes pack alternately into stacked columns where the



**Figure 32.** The use of the phenyl–perfluorophenyl synthon to predispose molecules for photochemical reactions in the solid state.<sup>[363, 365]</sup> a) Precursors for *cis*-polybutadiynes. b) The X-ray structure of **38** (ca. 3.7 Å distance between layers, CSD code: RIHGQE). c) The [2+2] photocycloaddition reaction of **39** proceeds with regiochemical and stereochemical control to give **40** quantitatively in the crystal.

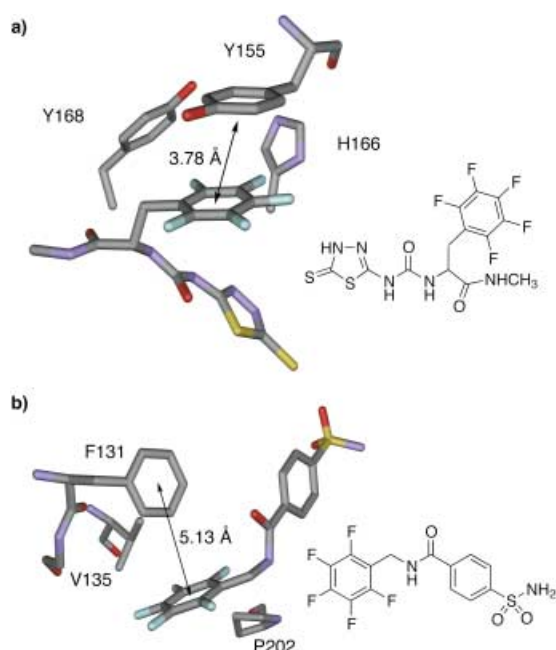
individual molecules are only slightly longitudinally slipped with respect to one another ( $d = 3.69$  Å, not shown). Difunctional **38** packs similarly (although slightly staggered) and in a head-to-tail arrangement (Figure 32b). Both types of complexes ( $(\mathbf{36-37})_n$  and  $(\mathbf{38})_n$ ) are predisposed to form *cis*-polybutadiynes upon irradiation;<sup>[364]</sup> however, although approximately 20% of the polymerization product has been obtained in each case, its stereochemistry (*cis* or *trans*) has yet to be reported.

Subsequent studies used phenyl–perfluorophenyl interactions to orient distyrylbenzenes in the solid state for photo-dimerization reactions.<sup>[365, 366]</sup> *trans*-Pentafluorostilbene **39** could be converted into cyclobutane **40** in nearly quantitative yield and with excellent stereocontrol (Figure 32c). There has since been considerable interest in using this motif to control the solid-state packing of distyrylbenzene derivatives for use in optoelectronic technologies.<sup>[367]</sup> More recent studies, and more are sure to come, have utilized interactions between aromatic and perfluoroaromatic compounds to control supramolecular organization in reversible media; these include modulating the behavior of liquid-crystalline phases,<sup>[368]</sup> formation of hydrogels,<sup>[369]</sup> and templation effects in cyclophane synthesis.<sup>[370]</sup>

### 7.3. Perfluoroarene Interactions in Biological Recognition

Fluorine-containing compounds have enjoyed a rich history in bioorganic and medicinal chemistry and have been widely studied.<sup>[371–373]</sup> The function of the fluorine atom in these settings is diverse: from an isosteric and isoelectronic replacement of the hydroxy group,<sup>[374]</sup> to a means of enhancing the metabolic stability of drugs<sup>[371]</sup> and modifying electronic and physical properties (for example, lipophilicity, acidity, steric hindrance). Introduction of perfluoroaromatic groups in biological systems, particularly with the intention of exploiting their unique electronic properties, has been somewhat more limited. A few systems are discussed here.<sup>[375]</sup> Fluorinated tryptophan side chains have been installed in the ligand binding site of acetylcholine receptors to assess the contributions of cation– $\pi$  interactions to substrate binding.<sup>[270, 354]</sup> A linear correlation in a “fluorination plot” between  $\lg(\text{EC}_{50})$ <sup>[376]</sup> and the cation– $\pi$  binding ability of the side chains (as given by their degree of fluorine substitution) provides direct evidence for the presence of a single ammonium–Trp interaction that is essential to ligand binding.

Interactions between Tyr155 and the pentafluorophenyl group of a 1,3,4-thiadiazole-2-thione-based inhibitor of the metalloproteinase stromelysin (Figure 33a) contribute to its high binding affinity ( $K_i = 18$  nM) and slowed the rates of ring flip relative to other analogues.<sup>[377]</sup> Although the familiar quadrupole–quadrupole interaction dominates here, Christenson, Doyon, and co-workers<sup>[378–380]</sup> have shown with fluorinated inhibitors of carbonic anhydrase II (CAII) that the quadrupolar interaction need not always dominate substrate recognition, but rather a variety of electrostatic forces (for example, dipole–induced dipole, dipole–quadrupole) may contribute differently to the binding depending on the patterns and degree of fluorine substitution in the inhibitor.



**Figure 33.** Perfluoroaromatic interactions involving enzymes and their inhibitors. a) Face-to-face interaction between Tyr155 and the pentafluorophenyl group of a 1,3,4-thiadiazole-2-thione inhibitor of a metalloproteinase (PDB code: 1USN).<sup>[377]</sup> b) A rather unexpected edge-to-face arrangement between the pentafluorophenyl substituent of a carbonic anhydrase II inhibitor and Phe 131 of the enzyme (PDB code: 1G54).<sup>[379]</sup>

Testament to this is the rarely seen edge-to-face orientation between Phe 131 of CAII and the pentafluorophenyl derivative of an *N*-(4-sulfamylbenzoyl)benzylamine inhibitor (Figure 33b) in their system.<sup>[379]</sup>

Finally Kool and co-workers have elegantly shown difluorotoluene, although not a perfluorinated aromatic compound, to be a versatile isostere of the natural nucleobase thymine.<sup>[165b,381]</sup> In the context of formation of duplex DNA, the fluorinated “base” stacks with its nearest neighbor in a geometry dictated by the helix. The marked increase in DNA stability upon substitution of thymine for difluorotoluene has been attributed to differences in hydrophobicity between the bases (their size, shape, surface area, and polarizability are comparable). However, although not specifically addressed, electronic effects in terms of  $\pi$ - $\pi$  stacking may also play a role in these interactions.

#### 7.4. Additional Perfluoroarene Interactions

Although there has been considerable debate regarding the effectiveness of organofluorine as a hydrogen-bond acceptor, many of the solid-state studies described above have implicated  $C_{\text{aryl}}-F\cdots H-C$  interactions<sup>[335,373,382]</sup> as important intercolumnar and interlayer stabilizing contacts. The conclusion from these studies as well as systematic database analysis<sup>[382]</sup> is that the  $C_{\text{aryl}}-F\cdots H-C$  contact may show an orientation dependence and be structure-directing when the C-F carbon atom is sufficiently electropositive and there are no competing H-bond acceptors in the crystal. In general,

$F\cdots C$  distances ( $d$ ) lie between 3.3 and 3.6 Å while the  $C_{\text{aryl}}-F\cdots H$  angle approaches linearity as  $d$  decreases. Other contacts, such as  $C_{\text{aryl}}-F\cdots M^+$  ( $M^+$  is an alkali metal), naturally extend from the polarization of the  $C_{\text{aryl}}-F$  bond.<sup>[383]</sup>

The electron deficiency of perfluorinated aromatic compounds makes them excellent acceptors of electron density at their  $\pi$  faces.<sup>[384]</sup> Hexafluorobenzene has been calculated through DFT and ab initio protocols to form strong complexes with anions (such as  $Cl^-$ ,  $Br^-$ ,  $CN^-$ ,  $F^-$ ),<sup>[385]</sup> and calculated interaction energies ( $-10$  to  $-19$  kcal mol $^{-1}$  for the series given) are comparable to those obtained for cation- $\pi$  interactions with benzene (see Section 6). The contact distances can be quite short ( $C_6F_6$  centroid $\cdots F^-$ : 2.65 Å). Neutral molecules (of various polarity) possessing donor atoms also form complexes with perfluoroaromatic compounds; the interaction with water is the most well-studied.<sup>[379,380,386,387]</sup> The most stable complex displays a geometry wherein the oxygen lone pairs are directed into the  $\pi$  face, and surprisingly good agreement among computational protocols has been found ( $\Delta E$  lies between  $-1.6$  and  $-2.1$  kcal mol $^{-1}$ ,  $C_6F_6$  centroid $\cdots OH_2$ : 3.2 Å in all cases).<sup>[386]</sup> The interaction values reported are only slightly higher than the orientationally averaged binding energy for water-hexafluorobenzene calculated from gas-phase calorimetric data ( $-1.3$  kcal mol $^{-1}$ ).<sup>[387]</sup> Finally, as with other donors (for example, molecular oxygen),<sup>[388,389]</sup> the interactions are generally stronger with  $C_6F_6$  than with the parent  $C_6H_6$ .

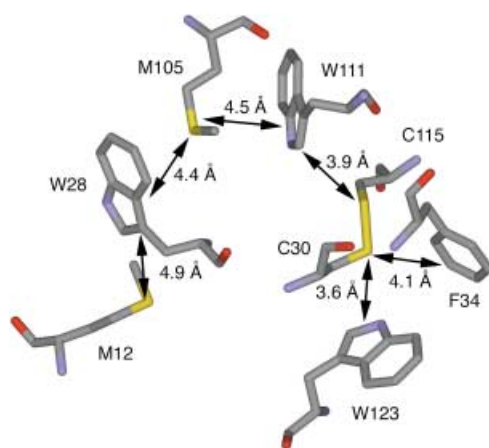
## 8. Sulfur-Arene Interactions

### 8.1. Crystallographic and Computational Analysis

#### 8.1.1. Sulfur-Arene Interactions in Proteins

Close and frequent contacts ( $< 5$  Å from the sulfur center to the center of the ring system) between sulfur-containing amino acid side chains (Met, Cys) and aromatic side chains (Tyr, Trp, Phe) were first recognized in globular protein crystal structures in the late 1970s.<sup>[390]</sup> Morgan et al. identified eight proteins that contained one or more chains of alternating “sulfur and  $\pi$ -bonded atoms”; a compelling early example is the lysozyme from hen egg-white shown in Figure 34.<sup>[391]</sup> The distances between the sulfur atoms and ring carbon atoms are 3.5–4.9 Å in this example; this range falls within the distance minimum established by the authors for  $S\cdots C(sp^2)$  van der Waals contacts (5 Å).

The nature of the interaction between sulfur and its neighboring aromatic rings could in no way be elucidated from these structures, although the following factors were considered important: 1) the filled 3p and empty 3d orbitals on sulfur, 2) the related enhanced polarizability of sulfur atoms (and C-S or S-S bonds) relative to carbon atoms (or C-C bonds), and 3) the known ability of divalent sulfur-containing molecules (particularly disulfides) to quench the fluorescence of aromatic amino acids (for example, Trp, Tyr),<sup>[392]</sup> a phenomenon still actively researched.<sup>[393]</sup> We can add the acidity of the S-H group to this list in the case of cysteine residues, which should interact favorably with  $\pi$  surfaces (see below and Section 5).

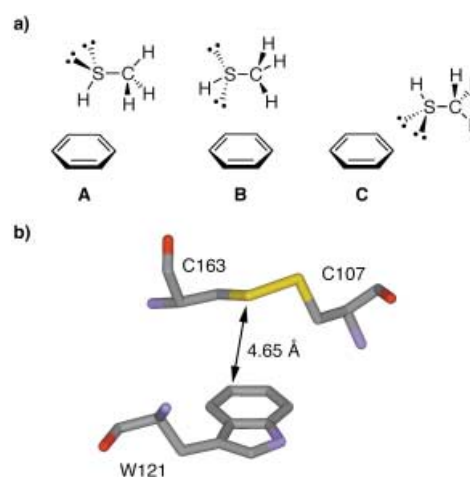


**Figure 34.** A chain of alternating “sulfur and  $\pi$ -bonded atoms” as identified in hen egg-white lysozyme (PDB code: 6LYZ).<sup>[391]</sup>

Subsequent analysis of 36 proteins by Reid et al. resulted in the first statistical analysis of PDB data and the development of a structural model.<sup>[394]</sup> A preference was identified for placement of divalent sulfur ( $-\text{SH}$ ,  $\text{S-S}$ , and  $-\text{CH}_2\text{-S-CH}_3$ ) at the edge and slightly above the plane of aromatic rings. The same trend was observed with oxygen in similar analyses and suggested that there were significant electrostatic interactions between the heteroatom and the aromatic hydrogen atoms.

More recent structural studies have considered methionine, cysteine, and cystine ( $\text{S-S}$ ) residues separately, and rightfully so given the different structural and electronic properties of these species. Recent PDB analyses<sup>[395]</sup> find that methionine is as favored as aromatic amino acids, specifically Tyr and Trp, to be within (distance ( $d$ )  $< 4.0$  Å between Met S atom and ring heavy atoms) the environment of the Trp indol ring. In a survey of 1276 Met residues, 9% were found in contact with an aromatic edge (average  $d$  below search cut-off: 3.7(1) Å) and 8% with an aromatic face (average  $d$  below search cut-off: 3.6(1) Å). Despite the statistically equivalent distribution of the geometric signatures of the two interaction types, they were found to be quite different, with more structural regularity and closer distances being associated with facial contacts. However, the orientation of the aromatic partner was not considered in these studies, thus making energetic conclusions tenuous. Similar studies have shown an even stronger preference for cysteine residues to experience facial contacts with aromatic residues.<sup>[396]</sup>

The recent work of Smith and co-workers on cystine–arene interactions correlates interaction structure with energy values.<sup>[206,397,398]</sup> Three structural motifs were considered for the interaction of methanethiol with an aromatic ring (Figure 35 a). Initial ab initio calculations (MP2/6-311G(2d,p)) revealed **A** to be the most stable ( $-3.7$  kcal mol $^{-1}$ ), followed by **C** ( $-1.7$  kcal mol $^{-1}$ ), and **B** ( $-1.5$  kcal mol $^{-1}$ ). The sulfur atom in structure **A** is positioned 3.5–4.0 Å above the ring. The  $\text{S-H}/\pi$  interaction, a consequence of favorable electrostatic interactions between a positively polarized  $\text{S-H}$  hydrogen atom and a  $\pi$  system (negatively polarized at this distance),<sup>[209,399]</sup> and dispersion interactions between the sulfur atom and a  $\pi$  surface account



**Figure 35.** Sulfur–arene interactions involving sulfides and disulfides: a) The three lowest energy arrangements derived from ab initio calculations for methylthiol interacting with benzene (the stability series is  $\text{A} > \text{C} > \text{B}$ , least stable);<sup>[206]</sup> b) an example of the conserved disulfide–tryptophan interaction in immunoglobulin (Ig) proteins (PDB code: 1IEA).<sup>[403]</sup>

for 2.6 kcal mol $^{-1}$  of the interaction energy (the 1.1 kcal mol $^{-1}$  remaining is attributed to favorable dispersion interactions between the  $\text{CH}_3$  group and the arene).<sup>[400]</sup> Structure **B** is highest in energy since it suffers from a repulsive interaction between an aromatic ring and a lone pair of electrons which is only partially compensated by dispersion contacts between the  $\text{CH}_3$  group and the arene. We refer the reader here to computational studies performed on dimethylsulfide–benzene complexes that reveal the importance of such dispersive interactions.<sup>[401]</sup> Finally, the sulfur atom in structure **C** is positioned slightly above ( $\leq 2.5$  Å) and to the edge (4.5–6.0 Å from ring centroid) of the aromatic ring in a positively polarized region (based on the MEP at this distance).<sup>[209]</sup> In this arrangement favorable interactions between the lone pair of electrons and the aromatic ring occur, which are calculated to contribute 1.5 kcal mol $^{-1}$  to the interaction energy. These results are in reasonable, but not complete, agreement with earlier ab initio experiments (MP2/6-31G\*//HF/3-21G\*) performed on the benzene–methanethiol complex.<sup>[402]</sup> The most stable arrangement in these studies positioned the  $\text{CH}_3$  group directly above the ring (for  $\text{S-CH}/\pi$  interactions) and the sulfur atom near the ring edge. The  $\text{S-H}$  hydrogen atom did not participate in the binding at all. An additional finding from these investigations, and one that has yet to be fully explored for sulfur–arene interactions, is a marked dependence of the interaction strength and structure on the local electric field (that is, nearby charge centers).

A subsequent search of the PDB by Smith and co-workers<sup>[206]</sup> revealed that of 682 cysteine residues (in 609 protein structures) that do not form disulfide bonds, 268 undergo interactions with aromatic rings to give structures such as **A–C** in Figure 35. However, of these, 207 involve attractive interactions between arenes and lone pairs of electrons (such as in **C**) and only 4 display the  $\text{S-H}/\pi$ -bonding configuration (such as in **A**). It appears that in the majority of cases the protein structure is better served by having the thiol

participate in conventional hydrogen bonding (for example,  $S-H\cdots O(\text{or } N)$ ), and this happens in 82 % of the total residues considered.

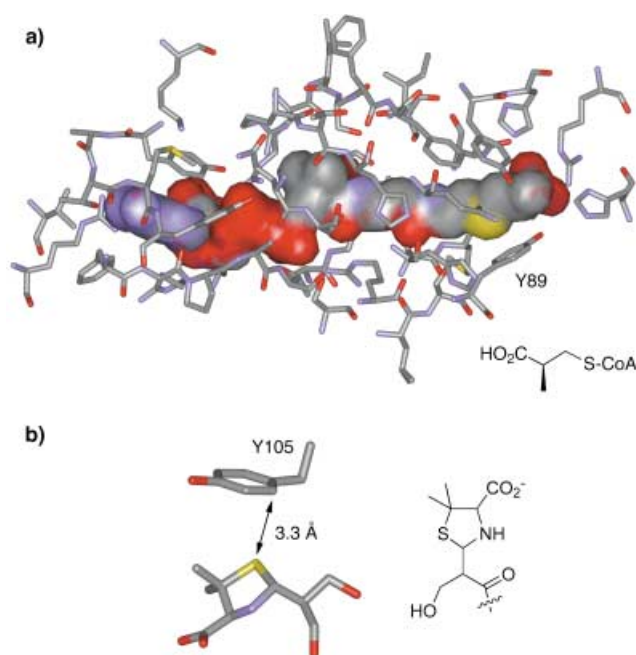
Ioerger et al. have studied cysteine–arene interactions in immunoglobulin (Ig) proteins.<sup>[403]</sup> Their results from a survey of over 60 structures have revealed a highly conserved  $(\text{Cys})_2\cdots\text{Trp}$  interaction within the Ig fold motif, an example of which is shown in Figure 35 b.<sup>[404]</sup> The average distance between the S–S midpoint and the center of the indol ring for the surveyed structures is 4.5 Å, where stabilization of the complexes clearly comes through a combination of favorable dispersion interactions between one of the  $\text{CH}_2$  groups and one of the sulfur atoms with the  $\pi$  surface. This geometry is quite similar to the lowest energy structure calculated for 1:1 benzene–dimethyldisulfide complexes by empirical methods<sup>[405]</sup> that predict direct contacts between one of the sulfur atoms and the benzene ring to make an additional contribution of 0.8 kcal mol<sup>-1</sup> to the interaction energy.

Statistical analysis of the crystal structures of small molecules in the Cambridge Structural Database has provided convincing evidence for the interaction between divalent sulfur (C–S–C) units and aromatic rings.<sup>[406]</sup> Local maxima of the probability distributions obtained from the searches were used to define a preferred geometry for the interaction; it was found that the sulfur atom lies essentially in the plane of the aromatic ring approximately 5.0 Å from the center of the aromatic ring.<sup>[407]</sup> This distance maximum was not identified in analogous searches performed with X–CH<sub>2</sub>–X fragments. We have seen in X-ray crystal structures of complexes formed in our own research between Rebek imide-type receptors with appended methylthioether side chains and adenine (Figure 15) an average distance of 4 Å between the heavy atoms of adenine and the sulfur atom located above the heterocycle.<sup>[167]</sup> However, as discussed in Section 3 and ref. [406], the contribution of crystal-packing forces in these small-molecule structures are likely to be significant and biasing.

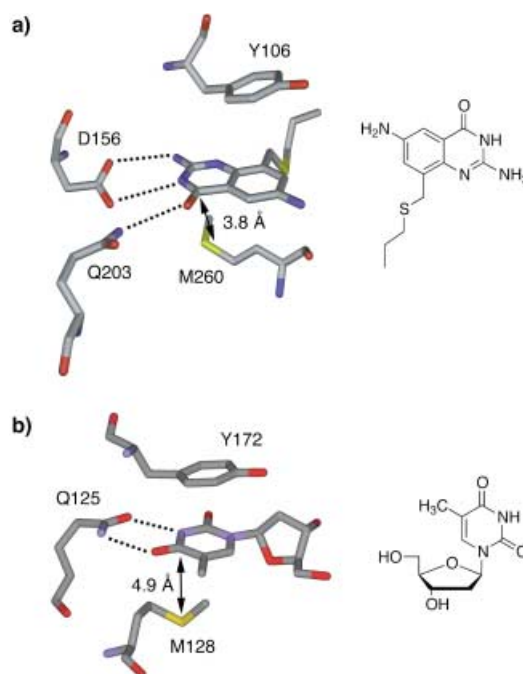
### 8.1.2. Protein–Ligand Complexes

Figure 36 shows just two of several results from a PDB search<sup>[408]</sup> for sulfur–arene contacts between substrates containing divalent sulfur and their enzyme hosts.<sup>[409–411]</sup> In the first (Figure 36 a), methylmalonyl-CoA mutase employs an  $S\cdots\text{Ar}$  (Y) contact to stabilize the lipophilic region of its flexible 2-carboxy-(*R*)-propyl-CoA substrate.<sup>[409]</sup> The second (Figure 36 b) shows a portion of the acyl–enzyme complex solved at 1.95 Å between 6 $\alpha$ -(hydroxymethyl)penicillanate and  $\beta$ -lactamase from *Escherichia coli*, wherein a “sub-van der Waals contact” (3.3 Å) is observed between the thiazolidine sulfur atom and the Tyr 105 ring.<sup>[410]</sup> The sulfur atom is located below and to the edge of the aromatic ring.

The frequency of enzyme binding sites that involve a “sandwiching” of an aromatic substrate between two hydrophobic fragments (particularly Tyr, Phe, Trp, and Met) residues is striking. A poignant example of this motif is seen at the active site of tRNA-guanine transglycosylase (TGT), as shown in Figure 37 a.<sup>[412]</sup> Here, Tyr 106 undergoes  $\pi$  stacking with the complexed inhibitor on one face while Met 260



**Figure 36.** Sulfur–arene contacts between sulfur-bearing substrates and their biological receptors: a) X-ray crystal structure (2.2 Å) of *S*-((*R*)-2-carboxypropyl)-CoA bound to methylmalonyl-CoA mutase. The van der Waals surface of the substrate is shown and colored by atom (PDB code: 7REQ).<sup>[409]</sup> b) A portion of the acyl–enzyme complex formed between 6 $\alpha$ -(hydroxymethyl)penicillanate and  $\beta$ -lactamase (PDB code: 1TEM).<sup>[410]</sup>



**Figure 37.** “Sandwich”-type complexation involving methionine. a) A tight-binding quinazoline inhibitor is held between Tyr 106 and Met 260 within the active site of TGT (PDB code: 1K4H).<sup>[412]</sup> b) Thymidine within the thymidine kinase HSV1 TK (PDB code: 2VTK).<sup>[415]</sup>

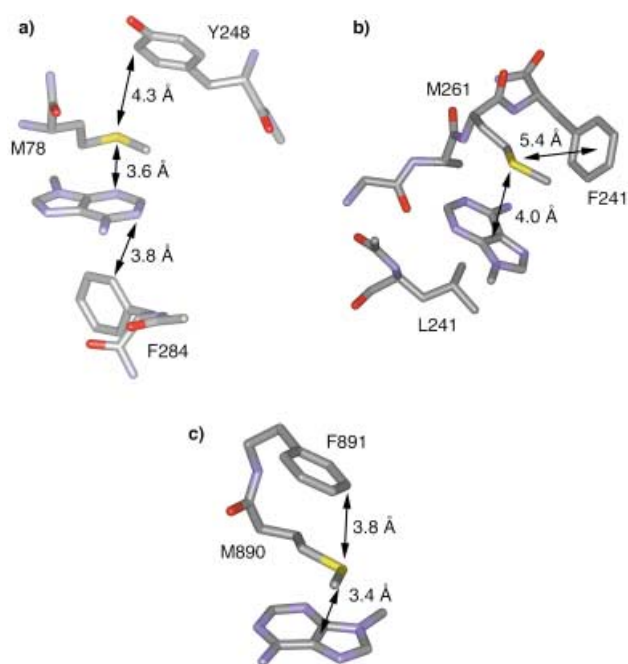
makes a contact distance (sulfur atom to the center of the ring system) of approximately 3.8 Å on the other side. The positioning of the methionine residue in the complex is also notable. Dispersion interactions appear maximized as the planar  $-\text{CH}_2\text{-S-CH}_3$  fragment lies essentially coplanar with the quinazoline heterocycle.

The role of a highly conserved methionine in substrate binding has been carefully assessed by Folkers and co-workers in their complexes of herpes simplex virus type 1 thymidine kinase (HSV1 TK) with thymidine (Figure 37b).<sup>[413,414]</sup> The common sandwiching motif of the nucleobase between Met 128 and Tyr 172 in the enzyme active site for this system was revealed by X-ray crystallographic analysis.<sup>[415]</sup> The sulfur atom is positioned 4.9 Å below the pyrimidine ring, with the terminal methyl group of methionine located within van der Waals distance of the heterocycle (Figure 37b). DFT calculations on a simplified system (dimethylsulfide, thymine, *p*-cresole, and ammonium ion (mimicking the Arg side chain above Tyr 172; not shown)) revealed that the sulfur atom, although polarizable, does not experience any significant inductive effects in this arrangement; hence, the contribution of the sulfur atom to substrate binding comes solely in the form of steric, dispersion, and hydrophobic effects.<sup>[413]</sup> Subsequent experimental results showed that the mutant with the bio-isosteric modification of methionine to isoleucine indeed exhibited nearly identical activity to that of the wild-type enzyme.<sup>[414]</sup>

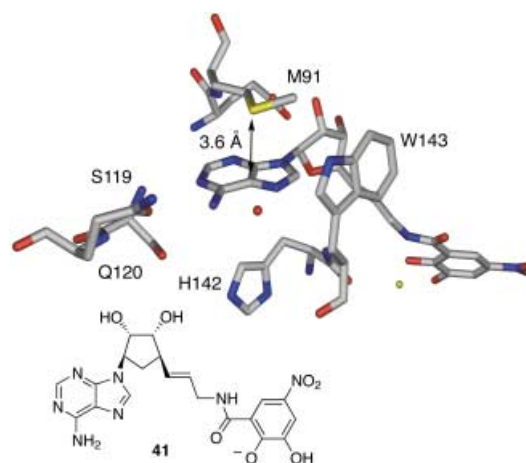
### 8.1.3. $S_{\text{Met}}$ -Adenine Interactions in Proteins

As with the thymidine kinase discussed above, PDB searches have revealed that adenine substrates or cofactors (ATP, ADP, AMP, FAD, *S*-adenosyl methionine (SAM), etc.) are often stabilized in the binding sites of enzymes (for example, kinases, hydrolases) by methionine side chains. While geometries similar to that shown in Figure 37b for the HSV1 TK complex are also common in these systems, we highlight here the arrangement that is similar to that found in the TGT active site (Figure 37a), namely, one that positions the C-S-C fragment coplanar with and directly above the purine ring, essentially at van der Waals distance (ca. 4.0 Å). Representative examples of  $S_{\text{Met}}$ -adenine interactions are shown in excerpts from the X-ray crystal structures of a ternary complex of retinol dehydratase (Figure 38a),<sup>[416]</sup> a ternary complex of chalcone *O*-methyltransferase (Figure 38b),<sup>[417]</sup> and a NAD<sup>+</sup> analogue complex of poly(ADP-ribose) polymerase (Figure 38c).<sup>[418]</sup> The common motif is intriguing as it directs one of the sulfur lone pairs into the  $\pi$  system—the distance must represent a subtle balance between repulsive and attractive forces. Analysis of these geometries by high-level computations is underway to shed light on the nature of the interaction. Also apparent from Figure 38 are the sandwich motifs common in these adenine-binding systems.

The bisubstrate inhibitor **41** has been shown to bind to Mg<sup>2+</sup>-containing catechol *O*-methyltransferase (COMT) with an IC<sub>50</sub> value of 9 nM; this enzyme is relevant in the treatment of Parkinson's disease.<sup>[419]</sup> The X-ray crystal structure of the ternary complex of COMT, **41**, and Mg<sup>2+</sup> ions (Figure 39)<sup>[419b]</sup>



**Figure 38.** Methionine–adenine interactions in transferases (for a more detailed description of the enzymes, see text). PDB codes: a) 1FML;<sup>[416]</sup> b) 1FP1;<sup>[417]</sup> c) 1A26.<sup>[418]</sup>



**Figure 39.**  $S_{\text{Met}}\cdots$ adenine interaction in the SAM binding pocket of the enzyme catechol *O*-methyltransferase complexed to the bisubstrate inhibitor **41** (PDB code: 1JR4; red sphere: water molecule, green sphere: magnesium ion).<sup>[419b]</sup>

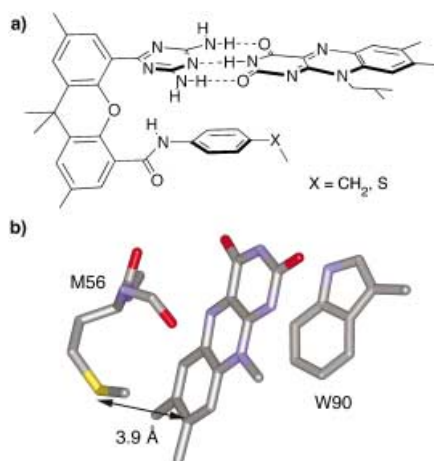
revealed that the adenine moiety (which occupies the *S*-adenosylmethionine (SAM) pocket of the enzyme) experiences favorable sulfur–arene contacts with Met91, and again depicts a planar C-S-C fragment positioned over the purine ring. The distance between the sulfur atom and the closest ring atom is 3.6 Å. A nearly identical sulfur–arene contact is found in the SAM–enzyme complex between Met 91 and the adenine moiety of the SAM cofactor.<sup>[420]</sup>

## 8.2. Energetic Aspects in Chemical and Biological Systems

### 8.2.1. Model Studies

The earliest studies by Morgan and co-workers examined the complexation of dimethylsulfide (DMS) by various aromatic compounds (for example, 1-methylnaphthalene) in  $\text{CCl}_4$  by analysis of the chemical shifts in the  $^1\text{H}$  NMR spectra.<sup>[421]</sup> Job plots confirmed a 1:1 binding stoichiometry at relatively high concentrations (1.1–3.7 M) of the components, while variable-temperature experiments provided estimates of the binding enthalpies ( $\Delta H^\circ \approx -0.8 \text{ kcal mol}^{-1}$ ). Complexation-induced changes in the chemical shifts led the authors to conclude that in most cases the methyl group of the DMS molecule was positioned over the aromatic ring center while the sulfur atom was in proximity to the ring edge.<sup>[422]</sup> This conclusion is in good agreement with the computational experiments described in the previous sections.<sup>[423]</sup> Subsequent NMR studies performed on deamino-oxytocin analogues by Hruby and co-workers revealed differences in the chemical shifts of aromatic side chain protons in proximity to a disulfide bridge.<sup>[424]</sup> An “edge-on” interaction was reasoned on the basis of chemical shift data, even though the observed downfield shifts were small ( $\Delta\delta \approx 0.06\text{--}0.08 \text{ ppm}$ ).

The receptor shown in Figure 40a has been designed to evaluate the contributions of donor atoms for flavin binding in flavodoxins.<sup>[425, 426]</sup> The xantheno scaffold nicely positions an



**Figure 40.** Sulfur–flavin interactions in a) a synthetic model systems<sup>[425]</sup> and b) flavodoxin from *Clostridium beijerinckii* (PDB code: 5NLL).<sup>[430]</sup>

aromatic residue below a noncovalently bound flavin substrate;  $^1\text{H}$  NMR studies in  $\text{CDCl}_3$  show a binding free enthalpy difference  $-\Delta\Delta G$  of about  $1 \text{ kcal mol}^{-1}$  for hosts bearing  $\text{X} = \text{CH}_2$  ( $K_a = 960 \text{ M}^{-1}$ ) versus  $\text{X} = \text{S}$  ( $K_a = 4800 \text{ M}^{-1}$ ).<sup>[425]</sup> Further computational studies (DFT methods) have identified a significant electrostatic contribution to the interaction. This observation is consistent with the positioning of sulfur under the electron-deficient pyrimidine moiety of the flavin ring system, however, no detectable overlap of the sulfur and aromatic orbitals or significant inductive effects could be detected.<sup>[426]</sup>

### 8.2.2. Employing Biological Systems

Although there have been only a few examples of site-directed mutagenesis experiments in proteins, they have provided compelling evidence for the stabilizing role of  $\text{S}_{\text{Met}}$ –arene interactions. Substitutions between contacting  $i$  and  $i+4$  residues of  $\alpha$ -helical peptides have given  $\Delta G^\circ$  values between  $-0.65$  and  $-0.80 \text{ kcal mol}^{-1}$  for Phe $\cdots$ Met interactions in two independent cases.<sup>[427]</sup> Building on earlier theoretical work of Hirono and co-workers,<sup>[428]</sup> Spencer and Stites demonstrated protein destabilization ( $0.8 \text{ kcal mol}^{-1}$ ) upon mutation of a Met residue (to Leu) situated nearby Phe and Tyr side chains.<sup>[429]</sup> Swenson and co-workers have shown in comprehensive mutational experiments with flavodoxins that a Met/Ala mutation reduces flavin binding by  $0.5 \text{ kcal mol}^{-1}$ , wherein the Met residue is known through crystallographic analysis to be positioned approximately  $3.9 \text{ \AA}$  above the flavin ring (Figure 40b).<sup>[430, 431]</sup> While all of these studies do reach some consensus in terms of  $\text{S}_{\text{Met}}$ –arene interaction energies ( $0.5\text{--}0.8 \text{ kcal mol}^{-1}$ ), the nature of the interaction in each case certainly varies.<sup>[432]</sup>

## 8.3. Outlook

Understanding the  $\text{S}\cdots\text{Ar}$  interaction in enzyme–substrate complexes, namely, its contribution to binding strength and geometry, has important consequences for the design of de novo inhibitors. In fact,  $\text{S}\cdots\text{Ar}$  contacts have only recently been considered, a priori, in drug development.<sup>[412, 419, 433]</sup> We anticipate intensified contributions along these lines in the future, particularly as modest to significant enhancements in binding can be realized with such a conservative substitution ( $-\text{S}$  versus  $-\text{CH}_2$ ). In closing, we do, however, note that while the “sulfur–arene interaction” implies direct participation of sulfur atoms in binding, it appears that this may only be true in a narrow range of cases, and further theoretical and experimental work is required to elucidate when such contacts are likely to occur.<sup>[434]</sup>

## 9. Summary

The accomplishments of more than 20 years of supramolecular chemistry research in advancing the knowledge of structure and energetics of individual intermolecular bonding interactions are now increasingly also recognized in the biomedical community. Examples of investigations with chemical systems that have profoundly influenced biology include the discovery of the cation– $\pi$  interaction and the revised view of the hydrophobic effect as a driving force for apolar complexation. Nevertheless, it has also become apparent that a single research approach, such as studying solution complexation with artificial receptors, is insufficient for enhancing the knowledge of molecular recognition phenomena up to a level at which it becomes directly useful for application in drug design and lead optimization. This situation has been fully taken into account in this review which presents, in addition to findings from supramolecular

chemistry, quantitative investigations from biostructural research, crystallographic database mining, gas-phase study, and theoretical calculations. In particular, the analysis of the dramatically increasing number of protein crystal structures using modern software is increasingly becoming a fertile ground for advanced molecular recognition study. The more classical interactions involving  $\pi$ - $\pi$ -stacking and edge-to-face contacts between aromatic rings continue to attract interest in terms of further refined geometries and energy models. The discovery of cation- $\pi$  interactions has created a "hot" area of research in biology, and these contacts are increasingly finding application in modern drug design. Ample opportunities exist for further exploring fluorine-arene and sulfur-arene interactions; experimental studies targeting H bonding to  $\pi$  surfaces in solution complexes also remain poorly developed. While the complexity of ion pairs and their interactions with aromatic rings has been identified, both experimental and computational studies of these interactions are in their infancy. Add to this the true challenge in future computational chemistry of handling fully solvated chemical and biological complexation processes with acceptable speed at a high level of theory and accuracy. From these few examples, it becomes clear that molecular recognition studies in chemistry and biology will remain a fascinating area of future research.

We thank F. Hoffmann-La Roche Ltd (Basel), the ETH Research Council, the Fonds der Chemischen Industrie, and the U.S. National Science Foundation for their generous support of this research. Continuing fruitful discussions with Prof. Klaus Müller (Roche, Basel), Prof. Jack D. Dunitz (ETH Zürich), and Prof. Gerhard Klebe (Univ. Marburg) are gratefully acknowledged. Furthermore, F.D. wishes to thank all the scientists at Global Roche involved in biostructural research; their findings as discussed in numerous consulting sessions have initiated and stimulated many of the ongoing molecular recognition studies with biological receptors in the Diederich laboratories at ETH Zürich. Contributions of the many enthusiastic co-workers in the Diederich research group are acknowledged through the literature citations. R.K.C. is grateful to the U.S. National Science Foundation (postdoctoral fellowship) and the University of Florida for financial support. Finally, we thank Prof. G. W. Gokel, Prof. F.-G. Klärner, and Dr. K. Deshayes for providing drawings of their receptors and complexes.

Received: November 4, 2002 [A563]

- [1] a) G. Kryger, I. Silman, J. L. Sussman, *J. Physiol.* **1998**, *92*, 191–194; b) G. Kryger, I. Silman, J. L. Sussman, *Structure* **1999**, *7*, 297–307.
- [2] a) J.-M. Lehn, *Supramolecular Chemistry: Concepts and Perspectives*, VCH, New York, **1995**; b) *Comprehensive Supramolecular Chemistry*, Vols. 1–10 (Eds.: J. L. Atwood, J. E. D. Davies, D. D. MacNicol, F. Vögtle, J.-M. Lehn), Pergamon, Oxford, **1996**; c) *Chem. Rev.* **1997**, *97*, 1231–1734 (special issue on molecular recognition (Ed.: S. H. Gellman)); d) H.-J. Schneider, A. Yatsimirsky, *Principles and Methods in Supramolecular Chemistry*, Wiley, Chichester, **2000**; e) J. W. Steed, J. L. Atwood, *Supramolecular Chemistry*, Wiley, Chichester, **2000**; f) *Proc. Natl. Acad. Sci. USA* **2002**, *99*, 4755–5750 (special issue on supramolecular chemistry and self-assembly (Ed.: J. Halpern)).
- [3] *Curr. Opin. Chem. Biol.* **2002**, *6*, 11–12 (special issue on proteomics and genomics (Eds.: J. D. Hoheisel, D. Cahill)).
- [4] P. Betschmann, S. Sahli, F. Diederich, U. Obst, V. Gramlich, *Helv. Chim. Acta* **2002**, *85*, 1210–1245.
- [5] U. Obst, D. W. Banner, L. Weber, F. Diederich, *Chem. Biol.* **1997**, *4*, 287–295.
- [6] S. K. Burley, G. A. Petsko, *Science* **1985**, *229*, 23–28.
- [7] J. C. Ma, D. A. Dougherty, *Chem. Rev.* **1997**, *97*, 1303–1324.
- [8] A. Niedzwiecka, J. Marcotrigiano, J. Stepinski, M. Jankowska-Anyszka, A. Wyslouch-Cieszyńska, M. Dadlez, A.-C. Gingras, P. Mak, E. Darzynkiewicz, N. Sonenberg, S. K. Burley, R. Stolarski, *J. Mol. Biol.* **2002**, *319*, 615–635.
- [9] a) F. Diederich, *Angew. Chem.* **1988**, *100*, 372–396; *Angew. Chem. Int. Ed. Engl.* **1988**, *27*, 362–386; b) F. Vögtle, *Cyclophane Chemistry*, Teubner, Stuttgart, **1990**; c) C. Seel, F. Vögtle, *Angew. Chem.* **1992**, *104*, 542–563; *Angew. Chem. Int. Ed. Engl.* **1992**, *31*, 528–549; d) T. H. Webb, C. S. Wilcox, *Chem. Soc. Rev.* **1993**, *22*, 383–395; e) *Comprehensive Supramolecular Chemistry*, Vol. 2 (Ed.: F. Vögtle), Elsevier/Pergamon, Oxford, **1996**; this volume contains the following chapters on cyclophane complexation: H.-J. Schneider, A. K. Mohammad-Ali, pp. 69–101; A. Pochini, R. Ungaro, pp. 103–142; K. Odashima, K. Koga, pp. 143–194; D. A. Dougherty, pp. 195–209; F. Vögtle, C. Seel, P.-M. Windschief, pp. 211–265; Y. Aoyama, pp. 279–307; B. J. Whitlock, H. W. Whitlock, pp. 309–324; A. Collet, pp. 325–365; Y. Murakami, O. Hayashida, pp. 419–438; f) see also: M. Inouye, K. Fujimoto, M. Furusyo, H. Nakazumi, *J. Am. Chem. Soc.* **1999**, *121*, 1452–1458.
- [10] F. Diederich, *Cyclophanes*, The Royal Society of Chemistry, Cambridge, **1991**.
- [11] a) A. W. Schwabacher, J. Lee, H. Lei, *J. Am. Chem. Soc.* **1992**, *114*, 7597–7598; b) M. Fujita, S. Nagao, M. Ida, K. Ogata, K. Ogura, *J. Am. Chem. Soc.* **1993**, *115*, 1574–1576; c) H. Chen, S. Ogo, R. H. Fish, *J. Am. Chem. Soc.* **1996**, *118*, 4993–5001.
- [12] S. B. Ferguson, E. M. Sanford, E. M. Seward, F. Diederich, *J. Am. Chem. Soc.* **1991**, *113*, 5410–5419.
- [13] D. B. Smithrud, T. B. Wyman, F. Diederich, *J. Am. Chem. Soc.* **1991**, *113*, 5420–5426.
- [14] F. Diederich, D. B. Smithrud, E. M. Sanford, T. B. Wyman, S. B. Ferguson, D. R. Carcanague, I. Chao, K. N. Houk, *Acta Chem. Scand.* **1992**, *46*, 205–215.
- [15] S. B. Ferguson, E. M. Seward, F. Diederich, E. M. Sanford, A. Chou, P. Inocencio-Szweda, C. B. Knobler, *J. Org. Chem.* **1988**, *53*, 5593–5595.
- [16] For recent applications of cyclophanes such as **1**, see a) S. Anderson, R. T. Aplin, T. D. W. Claridge, T. Goodson III, A. C. Maciel, G. Rumbles, J. F. Ryan, H. L. Anderson, *J. Chem. Soc. Perkin Trans. 2* **1998**, 2383–2397; b) J. Huuskonen, J. E. H. Buston, N. D. Scotchmer, H. L. Anderson, *New J. Chem.* **1999**, *23*, 1245–1252; c) D. R. Benson, J. Fu, *Tetrahedron Lett.* **1996**, *37*, 4833–4836; d) D. R. Benson, J. Fu, C. F. Johnson, S. W. Pauls, D. A. Williamson, *J. Org. Chem.* **1998**, *63*, 9935–9945; e) D. A. Williamson, A. M. Barenberg, C. A. Coleman, D. R. Benson, *Chemosphere* **2000**, *40*, 1443–1446.
- [17] a) W. Kauzmann, *Adv. Protein Chem.* **1959**, *16*, 1–63; b) C. Tanford, *The Hydrophobic Effect: Formation of Micelles and Biological Membranes*, 2nd ed., Wiley, New York, **1980**; c) A. Ben-Naim, *Hydrophobic Interactions*, Plenum, New York, **1980**; d) N. T. Southall, K. A. Dill, A. D. J. Haymet, *J. Phys. Chem. B* **2002**, *106*, 521–533.
- [18] W. Blokzijl, J. B. F. N. Engberts, *Angew. Chem.* **1993**, *105*, 1610–1648; *Angew. Chem. Int. Ed. Engl.* **1993**, *32*, 1545–1579.

- [19] D. A. Stauffer, R. E. Barrans, Jr., D. A. Dougherty, *J. Org. Chem.* **1990**, *55*, 2762–2767.
- [20] E. L. Piatnitski, R. A. Flowers II, K. Deshayes, *Chem. Eur. J.* **2000**, *6*, 999–1006.
- [21] For other examples of enthalpy-controlled arene complexation by cyclophanes in water, see a) I. K. Chun, M. W. Lee, *J. Korean Pharm. Sci.* **1989**, *19*, 71–75; b) R. M. Izatt, K. Pawlak, J. S. Bradshaw, R. L. Bruening, *Chem. Rev.* **1995**, *95*, 2529–2586.
- [22] B. R. Peterson, P. Wallimann, D. R. Carcanague, F. Diederich, *Tetrahedron* **1995**, *51*, 401–421.
- [23] a) K. Harata, *Bull. Chem. Soc. Jpn.* **1979**, *52*, 1807–1812; b) K. Harata, K. Tsuda, K. Uekama, M. Otagiri, F. Hirayama, *J. Inclusion Phenom.* **1988**, *6*, 135–142; c) G. L. Bertrand, J. R. Faulkner, Jr., S. M. Han, D. W. Armstrong, *J. Phys. Chem. B* **1989**, *93*, 6863–6867; d) E. Junquera, V. G. Baonza, E. Aicart, *Can. J. Chem.* **1999**, *77*, 348–355.
- [24] J. C. Harrison, M. R. Eftink, *Biopolymers* **1982**, *21*, 1153–1166.
- [25] M. R. Eftink, M. L. Andy, K. Bystrom, H. D. Perlmutter, D. S. Kristol, *J. Am. Chem. Soc.* **1989**, *111*, 6765–6772.
- [26] E. Junquera, J. Laynez, M. Menéndez, S. Sharma, S. Penadés, *J. Org. Chem.* **1996**, *61*, 6790–6798.
- [27] K. Kano, T. Kitae, Y. Shimofuri, N. Tanaka, Y. Mineta, *Chem. Eur. J.* **2000**, *6*, 2705–2713.
- [28] M. V. Rekharsky, Y. Inoue, *Chem. Rev.* **1998**, *98*, 1875–1917.
- [29] H.-J. Böhm, G. Klebe, *Angew. Chem.* **1996**, *108*, 2750–2778; *Angew. Chem. Int. Ed. Engl.* **1996**, *35*, 2588–2614.
- [30] D. D. F. Shiao, J. M. Sturtevant, *Biochemistry* **1969**, *8*, 4910–4917.
- [31] a) L. Beres, J. M. Sturtevant, *Biochemistry* **1971**, *10*, 2120–2126; b) R. L. Biltonen, N. Langerman, *Methods Enzymol.* **1979**, *61*, 287–317; c) P. D. Ross, S. Subramanian, *Biochemistry* **1981**, *20*, 3096–3102; d) H.-J. Hinz, *Annu. Rev. Biophys. Bioeng.* **1983**, *12*, 285–317.
- [32] L. Sebo, B. Schweizer, F. Diederich, *Helv. Chim. Acta* **2000**, *83*, 80–92.
- [33] R. Talhout, J. B. F. N. Engberts, *Eur. J. Biochem.* **2001**, *268*, 1554–1560.
- [34] a) W. Y. Chou, L. A. Marky, S. Zaunczkowski, K. J. Breslauer, *J. Biomol. Struct. Dyn.* **1987**, *5*, 345–359; b) A. Kagemoto, A. Kunihiro, Y. Baba, *Thermochim. Acta* **1994**, *242*, 65–75; c) A. Odani, T. Sekiguchi, H. Okada, S. Ishiguro, O. Yamauchi, *Bull. Chem. Soc. Jpn.* **1995**, *68*, 2093–2102; d) J. Ren, T. C. Jenkins, J. B. Chaires, *Biochemistry* **2000**, *39*, 8439–8447; e) T.-K. Li, E. Bathory, E. J. LaVoie, A. R. Srinivasan, W. K. Olson, R. R. Sauers, L. F. Liu, D. S. Pilch, *Biochemistry* **2000**, *39*, 7107–7116.
- [35] H. P. Hopkins, Jr., Y. Ming, W. D. Wilson, D. W. Boykin, *Biopolymers* **1991**, *31*, 1105–1114.
- [36] D. P. Remeta, C. P. Mudd, R. L. Berger, K. J. Breslauer, *Biochemistry* **1993**, *32*, 5064–5073.
- [37] Since most of the minor-groove-binding drugs also possess cationic residues for ion pairing with the DNA phosphate backbone and additionally may undergo many H-bonding interactions, both favorable enthalpic and entropic terms are sometimes observed. a) L. A. Marky, K. J. Breslauer, *Proc. Natl. Acad. Sci. USA* **1987**, *84*, 4359–4363; b) N. Patel, H. Berglund, L. Nilsson, R. Rigler, L. W. McLaughlin, A. Gräslund, *Eur. J. Biochem.* **1992**, *203*, 361–366; c) D. S. Pilch, N. Poklar, C. A. Gelfand, S. M. Law, K. J. Breslauer, E. E. Baird, P. B. Dervan, *Proc. Natl. Acad. Sci. USA* **1996**, *93*, 8206–8311; d) D. S. Pilch, N. Poklar, E. E. Baird, P. B. Dervan, K. J. Breslauer, *Biochemistry* **1999**, *38*, 2143–2151.
- [38] K. J. Breslauer, D. P. Remeta, W.-Y. Chou, R. Ferrante, J. Curry, D. Zaunczkowski, J. G. Snyder, L. A. Marky, *Proc. Natl. Acad. Sci. USA* **1987**, *84*, 8922–8926.
- [39] Recent investigations show that the thermodynamic quantities for minor-groove intercalation are highly dependent on the structure, solvation, and sequence of the DNA binding site: L. Wang, A. Kumar, D. W. Boykin, C. Bailly, W. D. Wilson, *J. Mol. Biol.* **2002**, *317*, 361–374.
- [40] I. Jelesarov, L. Leder, H. R. Bosshard, *Methods* **1996**, *9*, 533–541.
- [41] C. P. Swaminathan, A. Nandi, S. S. Visweswariah, A. Surolia, *J. Biol. Chem.* **1999**, *274*, 31272–31278.
- [42] P. C. Ackroyd, J. Cleary, G. D. Glick, *Biochemistry* **2001**, *40*, 2911–2922.
- [43] a) J. Selig, *Biochim. Biophys. Acta* **1997**, *1331*, 103–116; b) T. Wieprecht, M. Beyermann, J. Selig, *Biochemistry* **1999**, *38*, 10377–10387.
- [44] S. R. Vippagunta, A. Dorn, H. Matile, A. K. Bhattacharjee, J. M. Karle, W. Y. Ellis, R. G. Ridley, J. L. Vennerstrom, *J. Med. Chem.* **1999**, *42*, 4630–4639.
- [45] S. R. Vippagunta, A. Dorn, R. G. Ridley, J. L. Vennerstrom, *Biochim. Biophys. Acta* **2000**, *1475*, 133–140.
- [46] Y. Inoue, Y. Liu, L.-H. Tong, B.-J. Shen, D.-S. Jin, *J. Am. Chem. Soc.* **1993**, *115*, 10637–10644.
- [47] a) E. Grunwald, C. Steel, *J. Am. Chem. Soc.* **1995**, *117*, 5687–5692; b) M. S. Searle, M. S. Westwell, D. H. Williams, *J. Chem. Soc. Perkin Trans. 1* **1995**, 141–151; c) J. D. Dunitz, *Chem. Biol.* **1995**, *2*, 709–712; d) L. Liu, Q.-X. Guo, *Chem. Rev.* **2001**, *101*, 673–695.
- [48] D. B. Smithrud, E. M. Sanford, I. Chao, S. B. Ferguson, D. R. Carcanague, J. Evanseck, K. N. Houk, F. Diederich, *Pure Appl. Chem.* **1990**, *62*, 2227–2236.
- [49] T. Z. Mordasini Denti, W. F. van Gunsteren, F. Diederich, *J. Am. Chem. Soc.* **1996**, *118*, 6044–6051.
- [50] C. Reichardt, *Solvent Effects in Organic Chemistry*, 2nd ed., VCH, Weinheim, **1988**, pp. 339–405.
- [51] a) H. J. Schneider, R. Kramer, S. Simova, U. Schneider, *J. Am. Chem. Soc.* **1988**, *110*, 6442–6448; b) A. Mirzoian, A. E. Kaifer, *J. Org. Chem.* **1995**, *60*, 8093–8095; c) M. S. Cubberley, B. L. Iverson, *J. Am. Chem. Soc.* **2001**, *123*, 7560–7563.
- [52] C. A. Berg-Brennan, D. I. Yoon, R. V. Slone, A. P. Kazala, J. T. Hupp, *Inorg. Chem.* **1996**, *35*, 2032–2035.
- [53] a) B. Zhang, R. Breslow, *J. Am. Chem. Soc.* **1997**, *119*, 1676–1681; b) C.-S. Kim, K. C. Russell, *Tetrahedron Lett.* **1999**, *40*, 3835–3838.
- [54] Ref. [10], p. 253.
- [55] W. Saenger, *Angew. Chem.* **1980**, *92*, 343–361; *Angew. Chem. Int. Ed. Engl.* **1980**, *19*, 344–362.
- [56] a) O. Sinanoglu in *Molecular Associations in Biology* (Ed.: B. Pullman), Academic Press, New York, **1968**, pp. 427–445; b) O. Sinanoglu in *Molecular Interactions, Vol. 3* (Ed.: W. J. Orville-Thomas), Wiley, Chichester, **1982**, pp. 283–342.
- [57] a) B. Lee, *Biopolymers* **1985**, *24*, 813–823; b) J. Canceill, L. Lacombe, A. Collet, *J. Am. Chem. Soc.* **1986**, *108*, 4230–4232; c) R. J. Clarke, J. H. Coates, S. F. Lincoln, *Adv. Carbohydr. Chem. Biochem.* **1988**, *46*, 205–249; d) A. Örstan, A. Ross, *J. Phys. Chem.* **1987**, *91*, 2739–2745.
- [58] C. Carey, Y.-K. Cheng, P. J. Rossky, *Chem. Phys.* **2000**, *258*, 415–425.
- [59] N. T. Southall, K. A. Dill, *J. Phys. Chem. B* **2000**, *104*, 1326–1331.
- [60] a) T. Lazaridis, M. E. Paulaitis, *J. Phys. Chem.* **1994**, *98*, 635–642; b) R. U. Lemieux, *Acc. Chem. Res.* **1996**, *29*, 373–380; c) B. D. Isbister, P. M. St. Hilaire, E. J. Toone, *J. Am. Chem. Soc.* **1995**, *117*, 12877–12878.
- [61] D. B. Smithrud, F. Diederich, *J. Am. Chem. Soc.* **1990**, *112*, 339–343.
- [62] a) A. Fersht, *Enzyme Structure and Mechanism*, Freeman, New York, **1985**, pp. 293–310; b) A. Fersht, C. Dingwall, *Biochemistry* **1979**, *18*, 1245–1249; c) J. A. McCammon, P. G. Wolynes, M. Karplus, *Biochemistry* **1979**, *18*, 927–942.
- [63] a) R. Castro, M. J. Berardi, E. Cordoba, M. Ochoa de Olza, A. E. Kaifer, J. D. Evanseck, *J. Am. Chem. Soc.* **1996**, *118*,



- 10257–10268; b) V. E. Williams, R. P. Lemieux, *J. Am. Chem. Soc.* **1998**, *120*, 11311–11315; c) M. Enescu, B. Levy, V. Gheorghe, *J. Phys. Chem. B* **2000**, *104*, 1073–1077; d) T. Liu, H.-J. Schneider, *Angew. Chem.* **2002**, *114*, 1418–1420; *Angew. Chem. Int. Ed.* **2002**, *41*, 1368–1370.
- [64] W. C. Cromwell, K. Bystrom, M. R. Eftink, *J. Phys. Chem.* **1985**, *89*, 326–332.
- [65] J. Espinosa, S. H. Gellman, *Angew. Chem.* **2000**, *112*, 2420–2423; *Angew. Chem. Int. Ed.* **2000**, *39*, 2330–2333.
- [66] S. Mecozzi, J. Rebek, Jr., *Chem. Eur. J.* **1998**, *4*, 1016–1022.
- [67] J. Dunitz in *Perspectives in Supramolecular Chemistry: The Crystal as a Supramolecular Entity* (Ed.: G. R. Desiraju), Wiley, Chichester, **1996**, pp. 1–30.
- [68] H. M. Berman, T. Battistuz, T. N. Bhat, F. Bluhm, P. E. Bourne, K. Burkhardt, Z. Feng, G. L. Gilliland, L. Iype, S. Jain, P. Fagan, J. Marvin, D. Padilla, V. Ravichandran, N. Thanki, H. Weissig, J. D. Westbrook, C. Zardecki, *Acta Crystallogr. Sect. D* **2002**, *58*, 899–907.
- [69] a) I. J. Bruno, J. C. Cole, J. P. M. Lommerse, R. S. Rowland, R. Taylor, M. L. Verdonk, *J. Comput.-Aided Mol. Des.* **1997**, *11*, 525–537; b) D. R. Boer, J. Kroon, J. C. Cole, B. Smith, M. L. Verdonk, *J. Mol. Biol.* **2001**, *312*, 275–287; c) A. Bergner, J. Günther, M. Hendlich, G. Klebe, M. Verdonk, *Biopolymers* **2002**, *61*, 99–110; Relibase+, V.1.1., CCDC, Cambridge, **2001**.
- [70] a) R. Taylor, *Acta Crystallogr. Sect. D* **2002**, *58*, 879–888; b) F. H. Allen, *Acta Crystallogr. Sect. B* **2002**, *58*, 380–388; c) I. J. Bruno, J. C. Cole, P. R. Edgington, M. Kessler, C. F. Macrae, P. McCabe, J. Pearson, R. Taylor, *Acta Crystallogr. Sect. B* **2002**, *58*, 389–397.
- [71] Over 257 000 structures have been deposited in the CSD (August 2002) while the last update (August 13, 2002) gave 18 464 structures in the PDB.
- [72] G. A. Jeffrey, *An Introduction to Hydrogen Bonding*, Oxford University Press, New York, **1997**.
- [73] G. A. Jeffrey, W. Saenger, *Hydrogen Bonding in Biological Structures*, Springer, Berlin, **1991**.
- [74] G. R. Desiraju, T. Steiner, *The Weak Hydrogen Bond*, Oxford University Press, New York, **1999**.
- [75] a) R. Taylor, O. Kennard, *J. Am. Chem. Soc.* **1982**, *104*, 5063–5070; b) Z. S. Derewenda, L. Lee, U. Derewenda, *J. Mol. Biol.* **1995**, *252*, 248–262; c) G. R. Desiraju, *Acc. Chem. Res.* **1996**, *29*, 441–449; d) M. C. Wahl, M. Sundaralingam, *Trends Biochem. Sci.* **1997**, *22*, 97–101; e) Y. Mandel-Gutfreund, H. Margalit, R. L. Jernigan, V. B. Zhurkin, *J. Mol. Biol.* **1998**, *277*, 1129–1140; f) G. R. Desiraju, *Acc. Chem. Res.* **2002**, *35*, 565–573.
- [76] J. D. Dunitz, A. Gavezzotti, *Acc. Chem. Res.* **1999**, *32*, 677–684.
- [77] E. G. Cox, D. W. J. Cruickshank, J. A. S. Smith, *Proc. R. Soc. London Ser. A* **1958**, *247*, 1–21.
- [78] D. E. Williams, Y. Xiao, *Acta Crystallogr. Sect. A* **1993**, *49*, 1–10.
- [79] B. P. van Eijck, A. L. Spek, W. T. M. Mooij, J. Kroon, *Acta Crystallogr. Sect. B* **1998**, *54*, 291–299, and references therein.
- [80] G. Klebe, F. Diederich, *Philos. Trans. R. Soc. London Ser. A* **1993**, *345*, 37–48.
- [81] a) M. Gurrath, G. Müller, H.-D. Höltje, *Perspect. Drug Discovery Des.* **1998**, *12*, 135–157; b) A. Vedani, P. Zbinden, J. P. Snyder, P. A. Greenidge, *J. Am. Chem. Soc.* **1995**, *117*, 4987–4994.
- [82] D. T. Bong, M. R. Ghadiri, *Angew. Chem.* **2001**, *113*, 2221–2224; *Angew. Chem. Int. Ed.* **2001**, *40*, 2163–2166.
- [83] A. Gavezzotti, *Synlett* **2002**, 201–214.
- [84] W. D. S. Motherwell, H. L. Ammon, J. D. Dunitz, A. Dzyabchenko, P. Erk, A. Gavezzotti, D. W. M. Hofmann, F. J. J. Leusen, J. P. M. Lommerse, W. T. M. Mooij, S. L. Price, H. Scheraga, B. Schweizer, M. U. Schmidt, B. P. van Eijck, P. Verwer, D. E. Williams, *Acta Crystallogr. Sect. B* **2002**, *58*, 647–661.
- [85] G. R. Desiraju, A. Gavezzotti, *J. Chem. Soc. Chem. Commun.* **1989**, 621–623.
- [86] G. R. Desiraju, *Angew. Chem.* **1995**, *107*, 2541–2558; *Angew. Chem. Int. Ed. Engl.* **1995**, *34*, 2311–2327.
- [87] C. V. K. Sharma, K. Panneerselvam, L. Shimoni, H. Katz, H. L. Carrell, G. R. Desiraju, *Chem. Mater.* **1994**, *6*, 1282–1292.
- [88] a) C. Janiak, *J. Chem. Soc. Dalton Trans.* **2000**, 3885–3896; for a recent review on aromatic interactions, see b) C. A. Hunter, K. R. Lawson, J. Perkins, C. J. Urch, *J. Chem. Soc. Perkin Trans. 2* **2001**, 651–669.
- [89] J. P. Glusker, *Top. Curr. Chem.* **1998**, *198*, 1–56.
- [90] S. K. Burley, G. A. Petsko, *Adv. Protein Chem.* **1988**, *39*, 125–189.
- [91] G. B. McGaughey, M. Gagné, A. K. Rappé, *J. Biol. Chem.* **1998**, *273*, 15458–15463.
- [92] a) J. Singh, J. M. Thornton, *FEBS Lett.* **1985**, *191*, 1–6; b) C. A. Hunter, J. Singh, J. M. Thornton, *J. Mol. Biol.* **1991**, *218*, 837–846; c) U. Samanta, D. Pal, P. Chakrabarti, *Acta Crystallogr. Sect. D* **1999**, *55*, 1421–1427.
- [93] R. Bhattacharyya, U. Samanta, P. Chakrabarti, *Protein Eng.* **2002**, *15*, 91–100, and references therein.
- [94] R. Chelli, F. L. Gervasio, P. Procacci, V. Schettino, *J. Am. Chem. Soc.* **2002**, *124*, 6133–6143.
- [95] N. Kannan, S. Vishveshwara, *Protein Eng.* **2000**, *13*, 753–761.
- [96] C. Ibarra, B. S. Nieslanik, W. M. Atkins, *Biochemistry* **2001**, *40*, 10614–10624.
- [97] F. A. Quirocho, G. Hu, P. D. Gershon, *Curr. Opin. Struct. Biol.* **2000**, *10*, 78–86.
- [98] a) D. Liu, D. A. Williamson, M. L. Kennedy, T. D. Williams, M. M. Morton, D. R. Benson, *J. Am. Chem. Soc.* **1999**, *121*, 11798–11812; b) K. Kano, K. Fukuda, H. Wakami, R. Nishiyabu, R. F. Pasternack, *J. Am. Chem. Soc.* **2000**, *122*, 7494–7502.
- [99] Y. Wang, X. Hu, *J. Am. Chem. Soc.* **2002**, *124*, 8445–8451.
- [100] E. Gazit, *FASEB J.* **2002**, *16*, 77–83.
- [101] S. R. Griffiths-Jones, M. S. Searle, *J. Am. Chem. Soc.* **2000**, *122*, 8350–8356.
- [102] C. D. Tatko, M. L. Waters, *J. Am. Chem. Soc.* **2002**, *124*, 9372–9373.
- [103] B. J. Hillier, H. M. Rodriguez, L. M. Gregoret, *Folding Des.* **1998**, *3*, 87–93.
- [104] L. Serrano, M. Bycroft, A. R. Fersht, *J. Mol. Biol.* **1991**, *218*, 465–475.
- [105] S. M. Butterfield, P. R. Patel, M. L. Waters, *J. Am. Chem. Soc.* **2002**, *124*, 9751–9755.
- [106] a) K. C. Janda, J. C. Hemminger, J. S. Winn, S. E. Novick, S. J. Harris, W. Klemperer, *J. Chem. Phys.* **1975**, *63*, 1419–1421; b) J. M. Steed, T. A. Dixon, W. Klemperer, *J. Chem. Phys.* **1979**, *70*, 4940–4946.
- [107] S. Sun, E. R. Bernstein, *J. Phys. Chem.* **1996**, *100*, 13348–13366.
- [108] R. Laatikainen, J. Ratilainen, R. Sebastian, H. Santa, *J. Am. Chem. Soc.* **1995**, *117*, 11006–11010.
- [109] G. D. Smith, R. L. Jaffe, *J. Phys. Chem.* **1996**, *100*, 9624–9630.
- [110] a) R. L. Jaffe, G. D. Smith, *J. Chem. Phys.* **1996**, *105*, 2780–2788; b) P. Hobza, H. L. Selzle, E. W. Schlag, *J. Phys. Chem.* **1996**, *100*, 18790–18794; c) F. Tran, J. Weber, T. A. Wesolowski, *Helv. Chim. Acta* **2001**, *84*, 1489–1503; d) M. O. Sinnokrot, E. F. Valeev, C. D. Sherril, *J. Am. Chem. Soc.* **2002**, *124*, 10887–10893.
- [111] a) S. Tsuzuki, K. Honda, T. Uchamaru, M. Mikami, K. Tanabe, *J. Am. Chem. Soc.* **2002**, *124*, 104–112  $D_0$ : stabilization energies, are given with a negative sign throughout the review. The zero-point vibration energy ( $\Delta ZPV$ ) has been calculated

- for the T-shaped dimer, which gives a  $D_0$  value of about  $-2.2 \text{ kcal mol}^{-1}$  ( $D_0 = D_c - \Delta ZPV$ ).
- [112] a) H. Krause, B. Ernstberger, H. J. Neusser, *Chem. Phys. Lett.* **1991**, *184*, 411–417; b) H. J. Neusser, H. Krause, *Chem. Rev.* **1994**, *94*, 1829–1843.
- [113] J. R. Grover, E. A. Walters, E. T. Hui, *J. Phys. Chem.* **1987**, *91*, 3233–3237.
- [114] P. Hobza, H. L. Selzle, E. W. Schlag, *J. Am. Chem. Soc.* **1994**, *116*, 3500–3506.
- [115] a) C. Gonzalez, E. C. Lim, *J. Phys. Chem. A* **2000**, *104*, 2953–2957; b) N. K. Lee, S. Park, S. K. Kim, *J. Chem. Phys.* **2002**, *116*, 7910–7917.
- [116] M. D. Blanchard, R. P. Hughes, T. E. Concolino, A. L. Rheingold, *Chem. Mater.* **2000**, *12*, 1604–1610.
- [117] G. R. Dennis, G. L. D. Ritchie, *J. Phys. Chem.* **1991**, *95*, 656–660.
- [118] C. A. Hunter, *Angew. Chem.* **1993**, *105*, 1653–1655; *Angew. Chem. Int. Ed. Engl.* **1993**, *32*, 1584–1586. The induction energies arising, for example, from the interaction of polarizable sites with the quadrupole moment, as well as charge-transfer, do not contribute significantly to the overall binding energy.
- [119] a) D. H. Rich, *Perspect. Med. Chem.* **1993**, 15–25; b) A. M. Davis, S. J. Teague, *Angew. Chem.* **1999**, *111*, 778–792; *Angew. Chem. Int. Ed.* **1999**, *38*, 736–749.
- [120] W. L. Jorgensen, D. L. Severance, *J. Am. Chem. Soc.* **1990**, *112*, 4768–4774.
- [121] P. Linse, *J. Am. Chem. Soc.* **1992**, *114*, 4366–4373.
- [122] C. Chipot, R. Jaffe, B. Maignet, D. A. Pearlman, P. A. Kollman, *J. Am. Chem. Soc.* **1996**, *118*, 11217–11224.
- [123] a) S. Ishikawa, T. Ebata, H. Ishikawa, T. Inoue, N. Mikami, *J. Phys. Chem.* **1996**, *100*, 10531–10535; b) F. L. Gervasio, R. Chelli, P. Procacci, V. Schettino, *J. Phys. Chem. A* **2002**, *106*, 2945–2948.
- [124] S. B. Ferguson, F. Diederich, *Angew. Chem.* **1986**, *98*, 1127–1129; *Angew. Chem. Int. Ed. Engl.* **1986**, *25*, 1127–1129.
- [125] The electron donor/acceptor (EDA) interaction has been introduced to qualitatively describe the attraction between two aromatic rings, one with strong donor and the other with strong acceptor character. This situation affects and introduces polarization as well as a dipole moment in addition to the dispersion and charge-transfer (CT) term. However, this concept can be misleading for describing interactions between aromatic rings, and the use of quadrupoles should be preferred.
- [126] a) M. Kamieth, F.-G. Klärner, F. Diederich, *Angew. Chem.* **1998**, *110*, 3497–3500; *Angew. Chem. Int. Ed.* **1998**, *37*, 3303–3306; b) F.-G. Klärner, U. Burkert, M. Kamieth, R. Boese, J. Benet-Buchholz, *Chem. Eur. J.* **1999**, *5*, 1700–1707.
- [127] a) C. A. Schalley, R. K. Castellano, M. S. Brody, D. M. Rudkevich, G. Siuzdak, J. Rebek, Jr., *J. Am. Chem. Soc.* **1999**, *121*, 4568–4579; b) C. Zonta, S. Cossu, O. De Lucchi, *Eur. J. Org. Chem.* **2000**, 1965–1971.
- [128] S. Kubik, R. Goddard, *Eur. J. Org. Chem.* **2001**, 311–322.
- [129] C. A. Hunter, J. K. M. Sanders, *J. Am. Chem. Soc.* **1990**, *112*, 5525–5534.
- [130] K. Müller-Dethlefs, P. Hobza, *Chem. Rev.* **2000**, *100*, 143–167.
- [131] a) A. Galán, D. Andreu, A. M. Echavarren, P. Prados, J. de Mendoza, *J. Am. Chem. Soc.* **1992**, *114*, 1511–1512; b) C. Raposo, M. Martín, M. L. Mussons, M. Crego, J. Anaya, M. C. Caballero, J. R. Morán, *J. Chem. Soc. Perkin Trans. 1* **1994**, 2113–2116; c) A. S. Shetty, J. Zhang, J. S. Moore, *J. Am. Chem. Soc.* **1996**, *118*, 1019–1027; d) J. Cuntze, F. Diederich, *Helv. Chim. Acta* **1997**, *80*, 897–911; e) J. N. H. Reek, A. H. Priem, H. Engelkamp, A. E. Rowan, J. A. A. W. Elemans, R. J. M. Nolte, *J. Am. Chem. Soc.* **1997**, *119*, 9956–9964; f) D. J. Hill, J. S. Moore, *Proc. Natl. Acad. Sci. USA* **2002**, *99*, 5053–5057.
- [132] F. J. Carver, C. A. Hunter, P. S. Jones, D. J. Livingstone, J. F. McCabe, E. M. Seward, P. Tiger, S. E. Spey, *Chem. Eur. J.* **2001**, *7*, 4854–4862.
- [133] F. J. Carver, C. A. Hunter, D. J. Livingstone, J. F. McCabe, E. M. Seward, *Chem. Eur. J.* **2002**, *8*, 2848–2859.
- [134] A. G. Martínez, J. O. Barcina, A. de Fresno Cerezo, *Chem. Eur. J.* **2001**, *7*, 1171–1175.
- [135] a) S. Paliwal, S. Geib, C. S. Wilcox, *J. Am. Chem. Soc.* **1994**, *116*, 4497–4498; b) E. Kim, S. Paliwal, C. S. Wilcox, *J. Am. Chem. Soc.* **1998**, *120*, 11192–11193.
- [136] For a review on intramolecular edge-to-face interactions, see W. B. Jennings, B. M. Farrell, J. F. Malone, *Acc. Chem. Res.* **2001**, *34*, 885–894.
- [137] a) T. Ren, Y. Jin, K. S. Kim, D. H. Kim, *J. Biomol. Struct. Dyn.* **1997**, *15*, 401–405; b) K. Nakamura, K. N. Houk, *Org. Lett.* **1999**, *1*, 2049–2051; c) for a recent theoretical calculation demonstrating backbone effects on the conformational preferences of the molecular torsional balance, see J. Ribas, E. Cubero, F. J. Luque, M. Orozco, *J. Org. Chem.* **2002**, *67*, 7057–7065.
- [138] U. Obst, P. Betschmann, C. Lerner, P. Seiler, F. Diederich, V. Gramlich, L. Weber, D. W. Banner, P. Schönholzer, *Helv. Chim. Acta* **2000**, *83*, 855–909.
- [139] J. A. Turk, D. B. Smithrud, *J. Org. Chem.* **2001**, *66*, 8328–8335.
- [140] a) P. J. Ala, E. E. Huston, R. M. Klabe, D. D. McCabe, J. L. Duke, C. J. Rizzo, B. D. Korant, R. J. DeLoskey, P. Y. S. Lam, C. N. Hodge, C.-H. Chang, *Biochemistry* **1997**, *36*, 1573–1580; b) N. O. Concha, C. A. Janson, P. Rowling, S. Pearson, C. A. Cheever, B. P. Clarke, C. Lewis, M. Galleni, J.-M. Frère, D. J. Payne, J. H. Bateson, S. S. Abdel-Meguid, *Biochemistry* **2000**, *39*, 4288–4298.
- [141] M. Brandl, M. S. Weiss, A. Jabs, J. Sühnel, R. Hilgenfeld, *J. Mol. Biol.* **2001**, *307*, 357–377.
- [142] Y. Umezawa, S. Tsuboyama, H. Takahashi, J. Uzawa, M. Nishio, *Bioorg. Med. Chem.* **1999**, *7*, 2021–2026.
- [143] For comparison with other systems, it is noteworthy to mention the methane–benzene complex with a stabilization energy of  $D_c = -1.45 \text{ kcal mol}^{-1}$  and a  $D_0 = -0.98 \text{ kcal mol}^{-1}$ : S. Tsuzuki, K. Honda, T. Uchimar, M. Mikami, K. Tanabe, *J. Am. Chem. Soc.* **2000**, *122*, 3746–3753.
- [144] a) M. Nishio, M. Hirota, Y. Umezawa, *The CH/π Interaction*, Wiley, New York, **1998**; b) <http://www.tim.hi-ho.ne.jp/dionisio/>
- [145] H. Suezawa, T. Hashimoto, K. Tsuchinaga, T. Yoshida, T. Yuzuri, K. Sakakibara, M. Hirota, M. Nishio, *J. Chem. Soc. Perkin Trans. 2* **2000**, 1243–1249.
- [146] N. K. Vyas, M. N. Vyas, F. A. Quijcho, *Science* **1988**, *242*, 1290–1295.
- [147] F. Cozzi, J. S. Siegel, *Pure Appl. Chem.* **1995**, *67*, 683–689.
- [148] V. E. Williams, R. P. Lemieux, G. R. J. Thatcher, *J. Org. Chem.* **1996**, *61*, 1927–1933.
- [149] M. J. Rashkin, M. L. Waters, *J. Am. Chem. Soc.* **2002**, *124*, 1860–1861.
- [150] N. J. Heaton, P. Bello, B. Herradón, A. Del Campo, J. Jiménez-Barbero, *J. Am. Chem. Soc.* **1998**, *120*, 12371–12384.
- [151] a) R. S. Lokey, B. L. Iverson, *Nature* **1995**, *375*, 303–305; b) J. Q. Nguyen, B. L. Iverson, *J. Am. Chem. Soc.* **1999**, *121*, 2639–2640.
- [152] a) J. F. Stoddart, *Pure Appl. Chem.* **1988**, *60*, 467–472; b) B. Odell, M. V. Reddington, A. M. Z. Slawin, N. Spencer, J. F. Stoddart, D. J. Williams, *Angew. Chem.* **1988**, *100*, 1605–1608; *Angew. Chem. Int. Ed. Engl.* **1988**, *27*, 1547–1550; c) D. Philp, A. M. Z. Slawin, N. Spencer, J. F. Stoddart, D. J. Williams, *J. Chem. Soc. Chem. Commun.* **1991**, *22*, 1584–1586; d) M. C. T. Fyfe, J. F. Stoddart, *Acc. Chem. Res.* **1997**, *30*, 393–401; e) C. G. Claessens, J. F. Stoddart, *J. Phys. Org. Chem.* **1997**, *10*, 254–272.
- [153] a) F. M. Raymo, J. F. Stoddart, *Chem. Rev.* **1999**, *99*, 1643–1663; b) F. M. Raymo, J. F. Stoddart in *Templated Organic*

- Synthesis* (Eds.: F. Diederich, P. J. Stang), Wiley-VCH, Weinheim, **2000**, pp. 75–104; c) V. Balzani, A. Credi, F. M. Raymo, J. F. Stoddart, *Angew. Chem.* **2000**, *112*, 3484–3530; *Angew. Chem. Int. Ed.* **2000**, *39*, 3348–3391; d) S. J. Rowan, S. J. Cantrill, G. R. L. Cousins, J. K. M. Sanders, J. F. Stoddart, *Angew. Chem.* **2002**, *114*, 938–993; *Angew. Chem. Int. Ed.* **2002**, *41*, 898–952.
- [154] For a theoretical analysis on the driving forces for complexation by **16**, see a) R. Castro, M. J. Berardi, E. Córdova, M. Ochoa de Olza, A. E. Kaifer, J. D. Evanseck, *J. Am. Chem. Soc.* **1996**, *118*, 10257–10268; b) F. M. Raymo, K. N. Houk, J. F. Stoddart, *J. Am. Chem. Soc.* **1998**, *120*, 9318–9322.
- [155] The most common approach to describe electrostatic effects in aromatic interactions is the use of atom-centered charges (ACC). A comparison of the various force fields implemented in the program package MacroModel for evaluating ACC effects is available: G. Chessari, C. A. Hunter, C. M. R. Low, M. J. Packer, J. G. Vinter, C. Zonta, *Chem. Eur. J.* **2002**, *8*, 2860–2867.
- [156] a) A. D. Hamilton, D. Van Engen, *J. Am. Chem. Soc.* **1987**, *109*, 5035–5036; b) A. V. Muehldorf, D. Van Engen, J. C. Warner, A. D. Hamilton, *J. Am. Chem. Soc.* **1988**, *110*, 6561–6562; c) A. D. Hamilton in *Supramolecular Chemistry, Vol. 371* (Eds.: V. Balzani, L. De Cola), Kluwer, Dordrecht, **1992**, pp. 137–144.
- [157] A. J. Goodman, E. C. Breinlinger, C. M. McIntosh, L. N. Grimaldi, V. M. Rotello, *Org. Lett.* **2001**, *3*, 1531–1534.
- [158] A. Weichsel, W. R. Montfort, *Nat. Struct. Biol.* **1995**, *2*, 1095–1101.
- [159] a) T. Benzing, T. Tjivikua, J. Wolfe, J. Rebek, Jr., *Science* **1988**, *242*, 266–268; b) S. C. Zimmerman, W. Wu, Z. Zeng, *J. Am. Chem. Soc.* **1991**, *113*, 196–201; c) J. E. Kickham, S. J. Loeb, S. L. Murphy, *Chem. Eur. J.* **1997**, *3*, 1203–1213; d) O. Baudoin, F. Gonnet, M.-P. Teulade-Fichou, J.-P. Vigneron, J.-C. Tabet, J.-M. Lehn, *Chem. Eur. J.* **1999**, *5*, 2762–2771; e) M. Inouye, M. S. Itoh, H. Nakazumi, *J. Org. Chem.* **1999**, *64*, 9393–9398; f) M. Sirish, H.-J. Schneider, *J. Am. Chem. Soc.* **2000**, *122*, 5881–5882; g) S. R. Waldvogel, R. Fröhlich, C. A. Schalley, *Angew. Chem.* **2000**, *112*, 2580–2583; *Angew. Chem. Int. Ed.* **2000**, *39*, 2472–2475.
- [160] a) Y. Hamuro, S. J. Geib, A. D. Hamilton, *J. Am. Chem. Soc.* **1997**, *119*, 10587–10593; b) A. J. Lovinger, C. Nuckolls, T. J. Katz, *J. Am. Chem. Soc.* **1998**, *120*, 264–268; c) J. H. K. K. Hirschberg, L. Brunsveld, A. Ramzi, J. A. J. M. Vekemans, R. P. Sijbesma, E. W. Meijer, *Nature* **2000**, *407*, 167–170; d) V. Berl, I. Huc, R. G. Khoury, J.-M. Lehn, *Chem. Eur. J.* **2001**, *7*, 2798–2809.
- [161] a) W. Saenger, *Principles of Nucleic Acid Structure*, Springer, New York, **1984**; b) A. Eschenmoser, E. Loewenthal, *Chem. Soc. Rev.* **1992**, *21*, 1–16; c) I. Detmer, D. Summerer, A. Marx, *Chem. Commun.* **2002**, 2314–2315.
- [162] a) J. Sponer, J. Leszczynski, P. Hobza, *THEOCHEM* **2001**, 573, 43–53; b) J. Sponer, J. Leszczynski, P. Hobza, *Biopolymers* **2002**, *61*, 3–31.
- [163] a) S. M. Freier, N. Sugimoto, A. Sinclair, D. Alkema, T. Neilson, R. Kierzek, M. H. Caruthers, D. H. Turner, *Biochemistry* **1986**, *25*, 3214–3219; b) S. Bommarito, N. Peyret, J. SantaLucia, Jr., *Nucleic Acids Res.* **2000**, *28*, 1929–1934.
- [164] a) Y.-P. Pang, J. L. Miller, P. A. Kollman, *J. Am. Chem. Soc.* **1999**, *121*, 1717–1725; b) K. M. Guckian, B. A. Schweitzer, R. X.-F. Ren, C. J. Sheils, D. C. Tahmassebi, E. T. Kool, *J. Am. Chem. Soc.* **2000**, *122*, 2213–2222; c) S. L. McKay, B. Haptonstall, S. H. Gellman, *J. Am. Chem. Soc.* **2001**, *123*, 1244–1245; d) H. Rosemeyer, F. Seela, *J. Chem. Soc. Perkin Trans. 2* **2002**, 746–750.
- [165] a) D. Barsky, E. T. Kool, M. E. Colvin, *J. Biomol. Struct. Dyn.* **1999**, *16*, 1119–1134; b) E. T. Kool, J. C. Morales, K. M. Guckian, *Angew. Chem.* **2000**, *112*, 1046–1068; *Angew. Chem. Int. Ed.* **2000**, *39*, 990–1009.
- [166] a) E. C. Long, J. K. Barton, *Acc. Chem. Res.* **1990**, *23*, 271–272; b) F. Gago, *Methods* **1998**, *14*, 277–292; c) K. E. Erkkila, D. T. Odom, J. K. Barton, *Chem. Rev.* **1999**, *99*, 2777–2795.
- [167] R. K. Castellano, V. Gramlich, F. Diederich, *Chem. Eur. J.* **2002**, *8*, 118–129.
- [168] P. Lustenberger, E. Martinborough, T. Mordasini Denti, F. Diederich, *J. Chem. Soc. Perkin Trans. 2* **1998**, 747–761.
- [169] J. A. M. Prates, N. Tarbouriech, S. J. Charnock, C. M. G. A. Fontes, L. M. A. Ferreira, G. J. Davies, *Structure* **2001**, *9*, 1183–1190.
- [170] C.-T. Chen, J. S. Siegel, *J. Am. Chem. Soc.* **1994**, *116*, 5959–5960.
- [171] S. E. Thompson, D. B. Smithrud, *J. Am. Chem. Soc.* **2002**, *124*, 442–449.
- [172] G. B. Jones, *Tetrahedron* **2001**, *57*, 7999–8016.
- [173] W. H. Pirkle, Y. Liu, *J. Chromatogr. A* **1996**, *749*, 19–24.
- [174] a) I. Dance, M. Scudder, *J. Chem. Soc. Dalton Trans.* **2000**, 1579–1585; b) A. Magistrato, P. S. Pregosin, A. Albinati, U. Rothlisberger, *Organometallics* **2001**, *20*, 4178–4184.
- [175] K. Kishikawa, M. Naruse, S. Kohmoto, M. Yamamoto, K. Yamaguchi, *J. Chem. Soc. Perkin Trans. 1* **2001**, 462–468.
- [176] a) T. Steiner, *Angew. Chem.* **2002**, *114*, 50–80; *Angew. Chem. Int. Ed.* **2002**, *41*, 48–76; b) L. J. Prins, D. N. Reinhoudt, P. Timmerman, *Angew. Chem.* **2001**, *113*, 2446–2492; *Angew. Chem. Int. Ed.* **2001**, *40*, 2382–2426.
- [177] D. A. Dixon, K. D. Dobbs, J. J. Valentini, *J. Phys. Chem.* **1994**, *98*, 13435–13439.
- [178] K. S. Kim, P. Tarakeshwar, J. Y. Lee, *Chem. Rev.* **2000**, *100*, 4145–4185.
- [179] D. H. Williams, M. S. Westwell, *Chem. Soc. Rev.* **1998**, *27*, 57–63.
- [180] a) P. Hobza, Z. Havlas, *Chem. Rev.* **2000**, *100*, 4253–4264; b) K. Hermansson, *J. Phys. Chem. A* **2002**, *106*, 4695–4702.
- [181] M. F. Perutz, G. Fermi, D. J. Abraham, C. Poyart, E. Bursaux, *J. Am. Chem. Soc.* **1986**, *108*, 1064–1078.
- [182] T. Steiner, G. Koellner, *J. Mol. Biol.* **2001**, *305*, 535–557.
- [183] G. Tóth, R. F. Murphy, S. Lovas, *J. Am. Chem. Soc.* **2001**, *123*, 11782–11790, and references therein.
- [184] A. Wlodawer, J. Walter, R. Huber, L. Sjölin, *J. Mol. Biol.* **1984**, *180*, 301–329.
- [185] G. Xiao, S. Liu, X. Ji, W. W. Johnson, J. Chen, J. F. Parsons, W. J. Stevens, G. L. Gilliland, R. N. Armstrong, *Biochemistry* **1996**, *35*, 4753–4765.
- [186] M. Sulpizi, P. Carloni, *J. Phys. Chem. B* **2000**, *104*, 10087–10091.
- [187] a) M. F. Perutz, *Philos. Trans. R. Soc. London Ser. A* **1993**, *345*, 105–112; b) G. B. Vázquez, X. Ji, C. Fronticelli, G. L. Guillard, *Acta Crystallogr. Sect. D* **1998**, *54*, 355–366; c) M. S. Weiss, M. Brandl, J. Sühnel, D. Pal, R. Hilgenfeld, *Trends Biochem. Sci.* **2001**, *26*, 521–523.
- [188] J. B. O. Mitchell, C. L. Nandi, I. K. McDonald, J. M. Thornton, S. L. Price, *J. Mol. Biol.* **1994**, *239*, 315–331.
- [189] K. A. Thomas, G. M. Smith, T. B. Thomas, R. J. Feldmann, *Proc. Natl. Acad. Sci. USA* **1982**, *79*, 4843–4847.
- [190] S. K. Burley, G. A. Petsko, *FEBS Lett.* **1986**, *203*, 139–143.
- [191] M. M. Flocco, S. L. Mowbray, *J. Mol. Biol.* **1994**, *235*, 709–717.
- [192] G. Tóth, C. R. Watts, R. F. Murphy, S. Lovas, *Proteins Struct. Funct. Genet.* **2001**, *43*, 373–381.
- [193] T. Steiner, A. M. M. Schreurs, J. A. Kanters, J. Kroon, *Acta Crystallogr. Sect. D* **1998**, *54*, 25–31.
- [194] J. L. Atwood, F. Hamada, K. D. Robinson, G. W. Orr, R. L. Vincent, *Nature* **1991**, *349*, 683–684.
- [195] G. Hummer, J. C. Rasaiah, J. P. Noworyta, *Nature* **2001**, *414*, 188–190.
- [196] K. Håkansson, *Int. J. Biol. Macromol.* **1996**, *18*, 189–194.

- [197] a) T. S. Zwier, *Annu. Rev. Phys. Chem.* **1996**, *47*, 205–241; b) B. Brutschy, *Chem. Rev.* **2000**, *100*, 3891–3920.
- [198] S. Tsuzuki, K. Honda, T. Uchimarui, M. Mikami, K. Tanabe, *J. Am. Chem. Soc.* **2000**, *122*, 11450–11458.
- [199] A. Courty, M. Mons, I. Dimicoli, F. Piuze, M.-P. Gageot, V. Brenner, P. de Pujo, P. Millié, *J. Phys. Chem. A* **1998**, *102*, 6590–6600.
- [200] S. Suzuki, P. G. Green, R. E. Bumgarner, S. Dasgupta, W. A. Goddard III, G. A. Blake, *Science* **1992**, *257*, 942–945.
- [201] P. Ruelle, M. Buchmann, H. Nam-Tran, U. W. Kesselring, *J. Comput.-Aided Mol. Des.* **1992**, *6*, 431–448.
- [202] M. P. Payne, L. C. Kenny, *J. Toxicol. Environ. Health Part A* **2002**, *65*, 897–931.
- [203] D. A. Rodham, S. Suzuki, R. D. Suenram, F. J. Lovas, S. Dasgupta, W. A. Goddard III, G. A. Blake, *Nature* **1993**, *362*, 735–737.
- [204] M. Mons, I. Dimicoli, B. Tardivel, F. Piuze, V. Brenner, P. Millié, *Phys. Chem. Chem. Phys.* **2002**, *4*, 571–576.
- [205] P. Tarakeswar, H. S. Choi, K. S. Kim, *J. Am. Chem. Soc.* **2001**, *123*, 3323–3331.
- [206] G. Duan, V. H. Smith, Jr., D. F. Weaver, *Mol. Phys.* **2001**, *99*, 1689–1699.
- [207] J. F. Malone, C. M. Murray, M. H. Charlton, R. Docherty, A. J. Lavery, *J. Chem. Soc. Faraday Trans.* **1997**, *93*, 3429–3436.
- [208] a) O. R. Wulf, U. Liddel, S. B. Hendricks, *J. Am. Chem. Soc.* **1936**, *58*, 2287–2293; b) W. Klemperer, M. W. Cronyn, A. H. Maki, G. C. Pimentel, *J. Am. Chem. Soc.* **1954**, *76*, 5846–5848; c) M. A. Viswamitra, R. Radhakrishnan, J. Bandekar, G. R. Desiraju, *J. Am. Chem. Soc.* **1993**, *115*, 4868–4869.
- [209] G. Duan, V. H. Smith, Jr., D. F. Weaver, *J. Phys. Chem. A* **2000**, *104*, 4521–4532.
- [210] G. Duan, V. H. Smith, Jr., D. F. Weaver, *Chem. Phys. Lett.* **1999**, *310*, 323–332.
- [211] G. Columberg, A. Bauder, *J. Chem. Phys.* **1997**, *106*, 504–510.
- [212] E. M. Duffy, P. J. Kowalczyk, W. L. Jorgensen, *J. Am. Chem. Soc.* **1993**, *115*, 9271–9275.
- [213] H. Adams, F. J. Carver, C. A. Hunter, N. J. Osborne, *Chem. Commun.* **1996**, 2529–2530.
- [214] C. Allot, H. Adams, P. L. Bernad, Jr., C. A. Hunter, C. Rotger, J. A. Thomas, *Chem. Commun.* **1998**, 2449–2450.
- [215] H. Adams, K. D. M. Harris, G. A. Hembury, C. A. Hunter, D. J. Livingstone, J. F. McCabe, *Chem. Commun.* **1996**, 2531–2532.
- [216] M. J. Cloninger, H. W. Whitlock, *J. Org. Chem.* **1998**, *63*, 6153–6159.
- [217] K. Brejc, W. J. van Dijk, R. V. Klaassen, M. Schuurmans, J. van der Oost, A. B. Smit, T. K. Sixma, *Nature* **2001**, *411*, 269–276.
- [218] J. P. Gollivan, D. A. Dougherty, *Proc. Natl. Acad. Sci. USA* **1999**, *96*, 9459–9464.
- [219] N. S. Scrutton, A. R. C. Raine, *Biochem. J.* **1996**, *319*, 1–8.
- [220] M. Levitt, M. F. Perutz, *J. Mol. Biol.* **1988**, *201*, 751–754.
- [221] W. Zhong, J. P. Gollivan, Y. Zhang, L. Li, H. A. Lester, D. A. Dougherty, *Proc. Natl. Acad. Sci. USA* **1998**, *95*, 12088–12093.
- [222] D. A. Dougherty, *Science* **1996**, *271*, 163–168.
- [223] M. O. Ortells, G. G. Lunt, *Trends Neurosci.* **1995**, *18*, 121–127.
- [224] N. Zacharias, D. A. Dougherty, *Trends Pharmacol. Sci.* **2002**, *23*, 281–287.
- [225] P. Lhoták, S. Shinkai, *J. Phys. Org. Chem.* **1997**, *10*, 273–285.
- [226] A. Arduini, A. Casnati, A. Pochini, R. Ungaro, *Curr. Opin. Chem. Biol.* **1997**, *1*, 467–474.
- [227] S. L. De Wall, E. S. Meadows, L. J. Barbour, G. W. Gokel, *Proc. Natl. Acad. Sci. USA* **2000**, *97*, 6271–6276.
- [228] G. W. Gokel, L. J. Barbour, S. L. De Wall, E. S. Meadows, *Coord. Chem. Rev.* **2001**, *222*, 127–154.
- [229] G. W. Gokel, L. J. Barbour, R. Ferdani, J. Hu, *Acc. Chem. Res.* **2002**, *35*, 878–886.
- [230] G. W. Gokel, A. Mukhopadhyay, *Chem. Soc. Rev.* **2001**, *30*, 274–286.
- [231] D. A. Stauffer, D. A. Dougherty, *Tetrahedron Lett.* **1988**, *29*, 6039–6042.
- [232] D. A. Dougherty, D. A. Stauffer, *Science* **1990**, *250*, 1558–1560.
- [233] J. L. Sussman, M. Harel, F. Frolow, C. Oefner, A. Goldman, L. Toker, I. Silman, *Science* **1991**, *253*, 872–879.
- [234] For a theoretical study, see K. S. Kim, J. Y. Lee, S. J. Lee, T.-K. Ha, D. H. Kim, *J. Am. Chem. Soc.* **1994**, *116*, 7399–7400.
- [235] H.-J. Schneider, *Angew. Chem.* **1991**, *103*, 1419–1439; *Angew. Chem. Int. Ed. Engl.* **1991**, *30*, 1417–1436.
- [236] H.-J. Schneider, F. Werner, T. Blatter, *J. Phys. Org. Chem.* **1993**, *6*, 590–594.
- [237] H.-J. Schneider, T. Schiestel, P. Zimmermann, *J. Am. Chem. Soc.* **1992**, *114*, 7698–7703.
- [238] H.-J. Schneider, *Chem. Soc. Rev.* **1994**, *23*, 227–234.
- [239] S. Y. Jon, J. Kim, M. Kim, S.-H. Park, W. S. Jeon, J. Heo, K. Kim, *Angew. Chem.* **2001**, *113*, 2174–2177; *Angew. Chem. Int. Ed.* **2001**, *40*, 2116–2119.
- [240] R. Méric, J.-P. Vigneron, J.-M. Lehn, *J. Chem. Soc. Chem. Commun.* **1993**, 129–131.
- [241] R. Méric, J.-M. Lehn, J.-P. Vigneron, *Bull. Soc. Chim. Fr.* **1994**, *131*, 579–583.
- [242] a) K. Araki, H. Shimizu, S. Shinkai, *Chem. Lett.* **1993**, 205–208; b) K. N. Koh, K. Araki, A. Ikeda, H. Otsuka, S. Shinkai, *J. Am. Chem. Soc.* **1996**, *118*, 755–758.
- [243] a) J. Canceill, L. Lacombe, A. Collet, *J. Chem. Soc. Chem. Commun.* **1987**, 219–221; b) A. Collet, J.-P. Dutasta, B. Lozach, J. Canceill, *Top. Curr. Chem.* **1993**, *165*, 103–129.
- [244] L. Garel, B. Lozach, J.-P. Dutasta, A. Collet, *J. Am. Chem. Soc.* **1993**, *115*, 11652–11653.
- [245] A. W. Schwabacher, S. Zhang, W. Davy, *J. Am. Chem. Soc.* **1993**, *115*, 6995–6996.
- [246] A. Sygula, P. W. Rabideau, *J. Chem. Soc. Chem. Commun.* **1994**, 2271–2272.
- [247] J. Gao, L. W. Chou, A. Auerbach, *Biophys. J.* **1993**, *65*, 43–47.
- [248] a) C. A. Schalley, *Mass Spectrom. Rev.* **2001**, *20*, 253–309; b) for earlier mass-spectrometric studies on ammonium complexes of calixarenes, see F. Inokuchi, Y. Miyahara, T. Inazu, S. Shinkai, *Angew. Chem.* **1995**, *107*, 1459–1462; *Angew. Chem. Int. Ed. Engl.* **1995**, *34*, 1364–1366.
- [249] a) K. Murayama, K. Aoki, *Chem. Commun.* **1997**, 119–120; b) K. Murayama, K. Aoki, *Chem. Commun.* **1998**, 607–608; c) B. Masci, M. Nierlich, P. Thuéry, *New J. Chem.* **2002**, *26*, 766–774.
- [250] G. Arena, A. Casnati, A. Contino, G. G. Lombardo, D. Sciotto, R. Ungaro, *Chem. Eur. J.* **1999**, *5*, 738–744.
- [251] G. Arena, A. Casnati, A. Contino, F. G. Gulino, D. Sciotto, R. Ungaro, *J. Chem. Soc. Perkin Trans. 2* **2000**, 419–423.
- [252] The Gibbs solvation free energy of  $N(CH_3)_4^+$  in water has been calculated to be more favorable by  $-70 \text{ kcal mol}^{-1}$  relative to  $C(CH_3)_4$ ; P. C. Kearney, L. S. Mizoue, R. A. Kumpf, J. E. Forman, A. McCurdy, D. A. Dougherty, *J. Am. Chem. Soc.* **1993**, *115*, 9907–9919.
- [253] S. Roelens, R. Torriti, *J. Am. Chem. Soc.* **1998**, *120*, 12443–12452.
- [254] S. Kubik, R. Goddard, *J. Org. Chem.* **1999**, *64*, 9475–9486.
- [255] T. Grawe, T. Schrader, P. Finocchiaro, G. Consiglio, S. Failla, *Org. Lett.* **2001**, *3*, 1597–1600.
- [256] M. Herm, O. Molt, T. Schrader, *Angew. Chem.* **2001**, *113*, 3248–3254; *Angew. Chem. Int. Ed.* **2001**, *40*, 3148–3151.
- [257] S. Rensing, T. Schrader, *Org. Lett.* **2002**, *4*, 2161–2164.
- [258] C. Jasper, T. Schrader, J. Panitzky, F.-G. Klärner, *Angew. Chem.* **2002**, *114*, 1411–1415; *Angew. Chem. Int. Ed.* **2002**, *41*, 1355–1358.

- [259] For *N*-alkylpyridinium interactions in rotaxanes and catenanes, see A. R. Pease, J. O. Jeppesen, J. F. Stoddart, Y. Luo, C. P. Collier, J. R. Heath, *Acc. Chem. Res.* **2001**, *34*, 433–444.
- [260] a) M. Meot-Ner, C. A. Deakne, *J. Am. Chem. Soc.* **1985**, *107*, 469–474; b) C. A. Deakne, M. Meot-Ner, *J. Am. Chem. Soc.* **1985**, *107*, 474–479.
- [261] a) B. Masci, M. Finelli, M. Varrone, *Chem. Eur. J.* **1998**, *4*, 2018–2030; b) Z. Zhong, A. Ikeda, S. Shinkai, *J. Am. Chem. Soc.* **1999**, *121*, 11906–11907; c) K. Araki, H. Hayashida, *Tetrahedron Lett.* **2000**, *41*, 1209–1213; d) F. Cuevas, S. Di Stefano, J. O. Magrans, P. Prados, L. Mandolini, J. de Mendoza, *Chem. Eur. J.* **2000**, *6*, 3228–3234; e) A. Dalla Cort, M. Nissinen, D. Mancinetti, E. Nicoletti, L. Mandolini, K. Rissanen, *J. Phys. Org. Chem.* **2001**, *14*, 425–431; f) A. Shivanyuk, J. Rebek, Jr., *Proc. Natl. Acad. Sci. USA* **2001**, *98*, 7662–7665; g) L. Frish, M. O. Vysotsky, S. E. Matthews, V. Böhmer, Y. Cohen, *J. Chem. Soc. Perkin Trans. 2* **2002**, 88–93.
- [262] A. Arduini, A. Pochini, A. Secchi, *Eur. J. Org. Chem.* **2000**, 2325–2334.
- [263] A. Arduini, G. Giorgi, A. Pochini, A. Secchi, F. Ugozzoli, *J. Org. Chem.* **2001**, *66*, 8302–8308.
- [264] S. Kubik, *J. Am. Chem. Soc.* **1999**, *121*, 5846–5855.
- [265] S. Kubik, R. Goddard, *Chem. Commun.* **2000**, 633–634.
- [266] a) K.-S. Jeong, S. H. Park, J. H. Kim, Y. L. Cho, *Bull. Korean Chem. Soc.* **1997**, *18*, 139–141; b) M. Kamieth, F.-G. Klärner, *J. Prakt. Chem.* **1999**, *341*, 245–251; c) M. Lämsä, S. Kiviniemi, E.-R. Kettukangas, M. Nissinen, J. Pursiainen, K. Rissanen, *J. Phys. Org. Chem.* **2001**, *14*, 551–558.
- [267] J. W. Caldwell, P. A. Kollman, *J. Am. Chem. Soc.* **1995**, *117*, 4177–4178.
- [268] S. Mecozzi, A. P. West, Jr., D. A. Dougherty, *J. Am. Chem. Soc.* **1996**, *118*, 2307–2308.
- [269] S. Mecozzi, A. P. West, Jr., D. A. Dougherty, *Proc. Natl. Acad. Sci. USA* **1996**, *93*, 10566–10571.
- [270] D. L. Beene, G. S. Brandt, W. Zhong, N. M. Zacharias, H. A. Lester, D. A. Dougherty, *Biochemistry* **2002**, *41*, 10262–10269.
- [271] E. Cubero, F. J. Luque, M. Orozco, *Proc. Natl. Acad. Sci. USA* **1998**, *95*, 5976–5980.
- [272] E. Cubero, M. Orozco, F. J. Luque, *J. Phys. Chem. A* **1999**, *103*, 315–321.
- [273] This has been extensively investigated through computational means; see, for example, a) H. Basch, W. J. Stevens, *THEOCHEM* **1995**, 338, 303–315; b) A. Pullman, G. Berthier, R. Savinelli, *J. Am. Chem. Soc.* **1998**, *120*, 8553–8554; c) H. Minoux, C. Chipot, *J. Am. Chem. Soc.* **1999**, *121*, 10366–10372; d) A. Pullman, G. Berthier, R. Savinelli, *THEOCHEM* **2001**, *537*, 163–172; e) C. Felder, H.-L. Jiang, W.-L. Zhu, K.-X. Chen, I. Silman, S. A. Botti, J. L. Sussman, *J. Phys. Chem. A* **2001**, *105*, 1326–1333; f) T. Liu, J. Gu, X.-J. Tan, W.-L. Zhu, X.-M. Luo, H.-L. Jiang, R.-Y. Ji, K.-X. Chen, I. Silman, J. L. Sussman, *J. Phys. Chem. A* **2001**, *105*, 5431–5437; g) T. Liu, J. Gu, X.-J. Tan, W.-L. Zhu, X.-M. Luo, H.-L. Jiang, R.-Y. Ji, K.-X. Chen, I. Silman, J. L. Sussman, *J. Phys. Chem. A* **2002**, *106*, 157–164; h) M. Aschi, F. Mazza, A. Di Nola, *THEOCHEM* **2002**, *587*, 177–188; i) E. Grunwald, S. Highsmith, T.-P. I in *Ions and Ion Pairs in Organic Reactions*, Vol. 2 (Ed.: M. Szwarc), Wiley, New York, **1974**, pp. 447–519.
- [274] C. Chipot, B. Maigret, D. A. Pearlman, P. A. Kollman, *J. Am. Chem. Soc.* **1996**, *118*, 2998–3005.
- [275] Y. Mo, G. Subramanian, J. Gao, D. M. Ferguson, *J. Am. Chem. Soc.* **2002**, *124*, 4832–4837.
- [276] S. Rensing, M. Arendt, A. Springer, T. Grawe, T. Schrader, *J. Org. Chem.* **2001**, *66*, 5814–5821.
- [277] S. Hashimoto, S. Ikuta, *THEOCHEM* **1999**, *468*, 85–94.
- [278] C. A. Hunter, C. M. R. Low, C. Rotger, J. G. Vinter, C. Zonta, *Proc. Natl. Acad. Sci. USA* **2002**, *99*, 4873–4876.
- [279] C. W. Davies, *Ion Association*, Butterworth, London, **1962**.
- [280] a) P. B. Savage, S. K. Holmgren, S. H. Gellman, *J. Am. Chem. Soc.* **1994**, *116*, 4069–4070; b) R. Arnecke, V. Böhmer, R. Cacciapaglia, A. Dalla Cort, L. Mandolini, *Tetrahedron* **1997**, *53*, 4901–4908.
- [281] A. Arduini, W. M. McGregor, D. Paganuzzi, A. Pochini, A. Secchi, F. Ugozzoli, R. Ungaro, *J. Chem. Soc. Perkin Trans. 2* **1996**, 839–846.
- [282] M. T. Reetz in *Comprehensive Supramolecular Chemistry*, Vol. 2 (Ed.: F. Vögtle), Pergamon, Oxford, **1996**, pp. 553–562.
- [283] a) K.-S. Jeong, K.-M. Hahn, Y. L. Cho, *Tetrahedron Lett.* **1998**, *39*, 3779–3782; b) V. Böhmer, A. Dalla Cort, L. Mandolini, *J. Org. Chem.* **2001**, *66*, 1900–1902.
- [284] S. Bartoli, S. Roelens, *J. Am. Chem. Soc.* **1999**, *121*, 11908–11909.
- [285] S. Bartoli, S. Roelens, *J. Am. Chem. Soc.* **2002**, *124*, 8307–8315.
- [286] G. De Iasi, B. Masci, *Tetrahedron Lett.* **1993**, *34*, 6635–6638.
- [287] It is worth noting that the anion's role often extends beyond modulating the electrostatics of the cation. Kubik and co-workers have shown that, upon complexation of a variety of *n*-butyltrimethylammonium salts by their cyclic peptide hosts,<sup>[128,254,264,265]</sup> a remarkable 10<sup>3</sup>–10<sup>4</sup>-fold cation binding enhancement is observed. This result is attributable to binding of the anion to the host that results in conformational changes that preorganize the host for cation binding, as well as simultaneous binding of the cation and anion to the host in a favorable position for attractive Coulombic interactions. These types of allosteric phenomena appear to be quite universal in cation- $\pi$  host-guest studies.
- [288] a) C. L. Nandi, J. Singh, J. M. Thornton, *Protein Eng.* **1993**, *6*, 247–259.
- [289] J. P. Gallivan, D. A. Dougherty, *J. Am. Chem. Soc.* **2000**, *122*, 870–874.
- [290] E. C. Meng, P. Cieplak, J. W. Caldwell, P. A. Kollman, *J. Am. Chem. Soc.* **1994**, *116*, 12061–12062.
- [291] A. M. de Vos, M. Ultsch, A. A. Kossiakoff, *Science* **1992**, *255*, 306–312.
- [292] O. Livnah, E. A. Stura, D. L. Johnson, S. A. Middleton, L. S. Mulcahy, N. C. Wrighton, W. J. Dower, L. K. Jolliffe, I. A. Wilson, *Science* **1996**, *273*, 464–471.
- [293] a) Y. Inoue, S. Sugio, J. Andzelm, N. Nakamura, *J. Phys. Chem. A* **1998**, *102*, 646–648; b) P.-O. Norrby, T. Liljefors, *J. Am. Chem. Soc.* **1999**, *121*, 2303–2306; c) many of these polarization effects appear in metalloproteins; see S. D. Zaric, D. M. Popovic, E.-W. Knapp, *Chem. Eur. J.* **2000**, *6*, 3935–3942.
- [294] V. Dvornikovs, D. B. Smithrud, *J. Org. Chem.* **2002**, *67*, 2160–2167.
- [295] For the influence of remote carboxylate groups on cation- $\pi$  binding in the context of salt bridges, see S. M. Ngola, P. C. Kearney, S. Mecozzi, K. Russell, D. A. Dougherty, *J. Am. Chem. Soc.* **1999**, *121*, 1192–1201.
- [296] a) R. L. Woodin, J. L. Beauchamp, *J. Am. Chem. Soc.* **1978**, *100*, 501–508; b) R. A. Kumpf, D. A. Dougherty, *Science* **1993**, *261*, 1708–1710; c) A. Andersen, F. Muntean, D. Walter, C. Rue, P. B. Armentrout, *J. Phys. Chem. A* **2000**, *104*, 692–705; d) R. Amunugama, M. T. Rodgers, *J. Phys. Chem. A* **2002**, *106*, 5529–5539.
- [297] J. Sunner, K. Nishizawa, P. Kebarle, *J. Phys. Chem.* **1981**, *85*, 1814–1820.
- [298] B. C. Guo, J. W. Purnell, A. W. Castleman, Jr., *Chem. Phys. Lett.* **1990**, *168*, 155–160.
- [299] A. Gapeev, R. C. Dunbar, *J. Am. Soc. Mass Spectrom.* **2002**, *13*, 477–484.
- [300] X-ray crystallographic studies of hexasubstituted benzene-cation complexes have shown M<sup>+</sup>... $\pi$ (arene) contacts with reversed affinity trends (for example, Cs<sup>+</sup>  $\approx$  Rb<sup>+</sup> > K<sup>+</sup> > Na<sup>+</sup>), see G. K. Fukin, S. V. Lindeman, J. K. Kochi, *J. Am. Chem. Soc.* **2002**, *124*, 8329–8336.

- [301] a) O. M. Cabarcos, C. J. Weinheimer, J. M. Lisy, *J. Chem. Phys.* **1998**, *108*, 5151–5154; b) O. M. Cabarcos, C. J. Weinheimer, J. M. Lisy, *J. Chem. Phys.* **1999**, *110*, 8429–8435.
- [302] G. W. Gokel, S. L. De Wall, E. S. Meadows, *Eur. J. Org. Chem.* **2000**, 2967–2978.
- [303] E. S. Meadows, S. L. De Wall, L. J. Barbour, G. W. Gokel, *J. Am. Chem. Soc.* **2001**, *123*, 3092–3107.
- [304] J. Hu, L. J. Barbour, G. W. Gokel, *Proc. Natl. Acad. Sci. USA* **2002**, *99*, 5121–5126.
- [305] a) V. Ryzhov, R. C. Dunbar, B. Cerda, C. Wesdemiotis, *J. Am. Soc. Mass Spectrom.* **2000**, *11*, 1037–1046; b) A. Gapeev, R. C. Dunbar, *J. Am. Chem. Soc.* **2001**, *123*, 8360–8365.
- [306] J. M. Talley, B. A. Cerda, G. Ohanessian, C. Wesdemiotis, *Chem. Eur. J.* **2002**, *8*, 1377–1388.
- [307] a) O. Donini, D. F. Weaver, *J. Comput. Chem.* **1998**, *19*, 1515–1525; b) J. Wouters, *J. Comput. Chem.* **2000**, *21*, 847–855.
- [308] a) R. C. Dunbar, *J. Phys. Chem. A* **2000**, *104*, 8067–8074; b) F. M. Siu, N. L. Ma, C. W. Tsang, *J. Am. Chem. Soc.* **2001**, *123*, 3397–3398.
- [309] S. Hoyau, K. Norrman, T. B. McMahon, G. Ohanessian, *J. Am. Chem. Soc.* **1999**, *121*, 8864–8875.
- [310] a) J. B. Nicholas, B. P. Hay, D. A. Dixon, *J. Phys. Chem. A* **1999**, *103*, 1394–1400; b) P. B. Armentrout, M. T. Rodgers, *J. Phys. Chem. A* **2000**, *104*, 2238–2247; c) D. Feller, D. A. Dixon, J. B. Nicholas, *J. Phys. Chem. A* **2000**, *104*, 11414–11419; d) J. C. Amicangelo, P. B. Armentrout, *J. Phys. Chem. A* **2000**, *104*, 11420–11432.
- [311] a) M. A. L. Eriksson, P.-Y. Morgantini, P. A. Kollman, *J. Phys. Chem. B* **1999**, *103*, 4474–4480; b) W.-L. Zhu, X.-J. Tan, C. M. Pua, J.-D. Gu, H.-L. Jiang, K.-X. Chen, C. E. Felder, I. Silman, J. L. Sussman, *J. Phys. Chem. A* **2000**, *104*, 9573–9580.
- [312] J. D. Schmitt, C. G. V. Sharples, W. S. Caldwell, *J. Med. Chem.* **1999**, *42*, 3066–3074.
- [313] R. Loewenthal, J. Sancho, A. R. Fersht, *J. Mol. Biol.* **1992**, *224*, 759–770.
- [314] a) V. Muñoz, L. Serrano, *Nat. Struct. Biol.* **1994**, *1*, 399–409; b) J. Fernández-Recio, A. Vázquez, C. Civera, P. Sevilla, J. Sancho, *J. Mol. Biol.* **1997**, *267*, 184–197.
- [315] A. Y. Ting, I. Shin, C. Lucero, P. G. Schultz, *J. Am. Chem. Soc.* **1998**, *120*, 7135–7136.
- [316] J. Fernández-Recio, A. Romero, J. Sancho, *J. Mol. Biol.* **1999**, *290*, 319–330.
- [317] C. A. Olson, Z. Shi, N. R. Kallenbach, *J. Am. Chem. Soc.* **2001**, *123*, 6451–6452.
- [318] E. V. Pletneva, A. T. Laederach, D. B. Fulton, N. M. Kostic, *J. Am. Chem. Soc.* **2001**, *123*, 6232–6245.
- [319] T. P. Burghardt, N. Juranic, S. Macura, K. Ajtai, *Biopolymers* **2002**, *63*, 261–272.
- [320] Z. Shi, C. A. Olson, N. R. Kallenbach, *J. Am. Chem. Soc.* **2002**, *124*, 3284–3291.
- [321] B. J. Smith, *J. Comput. Chem.* **1999**, *20*, 428–442.
- [322] B. P. Orner, X. Salvatella, J. S. Quesada, J. de Mendoza, E. Giralt, A. D. Hamilton, *Angew. Chem.* **2002**, *114*, 125–127; *Angew. Chem. Int. Ed.* **2002**, *41*, 117–119.
- [323] S. M. Ngola, D. A. Dougherty, *J. Org. Chem.* **1996**, *61*, 4355–4360.
- [324] a) L. C. Hsieh-Wilson, P. G. Schultz, R. C. Stevens, *Proc. Natl. Acad. Sci. USA* **1996**, *93*, 5363–5367; b) C. Jenson, W. L. Jorgensen, *J. Am. Chem. Soc.* **1997**, *119*, 10846–10854; c) D. Barak, A. Ordentlich, Y. Segall, B. Velan, H. P. Benschop, L. P. A. De Jong, A. Shafferman, *J. Am. Chem. Soc.* **1997**, *119*, 3157–3158; d) P. C. Miklis, R. Ditchfield, T. A. Spencer, *J. Am. Chem. Soc.* **1998**, *120*, 10482–10489.
- [325] a) P. Lakshminarasimhan, R. B. Sunoj, J. Chandrasekhar, V. Ramamurthy, *J. Am. Chem. Soc.* **2000**, *122*, 4815–4816; b) S. Yamada, C. Morita, *J. Am. Chem. Soc.* **2002**, *124*, 8184–8185.
- [326] M. Rooman, J. Liévin, E. Buisine, R. Wintjens, *J. Mol. Biol.* **2002**, *319*, 67–76.
- [327] H. Ihm, S. Yun, H. G. Kim, J. K. Kim, K. S. Kim, *Org. Lett.* **2002**, *4*, 2897–2900.
- [328] M. Mascal, A. Armstrong, M. D. Bartberger, *J. Am. Chem. Soc.* **2002**, *124*, 6274–6276.
- [329] C. R. Patrick, G. S. Prosser, *Nature* **1960**, *187*, 1021.
- [330] J. S. W. Overell, G. S. Pawley, *Acta Crystallogr. Sect. B* **1982**, *38*, 1966–1972.
- [331] J. H. Williams, J. K. Cockcroft, A. N. Fitch, *Angew. Chem.* **1992**, *104*, 1666–1669; *Angew. Chem. Int. Ed. Engl.* **1992**, *31*, 1655–1657.
- [332] J. A. Ripmeester, D. A. Wright, C. A. Fyfe, R. K. Boyd, *J. Chem. Soc. Faraday Trans. 2* **1978**, *74*, 1164–1178.
- [333] a) V. B. Smith, A. G. Massey, *Tetrahedron* **1969**, *25*, 5495–5501; b) J. Potenza, D. Mastropaolo, *Acta Crystallogr. Sect. B* **1975**, *31*, 2527–2529; c) D. G. Naae, *Acta Crystallogr. Sect. B* **1979**, *35*, 2765–2768; d) M. I. Bruce, M. R. Snow, E. R. T. Tiekink, *Acta Crystallogr. Sect. C* **1987**, *43*, 1640–1641; e) T. Dahl, *Acta Chem. Scand. Ser. A* **1988**, *42*, 1–7; f) D. J. Parks, W. E. Piers, M. Parvez, R. Atencio, M. J. Zaworotko, *Organometallics* **1998**, *17*, 1369–1377; g) C. M. Beck, J. Burdeniuc, R. H. Crabtree, A. L. Rheingold, G. P. A. Yap, *Inorg. Chim. Acta* **1998**, *270*, 559–562; h) J. R. Gardinier, F. P. Gabbaï, *J. Chem. Soc. Dalton Trans.* **2000**, 2861–2865; i) J. A. C. Clyburne, T. Hamilton, H. A. Jenkins, *Cryst. Eng.* **2001**, *4*, 1–9; j) J. C. Collings, A. S. Batsanov, J. A. K. Howard, T. B. Marder, *Acta Crystallogr. Sect. C* **2001**, *57*, 870–872; k) A. S. Batsanov, J. C. Collings, J. A. K. Howard, T. B. Marder, D. F. Perepichka, *Acta Crystallogr. Sect. C* **2001**, *57*, 1306–1307; l) A. S. Batsanov, J. A. K. Howard, T. B. Marder, E. G. Robins, *Acta Crystallogr. Sect. C* **2001**, *57*, 1303–1305; m) J. C. Collings, A. S. Batsanov, J. A. K. Howard, T. B. Marder, *Cryst. Eng.* **2002**, *5*, 37–46.
- [334] J. C. Collings, K. P. Roscoe, R. L. Thomas, A. S. Batsanov, L. M. Stimson, J. A. K. Howard, T. B. Marder, *New J. Chem.* **2001**, *25*, 1410–1417.
- [335] V. R. Vangala, A. Nangia, V. M. Lynch, *Chem. Commun.* **2002**, 1304–1305.
- [336] T. Dahl, *Acta Chem. Scand.* **1994**, *48*, 95–106.
- [337] J. H. Williams, *Acc. Chem. Res.* **1993**, *26*, 593–598.
- [338] Not discussed in this chapter, although equally interesting, are the properties and behaviors of 1,3,5-trifluorobenzene derivatives that have negligible quadrupole moments. See, for example, M. I. Cabaco, Y. Danten, M. Besnard, Y. Guissani, B. Guillot, *Chem. Phys. Lett.* **1996**, *262*, 120–124.
- [339] a) J. Vrbancich, G. L. D. Ritchie, *J. Chem. Soc. Faraday Trans. 2* **1980**, *76*, 648–659; b) K. E. Laidig, *Chem. Phys. Lett.* **1991**, *185*, 483–489; c) we mostly consider fluoroaromatic compounds with four or more fluorine atoms that have appreciably positive quadrupole moments relative to benzene, see J. Hernández-Trujillo, M. Costas, A. Vela, *J. Chem. Soc. Faraday Trans.* **1993**, *89*, 2441–2443.
- [340] T. G. Beaumont, K. M. C. Davis, *J. Chem. Soc. B* **1967**, 1131–1134.
- [341] J. D. Laposa, M. J. McGlinchey, C. Montgomery, *Spectrochim. Acta Part A* **1983**, *39*, 863–866.
- [342] T. G. Beaumont, K. M. C. Davis, *Nature* **1968**, *218*, 865.
- [343] C. J. Aspley, C. Boxwell, M. L. Buil, C. L. Higgitt, C. Long, R. N. Perutz, *Chem. Commun.* **1999**, 1027–1028.
- [344] A. P. West, Jr., S. Mecozzi, D. A. Dougherty, *J. Phys. Org. Chem.* **1997**, *10*, 347–350.
- [345] J. Hernández-Trujillo, F. Colmenares, G. Cuevas, M. Costas, *Chem. Phys. Lett.* **1997**, *265*, 503–507.
- [346] O. R. Lozman, R. J. Bushby, J. G. Vinter, *J. Chem. Soc. Perkin Trans. 2* **2001**, 1446–1452.
- [347] S. Lorenzo, G. R. Lewis, I. Dance, *New J. Chem.* **2000**, *24*, 295–304.

- [348] W. J. Gaw, F. L. Swinton, *Nature* **1966**, *212*, 283–284.
- [349] W. J. Gaw, F. L. Swinton, *Trans. Faraday Soc.* **1968**, *64*, 2023–2034.
- [350] a) M. E. Baur, C. M. Knobler, D. A. Horsma, P. Perez, *J. Phys. Chem.* **1970**, *74*, 4594–4596; b) C. L. Watkins, W. S. Brey, Jr., *J. Phys. Chem.* **1970**, *74*, 235–240; c) K. Tanabe, J. Hiraishi, *J. Raman Spectrosc.* **1982**, *12*, 274–277; d) E. Bartsch, H. Bertagnolli, P. Chieux, *Ber. Bunsen-Ges.* **1986**, *90*, 34–46; e) T. Tassaing, Y. Danten, M. Besnard, E. Zoidis, J. Yarwood, *Chem. Phys.* **1994**, *184*, 225–231.
- [351] M. Neelakandan, D. Pant, E. L. Quitevis, *Chem. Phys. Lett.* **1997**, *265*, 283–292.
- [352] F. Cozzi, F. Ponzini, R. Annunziata, M. Cinquini, J. S. Siegel, *Angew. Chem.* **1995**, *107*, 1092–1093; *Angew. Chem. Int. Ed. Engl.* **1995**, *34*, 1019–1020.
- [353] X. Fei, Y.-Z. Hui, V. Rüdiger, H.-J. Schneider, *J. Phys. Org. Chem.* **1997**, *10*, 305–310.
- [354] S. M. Ngola, D. A. Dougherty, *J. Org. Chem.* **1998**, *63*, 4566–4567.
- [355] R. Amunugama, M. T. Rodgers, *J. Phys. Chem. A* **2002**, *106*, 9092–9103.
- [356] For related effects borne out in catenation formation, see R. Ballardini, V. Balzani, A. Credi, C. L. Brown, R. E. Gillard, M. Montalti, D. Philp, J. F. Stoddart, M. Venturi, A. J. P. White, B. J. Williams, D. J. Williams, *J. Am. Chem. Soc.* **1997**, *119*, 12503–12513.
- [357] H. Adams, J.-L. J. Blanco, G. Chessari, C. A. Hunter, C. M. R. Low, J. M. Sanderson, J. G. Vinter, *Chem. Eur. J.* **2001**, *7*, 3494–3503.
- [358] J. S. Brennan, N. M. D. Brown, F. L. Swinton, *J. Chem. Soc. Faraday Trans. 1* **1974**, *70*, 1965–1970.
- [359] U. H. F. Bunz, V. Enkelmann, *Chem. Eur. J.* **1999**, *5*, 263–266.
- [360] R. E. Gillard, J. F. Stoddart, A. J. P. White, B. J. Williams, D. J. Williams, *J. Org. Chem.* **1996**, *61*, 4504–4505.
- [361] M. C. Etter, *Acc. Chem. Res.* **1990**, *23*, 120–126.
- [362] F. Ponzini, R. Zagha, K. Hardcastle, J. S. Siegel, *Angew. Chem.* **2000**, *112*, 2413–2415; *Angew. Chem. Int. Ed.* **2000**, *39*, 2323–2325.
- [363] G. W. Coates, A. R. Dunn, L. M. Henling, D. A. Dougherty, R. H. Grubbs, *Angew. Chem.* **1997**, *109*, 290–293; *Angew. Chem. Int. Ed. Engl.* **1997**, *36*, 248–251.
- [364] a) G. Wegner, *Z. Naturforsch. B* **1969**, *24*, 824–832; b) V. Enkelmann, *Adv. Polym. Sci.* **1984**, *63*, 91–136.
- [365] G. W. Coates, A. R. Dunn, L. M. Henling, J. W. Ziller, E. B. Lobkovsky, R. H. Grubbs, *J. Am. Chem. Soc.* **1998**, *120*, 3641–3649.
- [366] For related recent studies on the photodimerization of (1E,3E)-1-phenyl-4-pentafluorophenylbuta-1,3-dienes, see K. Vishnumurthy, T. N. G. Row, K. Venkatesan, *Photochem. Photobiol. Sci.* **2002**, *1*, 427–430.
- [367] a) M. L. Renak, G. P. Bartholomew, S. Wang, P. J. Ricatto, R. J. Lachicotte, G. C. Bazan, *J. Am. Chem. Soc.* **1999**, *121*, 7787–7799; b) G. P. Bartholomew, X. Bu, G. C. Bazan, *Chem. Mater.* **2000**, *12*, 2311–2318; c) W. J. Feast, P. W. Lövenich, H. Puschmann, C. Taliani, *Chem. Commun.* **2001**, 505–506.
- [368] a) P. Kirsch, K. Tarumi, *Angew. Chem.* **1998**, *110*, 501–506; *Angew. Chem. Int. Ed.* **1998**, *37*, 484–489; b) M. Weck, A. R. Dunn, K. Matsumoto, G. W. Coates, E. B. Lobkovsky, R. H. Grubbs, *Angew. Chem.* **1999**, *111*, 2909–2912; *Angew. Chem. Int. Ed.* **1999**, *38*, 2741–2745; c) C. Dai, P. Nguyen, T. B. Marder, A. J. Scott, W. Clegg, C. Viney, *Chem. Commun.* **1999**, 2493–2494.
- [369] A. F. M. Kilbinger, R. H. Grubbs, *Angew. Chem.* **2002**, *114*, 1633–1636; *Angew. Chem. Int. Ed.* **2002**, *41*, 1563–1566.
- [370] M. J. Marsella, Z.-Q. Wang, R. J. Reid, K. Yoon, *Org. Lett.* **2001**, *3*, 885–887.
- [371] J. T. Welch, *Tetrahedron* **1987**, *43*, 3123–3197.
- [372] D. O'Hagan, H. S. Rzepa, *Chem. Commun.* **1997**, 645–652.
- [373] B. E. Smart, *J. Fluorine Chem.* **2001**, *109*, 3–11.
- [374] M. Hoffmann, J. Rychlewski, *Int. J. Quantum Chem.* **2002**, *89*, 419–427.
- [375] Numerous other perfluoroaromatic substituted inhibitors have been generated in various systems. Recent examples include: a) A. Scozzafava, C. T. Supuran, *J. Med. Chem.* **2000**, *43*, 1858–1865; b) A. Scozzafava, L. Menabuoni, F. Mincione, F. Briganti, G. Mincione, C. T. Supuran, *J. Med. Chem.* **2000**, *43*, 4542–4551; c) J. A. Watts, A. Watts, D. A. Middleton, *J. Biol. Chem.* **2001**, *276*, 43197–43204.
- [376] The EC<sub>50</sub> value is a measure of functional binding affinity; see T. Kenakin, *Trends Pharmacol. Sci.* **1999**, *20*, 400–405.
- [377] B. C. Finzel, E. T. Baldwin, G. L. Bryant, G. F. Hess, J. W. Wilks, C. M. Trepod, J. E. Mott, V. P. Marshall, G. L. Petzold, R. A. Poorman, T. J. O'Sullivan, H. J. Schostarez, M. A. Mitchell, *Protein Sci.* **1998**, *7*, 2118–2126.
- [378] a) J. B. Doyon, A. Jain, *Org. Lett.* **1999**, *1*, 183–185; b) J. B. Doyon, E. A. M. Hansen, C.-Y. Kim, J. S. Chang, D. W. Christianson, R. D. Madder, J. G. Voet, T. A. Baird, Jr., C. A. Fierke, A. Jain, *Org. Lett.* **2000**, *2*, 1189–1192.
- [379] C.-Y. Kim, J. S. Chang, J. B. Doyon, T. T. Baird, Jr., C. A. Fierke, A. Jain, D. W. Christianson, *J. Am. Chem. Soc.* **2000**, *122*, 12125–12134.
- [380] C.-Y. Kim, P. P. Chandra, A. Jain, D. W. Christianson, *J. Am. Chem. Soc.* **2001**, *123*, 9620–9627.
- [381] K. M. Guckian, B. A. Schweitzer, R. X. F. Ren, C. J. Sheils, P. L. Paris, D. C. Tahmassebi, E. T. Kool, *J. Am. Chem. Soc.* **1996**, *118*, 8182–8183.
- [382] V. R. Thalladi, H.-C. Weiss, D. Bläser, R. Boese, A. Nangia, G. R. Desiraju, *J. Am. Chem. Soc.* **1998**, *120*, 8702–8710.
- [383] a) H. Plenio, *Chem. Rev.* **1997**, *97*, 3363–3384; b) H. Takemura, H. Kariyazono, M. Yasutake, N. Kon, K. Tani, K. Sako, T. Shinmyozu, T. Inazu, *Eur. J. Org. Chem.* **2000**, 141–148.
- [384] I. Alkorta, I. Rozas, J. Elguero, *J. Org. Chem.* **1997**, *62*, 4687–4691.
- [385] I. Alkorta, I. Rozas, J. Elguero, *J. Am. Chem. Soc.* **2002**, *124*, 8593–8598.
- [386] a) J. P. Gallivan, D. A. Dougherty, *Org. Lett.* **1999**, *1*, 103–105; b) Y. Danten, T. Tassaing, M. Besnard, *J. Phys. Chem. A* **1999**, *103*, 3530–3534; c) I. Alkorta, I. Rozas, M. L. Jimeno, J. Elguero, *Struct. Chem.* **2001**, *12*, 459–464.
- [387] C. J. Wormald, B. Wurzberger, *Phys. Chem. Chem. Phys.* **2000**, *2*, 5133–5137.
- [388] N. Kato, K. Endo, T. Tada, *J. Mol. Struct.* **2002**, *602*, 373–379.
- [389] J. R. Grover, G. Hagenow, E. A. Walters, *J. Chem. Phys.* **1992**, *97*, 628–642.
- [390] R. S. Morgan, C. E. Tatsch, R. H. Gushard, J. M. McAdon, P. K. Warme, *Int. J. Peptide Protein Res.* **1978**, *11*, 209–217.
- [391] R. Diamond, *J. Mol. Biol.* **1974**, *82*, 371–391.
- [392] a) L. G. Augenstine, C. A. Ghiron, *Proc. Natl. Acad. Sci. USA* **1961**, *47*, 1530–1547; b) K. Dose, B. Rajewsky, *Photochem. Photobiol.* **1962**, *1*, 181–189; c) L. Augenstine, P. Riley, *Photochem. Photobiol.* **1964**, *3*, 353–367; d) K. L. Grist, T. Taylor, L. G. Augenstine, *Radiat. Res.* **1965**, *26*, 198–210; e) K. Dose, *Photochem. Photobiol.* **1967**, *6*, 437–443; f) S. Risi, K. Dose, T. K. Rathinasamy, L. Augenstine, *Photochem. Photobiol.* **1967**, *6*, 423–436; g) S. Arian, M. Benjamini, J. Feitelson, G. Stein, *Photochem. Photobiol.* **1970**, *12*, 481–487; h) J. Feitelson, E. Hayon, *Photochem. Photobiol.* **1973**, *17*, 265–274; i) D. V. Bent, E. Hayon, *J. Am. Chem. Soc.* **1975**, *97*, 2599–2606.
- [393] a) Z. Li, W. E. Lee, W. C. Galley, *Biophys. J.* **1989**, *56*, 361–367; b) G. Krause, A. Holmgren, *J. Biol. Chem.* **1991**, *266*, 4056–4066; c) Y. Chen, M. D. Barkley, *Biochemistry* **1998**, *37*, 9976–9982; d) M. T. Neves-Petersen, Z. Gryczynski, J. Lakowicz, P. Fojan, S. Pedersen, E. Petersen, S. B. Petersen, *Protein Sci.* **2002**, *11*, 588–600.

- [394] K. S. C. Reid, P. F. Lindley, J. M. Thornton, *FEBS Lett.* **1985**, *190*, 209–213.
- [395] a) U. Samanta, D. Pal, P. Chakrabarti, *Proteins Struct. Funct. Genet.* **2000**, *38*, 288–300; b) D. Pal, P. Chakrabarti, *J. Biomol. Struct. Dyn.* **2001**, *19*, 115–128.
- [396] D. Pal, P. Chakrabarti, *J. Biomol. Struct. Dyn.* **1998**, *15*, 1059–1072.
- [397] For S–H/ $\pi$  interactions in crystal structures, see ref. [74], pp. 253–265.
- [398] For a general structural and conformational analysis of cysteines in proteins, see M. T. N. Petersen, P. H. Jonson, S. B. Petersen, *Protein Eng.* **1999**, *12*, 535–548.
- [399] W. D. Cornell, P. Cieplak, C. I. Bayly, I. R. Gould, K. M. Merz, Jr., D. M. Ferguson, D. C. Spellmeyer, T. Fox, J. W. Caldwell, P. A. Kollman, *J. Am. Chem. Soc.* **1995**, *117*, 5179–5197.
- [400] The value of 2.6 kcal mol<sup>-1</sup> is greater than for either N–H or O–H/ $\pi$  interactions (see Section 5) because of the increased polarizability of the sulfur atom and the enhanced acidity of the S–H group.
- [401] J. Pranata, *Bioorg. Chem.* **1997**, *25*, 213–219.
- [402] B. V. Cheney, M. W. Schulz, J. Cheney, *Biochim. Biophys. Acta* **1989**, *996*, 116–124.
- [403] T. R. Ioerger, C. Du, D. S. Linthicum, *Mol. Immunol.* **1999**, *36*, 373–386.
- [404] D. H. Fremont, W. A. Hendrickson, P. Marrack, J. Kappler, *Science* **1996**, *272*, 1001–1004.
- [405] G. Némethy, H. A. Scheraga, *Biochem. Biophys. Res. Commun.* **1981**, *98*, 482–487.
- [406] R. J. Zauhar, C. L. Colbert, R. S. Morgan, W. J. Welsh, *Biopolymers* **2000**, *53*, 233–248.
- [407] This orientation differs from those commonly found from model computational experiments and in protein crystal structures.
- [408] Searches were performed using Relibase V.1.1 (see ref. [69]). Results will be reported in more detail in a future publication.
- [409] F. Mancia, G. A. Smith, P. R. Evans, *Biochemistry* **1999**, *38*, 7999–8005.
- [410] L. Maveyraud, I. Massova, C. Birck, K. Miyashita, J.-P. Samama, S. Mobashery, *J. Am. Chem. Soc.* **1996**, *118*, 7435–7440.
- [411] M. Yun, C.-G. Park, J.-Y. Kim, C. O. Rock, S. Jackowski, H.-W. Park, *J. Biol. Chem.* **2000**, *275*, 28093–28099.
- [412] E. A. Meyer, R. Brenk, R. K. Castellano, M. Furler, G. Klebe, F. Diederich, *ChemBioChem* **2002**, *3*, 250–253.
- [413] F. Alber, O. Kuonen, L. Scapozza, G. Folkers, P. Carloni, *Proteins Struct. Funct. Genet.* **1998**, *31*, 453–459.
- [414] B. D. Pilger, R. Perozzo, F. Alber, C. Wurth, G. Folkers, L. Scapozza, *J. Biol. Chem.* **1999**, *274*, 31967–31973.
- [415] a) K. Wild, T. Bohner, A. Aubry, G. Folkers, G. E. Schulz, *FEBS Lett.* **1995**, *368*, 289–292; b) K. Wild, T. Bohner, G. Folkers, G. E. Schulz, *Protein Sci.* **1997**, *6*, 2097–2106.
- [416] S. Pakhomova, M. Kobayashi, J. Buck, M. E. Newcomer, *Nat. Struct. Biol.* **2001**, *8*, 447–451.
- [417] C. Zubieta, X.-Z. He, R. A. Dixon, J. P. Noel, *Nat. Struct. Biol.* **2001**, *8*, 271–279.
- [418] A. Ruf, V. Rolli, G. de Murcia, G. E. Schulz, *J. Mol. Biol.* **1998**, *278*, 57–65.
- [419] a) B. Masjost, P. Ballmer, E. Borroni, G. Zürcher, F. K. Winkler, R. Jakob-Roetne, F. Diederich, *Chem. Eur. J.* **2000**, *6*, 971–982; b) C. Lerner, A. Ruf, V. Gramlich, B. Masjost, G. Zürcher, R. Jakob-Roetne, E. Borroni, F. Diederich, *Angew. Chem.* **2001**, *113*, 4164–4166; *Angew. Chem. Int. Ed.* **2001**, *40*, 4040–4042.
- [420] J. Vidgren, L. A. Svensson, A. Liljas, *Nature* **1994**, *368*, 354–358.
- [421] a) B. L. Bodner, L. M. Jackman, R. S. Morgan, *Biophys. J.* **1977**, *17*, A57; b) B. L. Bodner, L. M. Jackman, R. S. Morgan, *Biochem. Biophys. Res. Commun.* **1980**, *94*, 807–813.
- [422] The similar association strength demonstrated for THF and 1-methylnaphthalene ( $\Delta H \approx -0.9$  kcal mol<sup>-1</sup>) also suggests that the sulfur atom does not participate in the binding; the oxygen atom is considerably more electronegative and less polarizable than the sulfur atom, which suggests that the main attractive interactions involved are between the polarized CH<sub>2</sub> groups and the aromatic ring.
- [423] For an intriguing example of a short sulfur–arene contact that influences the reactivity in disubstituted dibenzothiophene chemistry, see T. Kimura, N. Furukawa, *Tetrahedron Lett.* **1995**, *36*, 1079–1080.
- [424] M. Lebl, E. E. Sugg, V. J. Hruby, *Int. J. Pept. Protein Res.* **1987**, *29*, 40–45.
- [425] E. C. Breinlinger, C. J. Keenan, V. M. Rotello, *J. Am. Chem. Soc.* **1998**, *120*, 8606–8609.
- [426] V. M. Rotello, *Heteroat. Chem.* **1998**, *9*, 605–606.
- [427] a) A. R. Viguera, L. Serrano, *Biochemistry* **1995**, *34*, 8771–8779; b) B. J. Stapley, C. A. Rohl, A. J. Doig, *Protein Sci.* **1995**, *4*, 2383–2391.
- [428] N. Yamaotsu, I. Moriguchi, S. Hirono, *Biochim. Biophys. Acta* **1993**, *1203*, 243–250.
- [429] D. S. Spencer, W. E. Stites, *J. Mol. Biol.* **1996**, *257*, 497–499.
- [430] M. L. Ludwig, K. A. Patridge, A. L. Metzger, M. M. Dixon, M. Eren, Y. Feng, R. P. Swenson, *Biochemistry* **1997**, *36*, 1259–1280.
- [431] L. J. Druhan, R. P. Swenson, *Biochemistry* **1998**, *37*, 9668–9678.
- [432] For an example of a mutational study involving a cytochrome c enzyme that does not show a binding enhancement upon sulfur introduction, see D. S. Auld, G. B. Young, A. J. Saunders, D. F. Doyle, S. F. Betz, G. J. Pielak, *Protein Sci.* **1993**, *2*, 2187–2197.
- [433] a) B. D. Palmer, S. Trumpp-Kallmeyer, D. W. Fry, J. M. Nelson, H. D. Hollis Showalter, W. A. Denny, *J. Med. Chem.* **1997**, *40*, 1519–1529; b) P. Traxler, J. Green, H. Mett, U. Séquin, P. Furet, *J. Med. Chem.* **1999**, *42*, 1018–1026; c) J. Ren, C. Nichols, L. E. Bird, T. Fujiwara, H. Sugimoto, D. I. Stuart, D. K. Stammers, *J. Biol. Chem.* **2000**, *275*, 14316–14320.
- [434] Since submission of the manuscript several new articles related to this review have appeared: a) “Anion– $\pi$  Interactions: Do They Exist?": D. Quiñero, C. Garau, C. Rotger, A. Frontera, P. Ballester, A. Costa, P. M. Deya, *Angew. Chem.* **2002**, *114*, 3539–3542; *Angew. Chem. Int. Ed.* **2002**, *41*, 3389–3392; b) “ $\sigma$ -Donor,  $\pi$ -Donor, and anion complexation in  $\pi$ -complexation of alkali metal cations”: J. Hu, L. J. Barbour, G. W. Gokel, *Chem. Commun.* **2002**, 1808–1809; c) “Aromatic interactions in model systems”: M. L. Waters, *Curr. Opin. Chem. Biol.* **2002**, *6*, 736–741; d) “Comparison of the nature of  $\pi$  and conventional H-bonds: a theoretical investigation”: P. Tarakeshwar, K. S. Kim, *J. Mol. Struct.* **2002**, *615*, 227–238; e) “Anion Effects on the Recognition of Ion Pairs by Calix[4]arene-Based Heteroditopic Receptors”: A. Arduini, E. Brindani, G. Giorgi, A. Pochini, A. Secchi, *J. Org. Chem.* **2002**, *67*, 6188–6194; f) “The Influence of Substituents on Cation– $\pi$  Interactions. 4. Absolute Binding Energies of Alkali Metal Cation-Phenol Complexes Determined by Threshold Collision-Induced Dissociation and Theoretical Studies”: R. Amunugama, M. T. Rodgers, *J. Phys. Chem. A* **2002**, *106*, 9718–9728; g) “The Indole Side Chain of Tryptophan as a Versatile  $\pi$ -Donor”: J. Hu, L. J. Barbour, G. W. Gokel, *J. Am. Chem. Soc.* **2002**, *124*, 10940–10941; h) “A Perturbed pK<sub>a</sub> at the Binding Site of the Nicotinic Acetylcholine Receptor: Implications for Nicotinic Binding”: E. J. Petersson, A. Choi, D. S. Dahan, H. A. Lester, D. A. Dougherty, *J. Am. Chem. Soc.* **2002**, *124*, 12662–12663; i) “Comparison of Various Types of Hydrogen Bonds Involving Aromatic Amino Acids”: S. Scheiner, T. Kar, J. Pattanayak, *J. Am. Chem. Soc.* **2002**, *124*, 13257–13264; j) “Simple Cation– $\pi$  Interaction between a Phenyl Ring and a Protonated Amine Stabilizes an  $\alpha$ -Helix in Water”: L. K. Tsou,



C. D. Tatko, M. L. Waters, *J. Am. Chem. Soc.* **2002**, *124*, 14917–14921; k) “Arene–perfluoroarene interactions in crystal engineering 8: structures of 1:1 complexes of hexafluorobenzene with fused-ring polyaromatic hydrocarbons”: J. C. Collings, K. P. Roscoe, E. G. Robins, A. S. Batsanov, L. M. Stimson, J. A. K. Howard, S. J. Clark, T. B. Marder, *New J. Chem.* **2002**, *26*, 1740–1746; l) “Analysis of the  $\pi$ - $\pi$  Stacking Interactions between the Aminoglycoside Antibiotic Kinase APH(3)-IIIa

and Its Nucleotide Ligands”: D. B. Boehr, A. R. Farley, G. D. Wright, J. R. Cox, *Chem. Biol.* **2002**, *9*, 1209–1217; m) “Aromatic Side-Chain Interactions in Proteins. 1. Main Structural Features”: A. Thomas, R. Meurisse, B. Charleaux, R. Brasseur, *Proteins Struct. Funct. Genet.* **2002**, *48*, 628–634; n) “The C–H/ $\pi$  bonds: Strength, identification, and hydrogen-bonded nature: a theoretical study” J. J. Novoa, F. Mota, *Chem. Phys. Lett.* **2000**, *318*, 345–354.

# Quality counts...

The best of chemistry every week



## Wiley-VCH

P.O. Box 10 11 61  
69451 Weinheim  
Germany  
Phone +49 (0) 6201-606-147  
Fax +49 (0) 6201-606-172  
e-mail: [angewandte@wiley-vch.de](mailto:angewandte@wiley-vch.de)  
[www.angewandte.org](http://www.angewandte.org)

21602403\_gu

 WILEY-VCH